พอลิเมอร์ไรเซชันของโอเลฟินโดยตัวเร่งปฏิกิริยาเมทัลโลซีนบนตัวรองรับเซอร์โคเนียทรงกลมที่ถูกปรับปรุง

นางสาวศศิรดี จันทสี

OLEFIN POLYMERIZATION WITH MODIFIED SPHERICAL ZIRCONIA-SUPPORTED METALLOCENE CATALYSTS

Miss Sasiradee Jantasee

A Dissertation Submitted in Partial Fulfillment of the Requirements

for the Degree of Doctor of Engineering Program in Chemical Engineering

Department of Chemical Engineering

Faculty of Engineering

Chulalongkorn University

Academic Year 2013

Thesis Title   OLEFIN POLYMERIZATION WITH
                      MODIFIED SPHERICAL ZIRCONIA-
                      SUPPORTED METALLOCENE CATALYSTS
By   Miss Sasiradee Jantasee
Field of Study   Chemical Engineering
Thesis Advisor   Associate Professor Bunjerd Jongsomjit, Ph.D.

Accepted by the Faculty of Engineering, Chulalongkorn University in
Partial Fulfillment of the Requirements for the Doctoral Degree

....Dean of the Faculty of Engineering

(Prof.Bundhit Eua-arporn, Ph.D.)

THESIS COMMITTEE

…………………………………….………..Chairman

(Associate Professor Anongnat Somwangthanaroj, Ph.D)

…………………………………….………..Thesis Advisor

(Associate Professor Bunjerd Jongsomjit, Ph.D.)

…………………………………….………..Examiner

(Associate Professor ML. Supakanok Thongyai, Ph.D.)

…………………………………….………..Examiner

(Assistant Professor Supoj Pattanasri, Ph.D.)

…………………………………….………..External Examiner

(Ekrachan Chaichana, D.Eng.)

ศศิรดี จันทสี: พอลิเมอร์ไรเซชันของโอเลฟินโดยตัวเร่งปฏิกิริยาเมทัลโลซีนบนตัวรองรับเซอร์โคเนียทรงกลมที่ถูกปรับปรุง (OLEFIN POLYMERIZATION WITH MODIFIED SPHERICAL ZIRCONIA-SUPPORTED METALLOCENE CATALYSTS) อ.ที่ปรึกษาวิทยานิพนธ์หลัก: รศ.ดร. บรรเจิด จงสมจิตร, 105 หน้า.

ในงานวิจัยนี้เอทิลีน/1-เฮกซีนพอลิเมอร์ไรเซชันถูกดำเนินการร่วมกับตัวเร่งปฏิกิริยาเรซิมิค-เอทิลีนบิสอินดีนิลเซอร์โคเนียมไดคลอไรด์ เพื่อเปรียบเทียบผลของเมทิลอะลูมินอกเซน (MAO) ที่ถูกยึดเกาะบนตัวรองรับเซอร์โคเนียทรงกลมที่ถูกปรับปรุงด้วยตัวปรับปรุงต่างชนิดกัน ได้แก่ โบรอนไตรคลอไรด์ (BCl_3) , ซิลิกอนเตตระคลอไรด์ ($SiCl_4$) และกลีเซอรอล พบว่าตัวปรับปรุงทุกชนิดช่วยเพิ่มความว่องไวของตัวเร่งปฏิกิริยาในระบบวิวิธพันธุ์นี้ เมื่อเปรียบเทียบกับตัวรองรับเซอร์โคเนียที่ไม่ถูกปรับปรุง แต่ไม่ส่งผลต่อโครงสร้างของโคพอลิเมอร์ ซึ่งการปรับปรุงตัวรองรับเซอร์โคเนียด้วย $SiCl_4$ ก่อนการยึดเกาะด้วย MAO ให้ค่าความว่องไวในการเกิดปฏิกิริยาสูงที่สุด อย่างไรก็ตามเหตุผลในการเพิ่มขึ้นของค่าความว่องไวในการเกิดปฏิกิริยาเมื่อมีการปรับปรุงด้วย $SiCl_4$ ยังไม่เป็นที่แน่ชัด ถ้าหากว่าระบบตัวเร่งปฏิกิริยาร่วมที่ถูกปรับปรุงนี้สามารถเกิดพฤติกรรมลีฟวิงพอลิเมอร์เซชันได้ น่าจะช่วยให้เข้าใจมากขึ้นว่าการปรับปรุงนี้ส่งผลต่อจำนวนตำแหน่งที่ว่องไวในการเกิดปฏิกิริยา (C^*) และ/หรือค่าคงที่ของการเกิดปฏิกิริยาในขั้นการต่อสายโซ่ (k_p) เมื่อพิจารณาพฤติกรรมลีฟวิงของตัวเร่งปฏิกิริยา $Me_2Si(\eta^3\text{-}C_{13}H_8)(\eta^1\text{-}N^tBu)TiMe_2$ พบว่าตัวเร่งปฏิกิริยาร่วม MAO ที่ถูกยึดเกาะบนตัวรองรับเซอร์โคเนียมีแนวโน้มที่จะเกิดพฤติกรรมแบบลีฟวิงในปฏิกิริยาพอลิเมอร์ไรเซชันของโพรพิวลีน ดังนั้นจึงได้นำตัวเร่งปฏิกิริยาชนิดนี้มาใช้ร่วมกับ MAO ที่ถูกยึดเกาะบนตัวรองรับเซอร์โคเนียที่ไม่ถูกปรับปรุงและที่ถูกปรับปรุงด้วย $SiCl_4$ เพื่อศึกษาผลของการปรับปรับปรุงตัวรองรับด้วย $SiCl_4$ ที่มีต่อประสิทธิภาพของตังเร่งปฏิกิริยาร่วม พบว่าความสัมพันธ์ของค่าน้ำหนักโมเลกุลเฉลี่ย (M_n) ของพอลิโพรพิวลีนเพิ่มขึ้นเป็นเส้นตรงกับเวลาในการพอลิเมอร์ไรเซชัน โดยไม่ขึ้นกับระบบของตัวเร่งปฏิกิริยาร่วมที่ใช้ และให้พอลิเมอร์ที่มีการกระจายตัวของน้ำหนักโมเลกุลแคบ ผลเหล่านี้แสดงถึงพฤติกรรมการกิดลีฟวิงของระบบข้างต้น ดังนั้นค่า k_p และค่า C^* สามารถทำนายได้จากค่า M_n และจำนวนสายโซ่พอลิเมอร์ เมื่อตัวรองรับเซอร์โคเนียถูกปรับปรุงด้วย $SiCl_4$ จะส่งผลให้ค่า k_p ลดลง แต่ค่า C^* เพิ่มขึ้น ซึ่งการเพิ่มขึ้นของค่า C^* มีผลสำคัญมากกว่า โดยรวมจึงส่งผลให้ค่าความว่องไวในการเกิดปฏิกิริยาเพิ่มขึ้น

ภาควิชา	วิศวกรรมเคมี	ลายมือชื่อนิสิต ....
สาขาวิชา	วิศวกรรมเคมี	ลายมือชื่อ อ.ที่ปรึกษาวิทยานิพนธ์หลัก ....
ปีการศึกษา	2556	

5271829221: MAJOR   CHEMICAL ENGINEERING

KEYWORDS: METALLOCENE CATALYST / OLEFIN POLYMERIZATION / MODIFICATION / SPHERICAL ZIRCONIA

SASIRADEE JANTASEE: OLEFIN POLYMERIZATION WITH MODIFIED SPHERICAL ZIRCONIA-SUPPORTED METALLOCENE CATALYSTS. ADVISOR: ASSOC. PROF. BUNJERD JONGSOMJIT, Ph.D., 105 pp.

In this research, ethylene/1-hexene copolymerizations were conducted with rac-Et(Ind)$_2$ZrCl$_2$ in order to compare effect of MAO supported on spherical zirconia modified with different modifiers; BCl$_3$, SiCl$_4$ and glycerol. All kind of modifiers can enhance the catalytic activity of this heterogeneous catalyst system compared to unmodified-ZrO$_2$ system, but did not affect the copolymers microstructure. The modification of ZrO$_2$ with SiCl$_4$ before supporting MAO showed the highest catalytic activity. However, the reason of the activity improvement by SiCl$_4$-modification has not been clear. In the event of living polymerization accomplished with the modified cocatalyst system, it becomes obvious whether the modification affects the number of active centers (C^*) or the propagation rate constant (k_p). Considering the living nature of Me$_2$Si(η^3-C$_{13}$H$_8$)(η^1-N^{t}Bu)TiMe$_2$-based catalytic systems, ZrO$_2$-supported MAO cocatalyst suggest the living behavior of propylene polymerization with this catalyst. Thus, this catalyst was used with MAO supported on unmodified and SiCl$_4$-modified ZrO$_2$ for clarifying the modification effect of SiCl$_4$ on cocatalyst abilities. The M_n values of polypropylenes increased linearly against the polymerization time regardless the cocatalyst used to give polymers with narrow molecular weight distribution, indicating the living nature of the catalytic systems. Thus, the k_p and C^* values were evaluated from M_n and the number of polymer chains. When the ZrO$_2$ was modified with SiCl$_4$, the k_p value decreased and the C^* increased. The latter effect was more significant to enhance the catalytic activity.

Department:	Chemical Engineering	Student's Signature	....
Field of Study:	Chemical Engineering	Advisor's Signature	....
Academic Year:	2013		

ACKNOWLEDGEMENTS

The author would like to express her special gratitude to her thesis advisor, Associate Professor Dr. Bunjerd Jongsomjit, for his generosity in providing constant encouragement and useful suggestions, not only throughout her research but also throughout her life. She would not have accomplished this far and this research would not have been completed without all supports that she have always received from him.

She would also like to express her profound gratitude to Professor Dr. Takeshi Shiono for his exemplary guidance in academic perspective throughout her dissertation and taking care of her by him together with by all her friends at Hiroshima University while she was spending her time in Japan.

She is sincerely grateful Associate Professor Anongnat Somwangthanaroj, as the chairman, and all the members of the thesis committee including Associate Professor Dr. ML. Supakanok Thongyai, Dr. Suphot Phatanasri as well as Dr. Ekrachan Chaichana for their invaluable information as the guidance of this research and all their help.

She would like to take this opportunity to thank the Thailand Research Fund (TRF), Royal Golden Jubilee Scholarship and Commission on Higher Education for the financial support.

In addition, she wishes to thank all her friends and members in the Center of Excellence on Catalysis and Catalytic Reaction Engineering, Department of Chemical Engineering, Chulalongkorn University for all their support and encouragement.

Finally, she thanks almighty her parents and her brother who always give her understandings, supports and endless love all the times. The achievement of graduation is dedicated to her family.

CONTENTS

LIST OF TABLES

LIST OF FIGURES

Page

LIST OF ABBREVIATIONS AND SYMBOLS

Abbreviations

BCl_3	Boron trichloride
$SiCl_4$	Silicon tetrachloride
CA	Cross-linking agent
SiO_2	Silica
ZrO_2	Zirconia
rac-Et(Ind)$_2$ZrCl$_2$	*rac*-ethylenebis indenyl zirconium dichloride
Me$_2$Si(η^3-C$_{13}$H$_8$)(η^1-N^{t}Bu)TiMe$_2$	*tert*-[butyl(dimethylfluorenylsilyl) amido]dimethyl titanium
CGC	Constrained geometry catalyst
MAO	Methylaluminoxane
MMAO	Modified methylaluminoxane
dMMAO	died-Modified methylaluminoxane
TMA	Trimethylaluminium
TIBA	Triisobuthylaluminium
PE	Polyethylene
PP	Polypropylene
HDPE	High density polyethylene
LDPE	Low density polyethylene
LLDPE	Linear low density polyethylene
SEM	Scanning electron microscopy
EDX	Energy dispersive X-ray spectroscopy
FTIR	Fourier transform infrared
GPC	Gel permeation chromatography
XPS	X-ray photoelectron spectroscopy
NMR	Neclear magnetic resonance
TGA	Thermogravimetric analysis
ICP	Inductively-coupled plasma

Symbols

[C*]	Active site concentration
k_p	Propagation rate constant
k_{tr}	Chain-transfer rate constant
N	Number of polymer chain
[M]	Monomer concentration
$\overline{M}_n$	Number-average molecular weight
M_o	Molecular weight of the monomer
M_w	Weight-average molecular weight
M_n	Number-average molecular weight
M_w/M_n	Molecular weight distribution
t	Polymerization time
Y	Polymer yield
r_E	Reactivity of ethylene
r_H	Reactivity of 1-hexene
$r_E r_H$	Reactivity ratio

CHAPTER I

INTRODUCTION

The worldwide consumption of polyolefins, such as polyethylene (PE), polypropylene (PP), and copolymers of other alkene monomers, according to recent study reports is the large volume commodity polymers. The attractive feature of polyolefins is a wide range of polymer properties depending on both the polymer microstructure and molecular weight of polymer [1-5]. Polymer properties and productivity strongly depend on not only the types of catalyst but also the types of cocatalyst employed ascribed to producing the different active species [6]. Thus, it is interesting to develop in the areas of catalysis and cocatalyst and to study the effects of them on olefin polymerization behavior [7].

For industrial production, polyolefins can be synthesized with varieties of catalysts such as Ziegler-Natta catalysts, metallocene catalysts and chromium oxide-based catalysts (Philips) [8]. Particularly, the discovery of metallocene catalyst has attracted much attention as the catalyst for olefins polymerization [9]. Metallocene catalyst activated by methylaluminoxane (MAO) affords extremely high activity. This catalyst is superior to other catalysts in terms of the homogeneity of active species that enable us to produce uniform polymer with narrow molecular weight distribution and narrow comonomer distribution [10-12]. Moreover, the exploration of the constrained geometry catalysts (CGCs), which *N*-based ligand was attached to the cyclopentadienyl ring, has also attracted a great deal of attention. The CGC catalysts presented much higher comonomer incorporation in copolymer, narrower molecular weight distribution and higher thermal stabilities compared to conventional metallocene catalysts [13-14].

Most of research and the existing commercial productions have been done in gas- or slurry-phase polymerizations. For homogeneous metallocene catalysts, the difficulties in controlling the polymer morphology in gas- or slurry-phase polymerizations and the requirement of a great deal of costly MAO for achievement

high activity are major drawbacks [12]. Therefore, heterogenization of metallocene catalysts on supports is required to overcome these drawbacks. The supported metallocene catalysts have advantages in controlling the morphology of polymer and reducing the possibility of reactor fouling [12,15,16]. A great category of inorganic supports for immobilizing single-site metallocene catalysts has been studied. Although silica is an inorganic carrier greatly used as a support for metallocene catalysts, other inorganic carriers have also been reported [17-20]. Recently, the use of zirconia for *rac*-Et(Ind)$_2$ZrCl$_2$/MAO catalyst for ethylene/1-olefin copolymerizations was investigated and compared to the conventional silica. It was found that the use of zirconia exhibited higher productivity than that of the conventional silica [21].

However, the heterogenized metallocene catalysts leads to a decrease in catalytic activity compared with that of the homogeneous system [12,16,22]. The lower catalytic activity of heterogeneous system should be ascribed to the presence of the support surface itself leading to steric hindrance around the active species, i.e. the counter anion on the support surface; consequently suppressed monomer coordination. Moreover, chemical properties of the support surface also play a significant role for catalyst performance [17]. Many studies have reported that either catalyst or cocatalyst is anchored on the modified support surface improving the catalytic activity. There are many ways to modify the support; using a spacer group such as silicon compound between support surface and metallocene catalyst [23-26], anchoring cocatalyst onto the support surface through coordination of Lewis acid metal promoting the acidic surface property of the supports [27-31], and employing chemically modified MAO with aliphatic or aromatic diols as cross-linking agent (CA) to form three-dimensional lattice of MAO [32]. Thus, the crucial key of this research is an immobilizing the catalyst or cocatalyst on the support for improving the polymer morphology together with keeping the merits of the homogeneous system such as high activity via the support modification.

Furthermore, the reason of activity improvement due to the support modification was investigated. In the event of living polymerization, in which neither chain transfer nor deactivation occurs, accomplished with the modified cocatalyst

system, it becomes obvious whether the modification affects the number of active centers (C^*) or the propagation rate constant (k_p). Although MAO is by far the prominent cocatalyst for activation of metallocene catalysts [1], the living polymerization probably was accomplished with other cocatalysts.

From such a viewpoint, the aims of this research were divided into three parts as following.

1. To study the effect of spherical zirconia modified with different modifiers including $SiCl_4$, BCl_3, and glycerol in terms of catalyst precursor properties, catalytic activity and copolymer properties (Part 1)

2. To investigate supporting effect of different cocatalysts on living behavior, catalytic activity, polymer properties (Part 2)

3. To investigate the possibility of living polymerization for clarifying the modification effect of $SiCl_4$ on cocatalyst abilities (Part 3)

This dissertation consists of five chapters. Chapter I is general introduction and the motivation to investigate this research. Chapter II involves in knowledge and brief literature reviews on metallocene catalysts, olefin polymerizations and the modifications of support. Chapter III focuses on the chemicals and instruments employed, support and catalyst preparation, modification and impregnation procedures as well as polymerization procedures, and characterization techniques. In the Chapter IV, the results of olefins polymerization regarding three parts of investigations as mentioned above are shown and discussed. Finally, conclusions of this work and the suggestions for future work are presented in Chapter V.

CHAPTER II

LITERATURE REVIEWS

2.1 Polyolefins

Polyolefins are a category of polymer synthesized from vinyl monomers. The examples of polyolefins popular produced in the petrochemical industry are polyethylene synthesized from ethylene monomer, and polypropylene prepared from propylene monomer. The global polyolefins consumptions are approximately 47.5 million metric tons of polypropylene, 32.3 million metric tons of high density polyethylene (HDPE), 19 million metric tons of low density polyethylene (LDPE) and 20.9 million metric tons of linear low density polyethylene (LLDPE) in 2010 [33]. Due to their extreme usefulness in term of flexibility, strength, lightness, stability, impermeability and easy processability, they are most employed in polymer industries including films, packaging, machinery parts, electrical insulators, inks, and additives [34].

2.1.1   Polyethylene [35,36]

Polyethylene can be classified based on its branching and its density into three main classes; HDPE, LDPE and LLDPE. First, HDPE is a long linear chain polyethylene and crystalline structure consequently is highest compared to LDPE and LLDPE. It is the strongest, toughest, most chemical resistant and least flexible of the three types of polyethylene. HDPE is commonly synthesized by coordination polymerization with Ziegler-Natta catalyst or metallocene catalyst. Second, LDPE is a long chain branched polyethylene having lowest crystalline structure compared to LLDPE and HDPE. It is very flexible. LDPE can be produced by free radical process under high temperature and high pressure conditions. The last, LLDPE is a short chain branched polyethylene. It is called linear low density due to the short chain branches, which seem to be linear chain. Commonly, α-olefin is used as a comonomer such as 1-

butene, 1-hexene, or 1-octene. LLDPE is prepared by coordination polymerization reaction with Zeigler-Natta catalyst or metallocene catalyst or chromium oxide-based catalysts under lower temperature and lower pressure than LDPE production. The production of LDPE has lower expanding rate than that of LLDPE. The long chains in LDPE lead to high cross linking between chains, which eventually affects physical and mechanical properties of LDPE. Moreover, LDPE production is operated at high temperature (100 – 300 °C) and high pressure (1500-3000 atm) besides initiator is required resulting in high production cost. In addition, LLDPE can be consumed in many applications namely films, which is the largest field for LLDPE resins, pipe/tubing, bottles/containers, electric wire, and cable insulation. The structures of them are illustrated in **Figure 2.1** and the densities of polyethylene series are compared in **Table 2.1**.
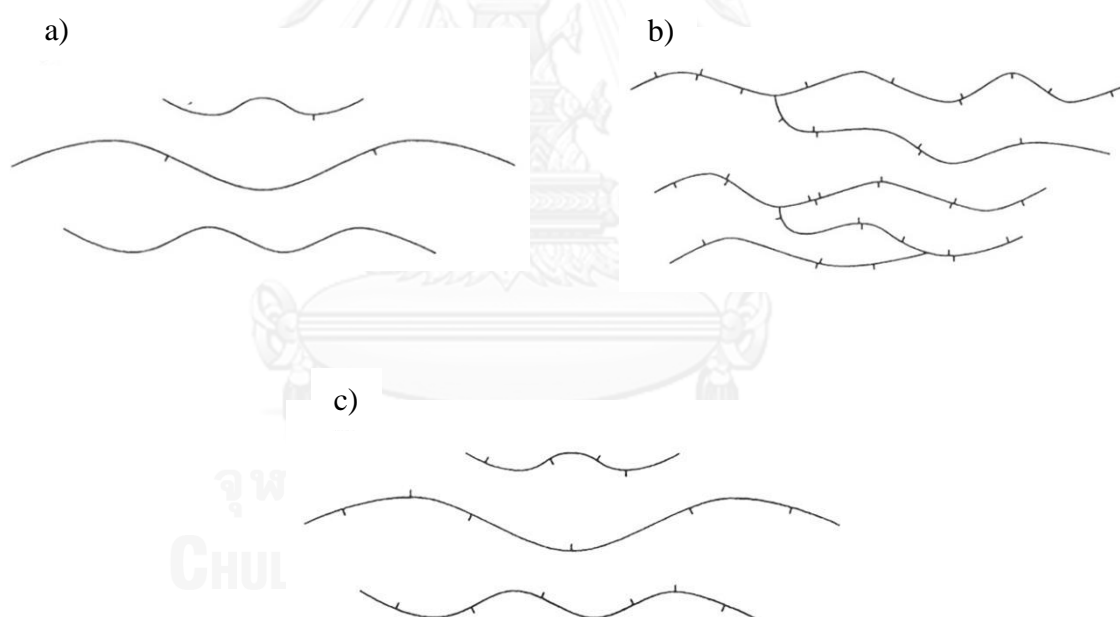
Figure 2.1 Typical structure of a) high density polyethylene; b) low density polyethylene; c) linear low density polyethylene [37]

Table 2.1 Densities of polyethylene series defined by the American Society for Testing and Material (ASTM) [36]

Type of polyethylene	Density (g/mL)
high density polyethylene	> 0.940
linear low density polyethylene	0.919 – 0.925
low density polyethylene	0.910 – 0.925

2.1.2 **Polypropylene** [35,38,39]

Another popular polyolefin in polymer market is polypropylene which is produced from propylene monomer. It was taken into commercial production in 1957. Polypropylene has been widely used in variety of applications namely packaging, containers, and automotive components. Polypropylene has higher thermal resistance than polyethylene. The methyl side-groups in propylene monomer can arrange themselves along the main chain of polymer in three different ways. If all methyl-side groups aligned uniformly on a side of main chain defined by meso-diad (m), this polymer has isotactic structure. If the methyl-side groups alternate in a regular location from one side of chain to another side defined by racemic-diad (r), this polymer has syndiotactic structure. Finally, atactic structure is polymer which the methyl-side groups random locate along the main chain. The tacticity has important influence on physical properties of polypropylene. Atactic polypropylene is amorphous polymer but isotactic and syndiotactic polypropylene are crystalline structure. The tacticity of polypropylene is present in **Figure 2.2**. Polypropylene can produce by chain-growth polymerization as well as coordination polymerization with Zeigler-Natta catalyst or metallocene catalyst.
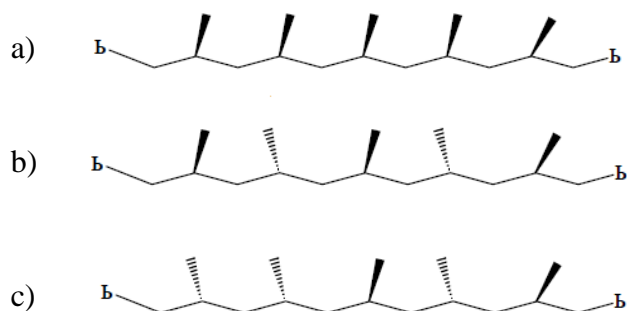
Figure 2.2 The tacticity of polypropylene a) isotactic,
b) syndiotactic and c) atactic [1]

2.2 Catalysts for olefin polymerization

Since the discovery of high efficiency catalyst which is Ziegler-Natta catalysts, these catalysts has played very important role in polyolefin industry up until now. The first development of these catalysts was occurred by Karl Ziegler in 1953 for the formation of high density polyethylene (HDPE). In 1954, Guilio Natta provided us next progress in these catalysts fields that was able to polymerize isotactic polypropylene. Ziegler-Natta catalysts are generated ground on titanium chlorides ($TiCl_4$) and alkylaluminum as a cocatalyst. These catalysts are commonly prepared by impregnation of $TiCl_4$ on solid support such as magnesium chloride and silica [35,40]. For Ziegler-Natta catalysts, the heterogeneous system has shown higher productivity than homogeneous system. As a matter of fact, the activated Ziegler-Natta catalysts have multiple types of active sites resulting in producing polymer with broad molecular weight distribution. This is due to different of stereochemical and reactivity of active site. The multi-site catalyst is shown in **Figure 2.3a)**. Over the past six decades, many industries and researchers have been consistently developed Ziegler-Natta catalysts in order to improve the productivity, selectivity and stereospecificity of polyolefins [40-42].

Not long after metallocene catalysts were discovered in 1980 by Sinn and Kaminsky, it has been the great revolution in olefin industry [1,40]. Metallocene

catalysts show in opposite to Ziegler-Natta catalysts which produce narrow molecular weight distribution polymer ($M_w/M_n \sim 2$). This is due to metallocene catalysts consist of only one type of active sites so called single-site catalyst while Ziegler-Natta catalysts have several types of active sites which produce polymer with broad molecular weight distribution. The active sites of metallocene catalyst are shown in **Figure 2.3b)**. Furthermore, their homogeneity nature of actives species allow for producing uniform polymer properties [42-44]. The homogeneous metallocene catalysts in combination with methylaluminoxane (MAO) provide large number of activity in olefin polymerization compared to Ziegler-Natta catalysts. They were able to control stereoregular isotactic and syndiotactic polypropylene of polypropylene in extreme high yield [45]. Thus, the metallocene catalysts can be fully thought to represent an important generation of olefin polymerization catalysts.
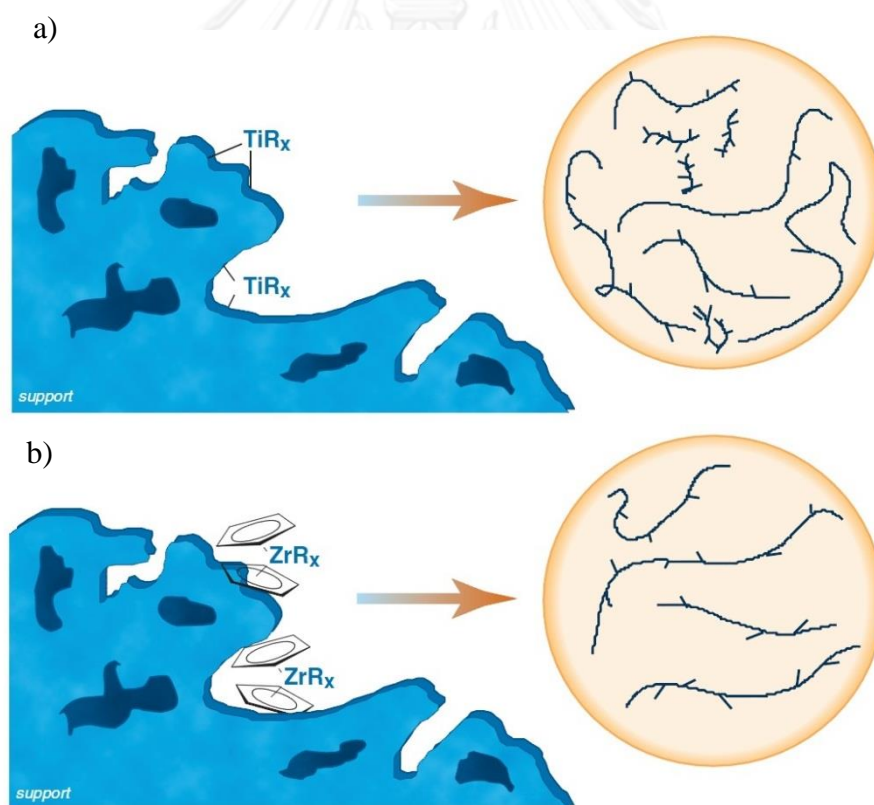
Figure 2.3 a) Different types of polymer produced from multi-site catalysts, and b) uniform polymer produced from single-site catalysts [46]

2.2.1 Meatallocene catalyst

Metallocene catalyst, which is organometallic compound, generally consists of group IV transition metal atom including titanium (Ti), zirconium (Zr), and hafnium (Hf) bound to one or two carbocyclic ligand such as cyclopentadienyl and its derivatives (ex. fluorenyl and indenyl etc.). The ligands are able to control the sterochemical and electronic of transition metal center that affect the polymer properties such as molecular weight, molecular weight distribution, and comonomer insertion [43]. The typical chemical structure of metallocene catalyst is illustrated in **Figure 2.4**. The general formula of metallocene catalyst is Cp′$_2$MX$_2$ [40]. The Cp′ ligands can be substituted by aromatic and aliphatic rings bridge through carbon or silicon atom. The "X" ligands are either halogen atoms (normally chloride) or alkyl groups or alcohols.

Figure 2.4 The typical chemical structure of metallocene catalyst [47]

Where

> M = transition metal (e.g. Zr, Ti or Hf)
>
> A = an optional bridging unit consisting of 1-3 atoms in the backbone usually Si or C atom
>
> R = hydrocarbyl substituents or fused ring system (indenyl, fluorenyl, and substituted derivatives)
>
> X = chlorine or other halogens from group 7 or an alkyl group

Table 2.2 Properties of metallocene catalysts [35]

Metallocene catalyst	Symmetry	Polymer structure
	C_{2v}	Atactic (variable)
	C_2	Isotactic
	C_s	Syndiotactic
	C_1	Variable

Metallocene catalysts are divided into several groups depending on structure symmetry. The symmetry types of the metallocene catalysts in **Table 2.2** have been examined. If two Cp rings on either sides of transition metal are unbridged, the metallocene is freely rotating non-stereorigid so called C_{2v}- symmetry. If two Cp rings are bridged, it is stereorigid metallocene and it is characterized by either C_1-, C_2- or C_s-symmetry depending upon the substitutions on two Cp rings and the bridging structure. C_s-symmetry catalysts have mirror planes containing the two-diastereotopic coordination sites. C_2-symmetry catalysts are a racemic mixture of an enantiomeric pair. The two sites are equivalent (homotopic) and enantioselective for the same monomer enantioface. C_2 ansa-metallocenes generally produce the most isoselective

polymerizations. C_1-symmetric (asymmetric) catalysts have unpredictable ligands. Many research proposed the substituents on the cyclopentadienyl ring as well as employing the suitable symmetry and geometry of catalyst to control stereoselective polymerization [35,40,43].

2.2.2 Constrain geometry catalyst (CGC)

In the early 1990s, a novel family of metallocene based catalysts known as constrained geometry catalysts (CGCs) has been found. They retain one cyclopentadienyl ring (or its derivatives) of the conventional metallocene catalysts, but replace the another ring with a nitrogen substituent that coordinates with the metal center (usually group IV metal). Such catalysts offer many attractions versus conventional metallocene catalysts, such as thermal stability which allows for higher polymerization temperatures and greater enchainment activity owing to the more open coordination sphere [14,48]. The efficiency in α-olefin insertion in ethylene/α-olefin copolymerization, that can be evaluated by using reactivity of ethylene values (r_E) under the similar conditions, increases in the order: Cp_2ZrCl_2 < *rac-*$Me_2Si[benz(e)Ind]_2ZrCl_2$ < $[Me_2Si(C_5Me_4)(N^tBu)]TiCl_2$ [49]. The reason has been explained as that the bridge constrains a more open Cp‑Ti‑N bond angle permits an even easier incorporation of bulky α-olefins in addition to that of ethylene macromonomers as illustrated in **Figure 2.5**.
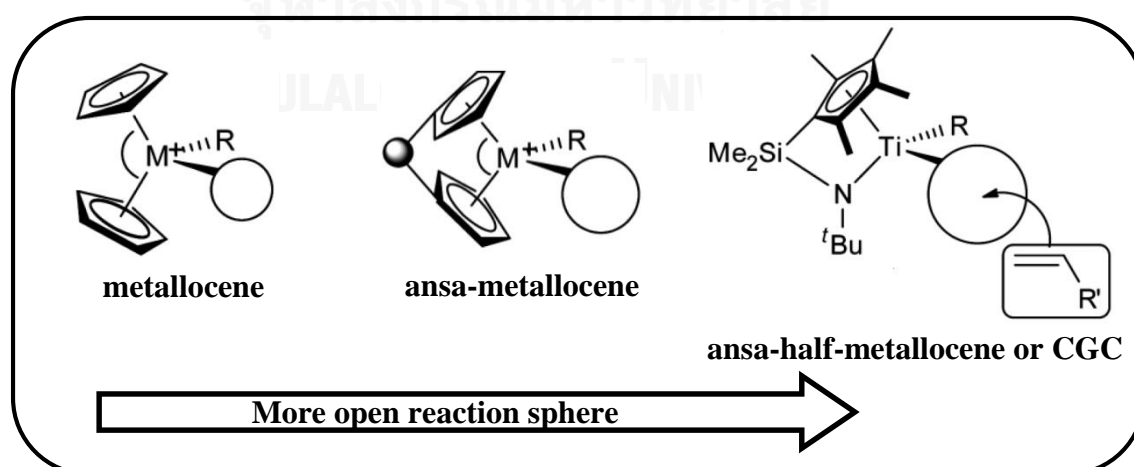
Figure 2.5 Comparative coordination sphere of catalysts [49]

The first CGC was reported by Bercaw et al. [14,48] as shown in **Figure 2.6a)**. These scandocene derivatives were found to undergo olefin insertion as well as β-hydride and β-alkyl elimination and to give low activity in olefin polymerization. Shortly later, the Group IV constrained geometry catalyst was developed industrially by Dow Chemical Company as shown in **Figure 2.6b)**. The reactive center is less steric hindrance than most other olefin polymerization catalysts due to the lack of a second cyclopentadienyl ring. However, CGCs typically do not have steric control over the polymerization of α-olefins due to the open nature of the active site resulting in atactic polymers [50]. They apparently have a lower tendency to undergo chain transfer, which produces very high molecular weight polymers or copolymers with ethylene and α-olefins. The molecular weight distribution of polymers produced by constrained geometry catalysts is similar to those of conventional metallocene catalysts, which is about 2 [51].

a)   b)

L= PMe$_3$
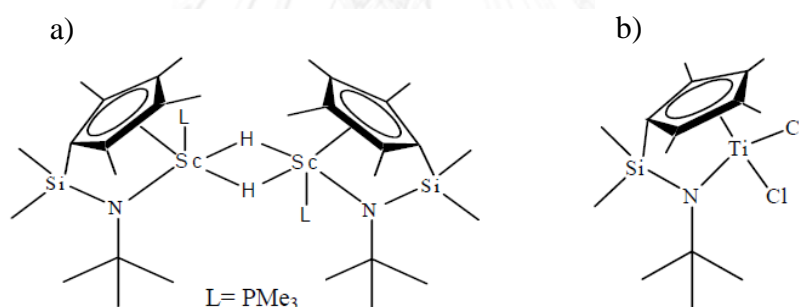
Figure 2.6 a) Scandium and b) titanium CGCs [14]

Stevens et al. claimed in their patent, that such a strain inducing link would improve catalyst performance. Thus, many researchers focused on designing with constrained geometry type by the CGCs structure modification, for example, modification of the ligand system [48,49], variation of the cyclopentadienyl fragment [49], variation of amido fragment [51], and variation of the metal center [52].

2.3 Cocatalyst

Metallocene catalyst is significant to be activated with cocatalysts, which are typically alkyl aluminum, resulting in the formation of active species. The abstraction of methyl group from the transition metal was occurred with the formation of the actives site as shown in **Figure 2.7** [12]. The conventional aluminum alkyl cocatalyst employed with Zeigler-Natta catalysts show very poor activity when they were used with metallocene. After the discovery of methylaluminoxane (MAO) by Sinn et al., in 1980, the metallocene catalysts in combination with MAO presented very high productivity about 10-100 times higher than that of classical Ziegler-Natta catalyst [1]. Thus, MAO plays a crucial role in olefin polymerization with metallocene catalysts.

$$Cp_2ZrCl_2 \xrightarrow{\text{MAO}} Cp_2ZrMe_2 \xrightarrow{\text{MAO}} [Cp_2ZrMe]^+[MeMAO]^-$$
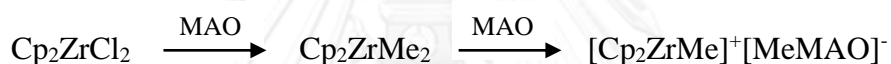
Figure 2.7 Formation of cationic metallocene active site

MAO is the most effective cocatalyst for metallocene catalysts. It is organoaluminoxanes which consist of aluminum atom and oxygen atom and free valence in aluminum atom are filled with methyl groups. MAO can prepare by partial hydrolysis reaction of trimethylaluminum (TMA) [53,54] This reaction need to carefully perform via the reaction with wet solvents or hydrated salts because of its extremely rapid exothermic reaction. It is accepted that MAO donates methyl group to replace halide atom (X) in metallocene catalyst. MAO is both the activator (abstracts methyl group) and the coordinator with the generated anion (acts as counter-ion to the cationic active center); meanwhile, it can act as an impurity scavenger which removes trace amounts of water and oxygen in polymerization system [1,53-55].

Although there are very extensive research concern with MAO structures in both academia and industry, the precise composition and structure of MAO have been not clear or well understood. This is due to multiple equilibrium between MAO oligomers and residual TMA. The TMA present in MAO solution are classified into

two types; "free" TMA and "associated" TMA as shown in **Figure 2.8**. Although the precise structure of MAO cannot specify, there are some researchers proposing possible structures of MAO according to **Figure 2.9** including linear chain and cyclic ring structure.

$$\left[\text{Al(Me)O}\right]_n \bullet x \; \text{AlMe}_3 \rightleftharpoons \left[\text{Al(Me)O}\right]_n \bullet (x\text{-}y) \; \text{AlMe}_3 \; + \; y \; \text{AlMe}_3$$

"associated"   "free"
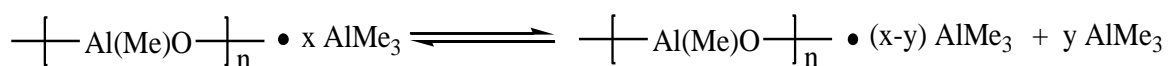
Figure 2.8 Types of TMA in MAO solution
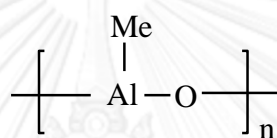
Linear structure
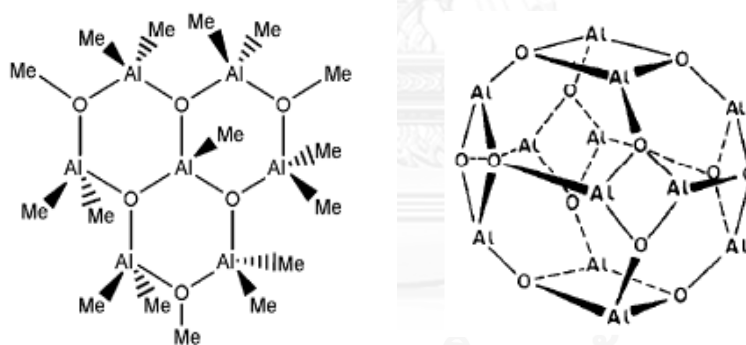
Cyclic structure

Figure 2.9 Examples of methylalumoxane structure proposed in general [53]

However, MAO has some drawbacks that conventional MAO has very low solubility in aliphatic solvents as well as poor storage stability in solution. To overcome these drawbacks, MAO can be modified. Commercial modified methylaluminoxane (MMAO) can be synthesized via the controlled reaction of trimethylaluminum (TMA) and triisobutylaluminum (TIBA) with water resulting in some methyl groups of MAO replaced by isobutyl groups. MMAO can improve solubility in aliphatic hydrocarbon

together with solution storage stability [56]. MMAO solution contains two types of residual alkylaluminum; free TMA and free TIBA. Hagimoto et al. [57] studied the additive effect of trialkylaluminiums in a chelating (diamide)dimethyltitanium complex ([ArN(CH$_2$)$_3$NAr]TiMe$_2$) with metal-oxide supported MMAO system. They found that when trialkylaluminiums were presented, the catalytic activity and the molecular weight of produced polymer were slightly lower than that of the corresponding MMAO/SiO$_2$ system due to a small amount of trialkylaluminium hindered the initiation reaction. Moreover, free alkylaluminum may promote chain transfer reaction during the polymerization; consequently the removal of free alkylaluminums should be required. The simple method for removing free alkylaluminums is evaporation of solvent in MAO or MMAO followed by washing with new solvent such as heptane and toluene. The resulting product is a white solid referred to dried MAO and dried MMAO [56]. Another method for removing free alkylaluminums is the chemical modification with diol such as *p*-hydroquinone under methane evolving [58,59] and 2,6-di-tert-butylphenol (*t*-Bu$_2$Ph-OH) [60].

The MAO modification by evacuation was investigated [61]. The results revealed that dried methylaluminoxane (dMAO) which was free of TMA, was more active than the standard MAO system, resulting in a steady polymerization rate and giving higher molecular weight of polypropylenes. Furthermore, the influences of trialkylaluminum addition on the dried MAO system were studied. It was found that the polymer yields were increased by the addition of triisobutylaluminum and trioctylaluminum, while the yields were decreased by trimethylaluminum and triethylaluminum.

In addition, there are other types of cocatalyst used to activate metallocene catalyst; borane [B(C$_6$F$_5$)$_3$], borate [(Ph$_3$C)B(C$_6$F$_5$)$_4$], and triethylaluminum (TEA). they also have been studied in the literature. For example, Intaragamjon [62] studied the effect of cocatalysts including methylaluminoxane (MAO), modified-methylalumonoxane (MMAO), dried-methylaluminoxane (dMAO), dried-modified-methylalumonoxane (dMMAO), borane (B(C$_6$F$_5$)$_3$), and borate (Ph$_3$CB(C$_6$F$_5$)$_4$) on ethylene polymerization and ethylene/1-hexene copolymerization with Me$_2$Si(η^3-

$C_{13}H_8)(\eta^1$-N^{t}Bu)TiMe$_2$ catalyst . They found that dMAO and dMMAO showed the highest activities in all types of polymerization attributed to less free alkylaluminum. The presence of TMA can promote chain transfer reaction and large amount of TMA can reduced Ti(IV) species to inactive lower vacant species.

2.4 Polymerization mechanisms

The olefin polymerization mechanisms by metallocene catalysts have been investigated in several experiments and theoretical studies [1,12,35]. Normally, polymerization mechanism with metallocene catalyst consists of three steps; initiation, propagation and termination.

For initiation step, it is generally accepted that the formation of cationic active species on metallocene catalyst is accomplished through alkylation of the metallocene by cocatalyst (generally MAO) resulting in the chloride ligands displacement. Then, the cocatalyst abstracts a methyl group from metal atom in metallocene catalyst, which generates the cationic metallocene species and weakly coordinated anion. These species are the active species for polymerization. The mechanism in this step is shown in **Figure 2.10**.
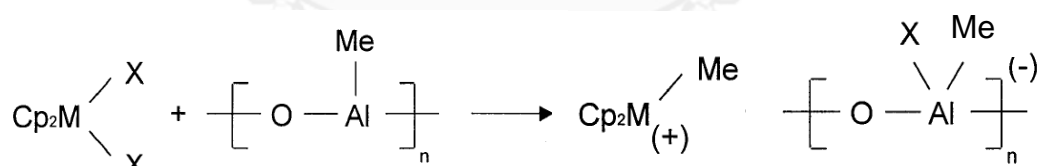
Figure 2.10 The active site formation of metallocene catalyst [65]

The mechanism of polymer chain propagation proceeds by coordination and insertion of monomer unit in the cationic active site. The monomer coordinates with highly electrophilic and coordinatively cationic complex. A four member transition state forms in this step. The stained four member transition state allows for the breaking of bond between metal atom and polymer chain (if this is the first monomer insertion, it is the breaking of a metal atom-methyl group bond), and a bond between monomer and metal atom as well as between monomer and polymer chain form. These lead to

the polymer chain growth by one monomer unit and a new vacant site formation which allows another monomer addition until polymer chain termination occurs. The mechanism in the propagation step is presented in **Figure 2.11**.
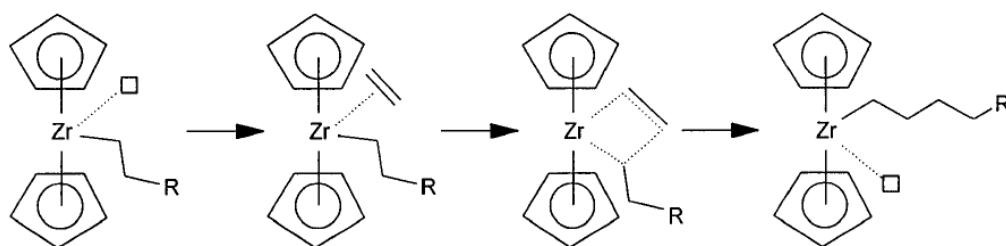
Figure 2.11 Propagation mechanism [65]

Chain termination reaction on olefin polymerization with metallocene catalyst occurs through the several reactions such as chain transfer by β-hydride elimination, chain transfer by β-alkyl elimination, chain transfer to monomer, chain transfer to aluminum and chain transfer to hydrogen. These chain transfer reactions are demonstrated in **Figure 2.12**. The relative importance of the different chain transfer reactions depends on the nature of the metallocene catalyst as well as the cocatalyst used and on the polymerization conditions [63,64]. Chain transfer by β-alkyl elimination can form the dead polymer chain with vinyl end groups, although much less common than β-hydride elimination. For chain transfer to monomer, after π-bond of the monomer opens, monomer coordinates with the active site and with the β-hydride of a growing polymer chain. Thus, this β-hydride is transferred to the approaching monomer. The first three chain transfer reactions form the dead polymer chain terminal double bonds.

a) β-hydride elimination
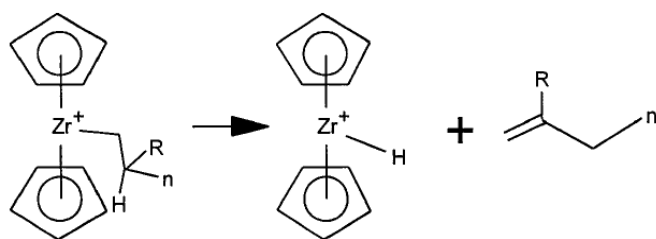
b) β-alkyl elimination
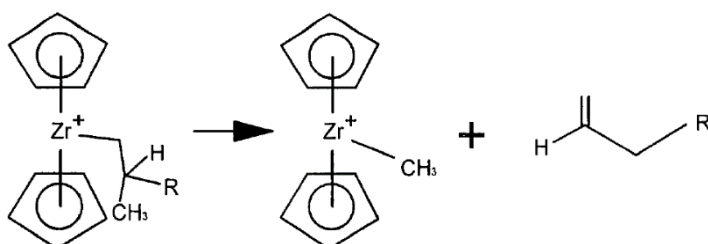
c) Chain transfer to monomer
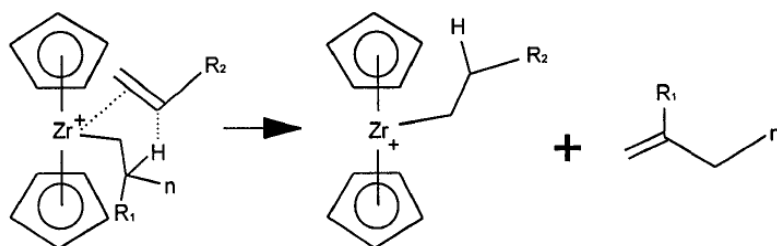
d) Chain transfer to aluminum
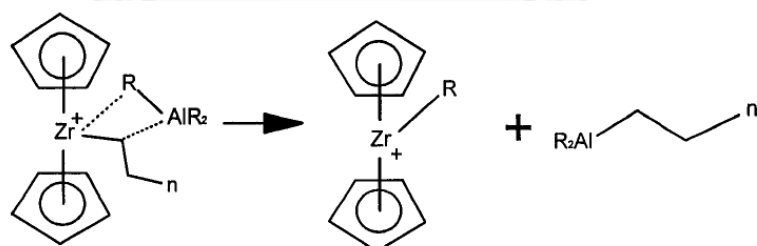
e) Chain transfer to hydrogen
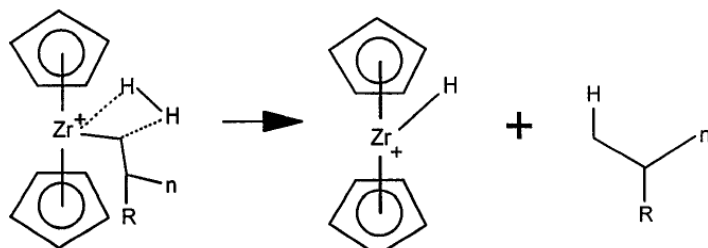
Figure 2.12 Chain transfer reactions [65]

Chain transfer to aluminum is transferred from alkyl group in cocatalyst to the cationic active center and the -AlR$_2$ is attached to the polymer chain. The bond between $-$AlR$_2$ and polymer chain can be removed by the addition of acidic methanol. Last but not least, it is chain transfer to hydrogen. Hydrogen is a common agent used to control the molecular weight of olefin polymerizations. A hydrogen molecule inserts to the growing polymer chain resulting in a dead polymer chain [12,64].

2.5 Living polymerization

Since the discovery of the metallocene catalysts for olefins polymerizations, one of the interesting fields developed by these catalysts is living polymerization. Metallocene catalysts allow us to conduct living polymerization at low temperature by suppressing chain transfer reactions such as β-hydride elimination [66]. Living polymerizations can produce polymers with predictable molecular weights and with narrow molecular weight distribution. These processes are useful for synthesis of terminally-functionalized polymers and block copolymers. However, living polymerization is not an efficient method for high polymer production volume because one active site produces only one polymer chain. There are very few reports of living polymerization by conventional metallocene catalysts [67]. The postmetallocene catalysts, such as constrained geometry catalysts, α-diimine chelate catalysts, phenoxy–imine chelate catalysts, offer the greatest potential for producing living and stereoselective polymerizations [68-71]. Some of metallocene catalysts for living olefin polymerization at low temperature are illustrated in **Figure 2.13**.
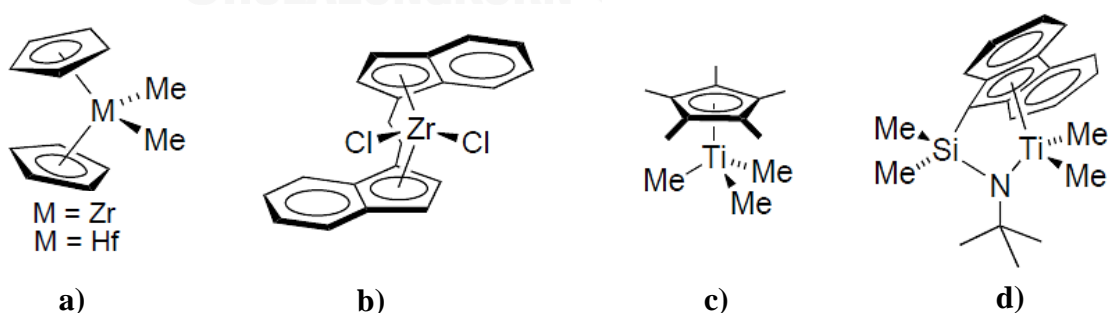
Figure 2.13 Metallocene catalysts for living olefin polymerization [67]

In an ideal living polymerization, all the active species simultaneously initiate the polymerization, with the rate constant for initiation greater than that for propagation as well as with neither chain transfer reactions nor termination reactions. Under these conditions, the polymers with very narrow molecular weight distribution ($M_w/M_n \sim 1$) are produced. There are seven basic accepted for living polymerization as follows [67]:

1) Polymerization proceeds to complete monomer conversion, and polymer chain growth continues upon further monomer addition.
2) Number average molecular weight (M_n) of polymer produced increases linearly with conversion.
3) Due to neither chain transfer nor deactivation, the number of active site remains constant during polymerization time.
4) Molecular weight of polymer can be predicted and be controlled.
5) The polymers with narrow molecular weight distribution ($M_w/M_n \sim 1$) are produced.
6) The living polymerization is useful for synthesis of block copolymer by sequential monomer addition.
7) It is also used to synthesize end-functionalized polymer.

The polymerization mechanisms with metallocene catalysts as mention in 2.4, monomer inserts to the active site. The polymer chain growth continues until chain transfer and chain termination reactions occur. If alkylaluminum is used as cocatalyst in the polymerization system, it can promote the occurring of chain transfer to the aluminum. Many investigations reveal the ways to reduce rate of chain transfer and chain termination reactions such that living behavior can be achieved. The simple method to accomplish living is a decrease of polymerization temperature in order to suppress chain transfer reaction [68]. Hagihara et al. [69] have reported $Me_2Si(\eta^3\text{-}C_{13}H_8)(\eta^1\text{-}N^tBu)TiMe_2$ catalyst activated with $B(C_6F_5)_3$ on polymerization proceeded in a living manner at -50 °C, and syndiotactic-rich polymer was obtained. However, deactivation occurred at 0 °C or at -50 °C when $Ph_3CB(C_6F_5)_4$ was used in place of $B(C_6F_5)_3$. Thus, the living nature of the $Me_2Si(\eta^3\text{-}C_{13}H_8)(\eta^1\text{-}N^tBu)TiMe_2$ catalyst

depended on polymerization temperature and cocatalyst. Hasan et al. [70] revealed that living polymerization of propylene proceeded at 0 °C with $Me_2Si(\eta^3\text{-}C_{13}H_8)(\eta^1\text{-}N^tBu)TiMe_2$ catalyst in combination with dried MAO as a cocatalyst, which was free from TMA. These results suggest that dried MAO able to be a cocatalyst for the living polymerization with the constrained geometry catalyst.

However, low polymerization temperature is the obstacle to occur living behavior due to precipitation of polymer. Thus, other ways has been reported such as modification of catalyst structure [72]. Another method to accomplish the living behavior focused on the synthesis of effective catalyst for occurring the living system at room temperature or higher. Camacho et al. [71] synthesized a cyclophane based Ni(II)-α-diimine complex which is highly active and robust catalyst for ethylene polymerization at high temperature. They studied the living polymerizations of propylene and 1-hexene using this catalyst together with MMAO as a cocatalyst at high temperatures. The results show that this catalyst system can achieve in living polymerization of propylene and 1-hexene at about 50-75 °C, that is higher than ambient temperature, because of the unusual cyclophane ligand framework.

The last method to succeed the living manner is to eliminate the use of alkyl aluminum causing chain transfer reaction in polymerization system. There is the development of weakly coordinating anions which made significant in living olefin polymerization possible [73].

2.5.1   Principal kinetics of living polymerization

One of the important features of living polymerization is its simple kinetics. Since neither chain transfer nor deactivation occurs in living system, the number of polymer chain (N) is equal to the number of active site (C^*), and the number average molecular weight (M_n) directly reflects the propagation rate. Based on the simple kinetic of living, we can investigate how the polymerization proceeds on the active sites formed by reaction between catalyst and cocatalyst and on the propagation rate according to the equation mentioned below.

Based on Natta equation [74].

$$\overline{M}_n = M_0 \cdot \frac{k_p \cdot [\mathrm{M}] \cdot t}{1 + k_{tr} \cdot t} \qquad (2.1)$$

$$\mathrm{Y} = k_p \cdot [\mathrm{M}] \cdot [C*] \cdot t \qquad (2.2)$$

Combining Equations 1 and 2 we obtain

$$\frac{1}{\overline{P}_n} = \frac{M_0}{\overline{M}_n} = \frac{k_{tr}}{k_p \cdot [M]} + \frac{1}{k_p \cdot [M]} \cdot \frac{1}{t} \qquad (2.3)$$

For the living polymerization, $k_{tr} \cong 0$, we obtain

$$\frac{\overline{M}_n}{M_0} = k_p [M] t \qquad (2.4)$$

And $\qquad [C*] = \dfrac{\mathrm{Y}[M_0]}{\overline{M}_n} = [N] \qquad (2.5)$

where

$\overline{M}_n$	=	number average molecular weight of the polymer
M_0	=	molecular weight of the monomer (g/mol)
[M]	=	monomer concentration
t	=	polymerization time
k_{tr}	=	chain transfer rate constant
k_p	=	propagation rate constant
Y	=	polymer yield
[$C*$]	=	number of active site
[N]	=	number of polymer chain

2.6 Heterogeneous single-site catalyst

In olefin production with traditional Ziegler-Natta catalysts currently use supported catalysts (heterogeneous) in slurry- and gas-phase processes. Replacement of the traditional Ziegler-Natta catalyst by a metallocene catalyst in the commercial processes should be accomplished by drop-in technology, which the existing polymerization processes are essentially unchanged except for using a different catalysts and adjusting processes conditions. Moreover, non-supported catalysts (homogeneous) produce fine particles of polymer (low bulk density) bringing about deposition of polymers on the walls and components of the reactor, commonly referred to reactor fouling [12]. Supported metallocene catalysts have the advantages including producing polymer particles with desired morphology, avoiding reactor fouling, lower Al/metal mole ratios required to obtain the maximum activities and improved stability of the catalyst due to much slower deactivation by bimolecular catalyst interactions [12,75,76]. Therefore, it is necessary to anchor the metallocene catalysts on the support.

2.6.1   Supported metallocene catalyst methods

Different methods have been studied for obtaining supported metallocene catalysts. The methods differ in the sequence used for reaction of support, catalyst and cocatalyst. There are three main methods for heterogenization of metallocene catalysts [76-78].

i) The metallocene or a mixture of the metallocene and MAO is anchored via physisorption or chemisorption onto the support (direct heterogenization). In the first case, the metallocene must be activated by external MAO.

ii) The metallocene catalyst is supported via covalent bonds between its ligand and the support followed by activated with external MAO. When a reaction between the surface hydroxyl groups and the metallocenes, multiple types of active sites are often formed, removing the single-sited nature of the system which is the possible drawback of these methods [79].

iii) The supporting cocatalyst first is the most commonly used method. Support is treated with cocatalyst followed by addition of the metallocene catalyst to produce the supported metallocene species (indirect heterogenization) which leads to an effective catalyst.

2.6.2 Replication and polymer morphology

Starting from the discovery of metallocene catalysts, many investigations on the catalysts made a continuous and very good progress in terms of yields achievable. However, another important fact in the technological and commercial developments was not just increase in the catalytic activity. It has been the capability of ideal catalyst to reduce the process constraints to zero. Thus, the complete control of the polymer granule should be highly desirable in olefins production in because of process economics and viability. A regular particle, which is particle with high density, regular shape and narrow particle size distribution, means good flowability and packing and even no need of further pelletization. The spherical form is the most attractive because the best to increase the flowability of polymers during processing, catalysts with controlled spherical morphology were developed allowing the full control of particle size and porosity of the related form polymers.

After polymerization starts at the primary particles surface, the particle is disrupted. The polymer is then growth around particle fragment eventually very compact. This means that the morphology of the catalyst particle could be replicated in the final polymer as the particle growth takes place during the polymerization [78,80] as exhibited in **Figure 2.14**. Steinmetz et al. [80] examined the particle growth of polypropylene made with a supported metallocene catalyst using scanning electron microscopy (SEM). They noticed formation of a polymer layer only on the outer surface of catalyst particles during the initial induction period. As the polymerization continued, the whole particle was filled with polymer. Particle fragmentation pattern depended on the type of supported metallocene.
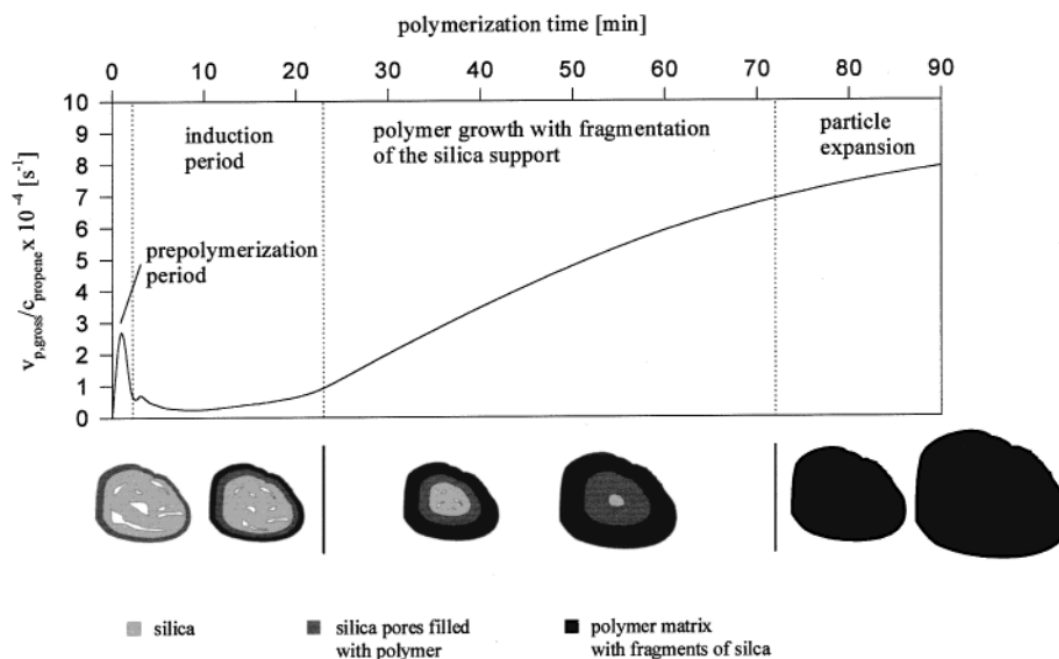
Figure 2.14 Scheme of polymer particle growth model [78]

2.6.3 Zirconia support

A great category of inorganic supports for immobilizing single-site metallocene catalysts has been studied [82]. The chemical properties of the support play an important role for anchoring the metallocene catalysis. This is because the interaction of catalyst with the support is importance for determination of the leaching possibility [75]. Recently, zirconia has been employed as catalyst and support due to its interesting chemical properties such as acidity, basicity, reducing or oxidizing ability [83]. Zirconia was used as a support for olefins polymerization in many academic researches which presented the interesting results.

Pothirat et al. [21] studied the efficiency of zirconia supported MAO as a cocatalyst with *rac*-Et(Ind)$_2$-ZrCl$_2$ catalyst for ethylene/α-olefins copolymerization, compared to the conventional silica. The results showed that the use of zirconia exhibited higher productivity than that of the conventional silica.

Jongsomjit et al. [85] studied the synthesis of linear low-density polyethylene (LLDPE)/ZrO_2 nanocomposites via *in-situ* polymerization with *rac*-Et(Ind)$_2$ZrCl$_2$/MAO catalyst. The nano-ZrO_2 filler exhibited good distribution and dispersion inside the polymer matrix. However, the melting temperature (T_m) and crystallization temperature (T_c) were found to slightly decrease with the addition of nano-ZrO_2 filler due to decreased crystallinity of polymer. Moreover, Jongsomjit [86] continue to investigate the use of the nano-SiO_2 and nano-ZrO_2 as the fillers for ethylene/1-octene with zirconocene/MAO catalyst. They found that when the nano-ZrO_2 filler was used, the copolymers productivity more increased than that employing nano-SiO_2 filler. Random copolymers were produced in both filler types.

2.6.4 Synthesis of zirconia

Zirconia can be synthesized by mean of several methods such as co-precipitation, sol-gel and solvothermal methods [87]. Particularly, solvothermal method can proceed at low reaction temperatures and no require post annealing treatments. Furthermore, solvothermal method allowed us to synthesize metal oxide with smaller particle, larger surface area, higher crystallinity and thermal stability than those obtained from other methods. This method was improved from the hydrothermal method except that organic solvents are used instead of water as the reaction medium. Solvothermal method is useful for controlling particle size and particle morphology by reaction conditions including temperature, pressure, solvent nature and aging time.

Wongmaneenil et al. [88] revealed the effects of solvents on morphology and other characteristics of zirconia and studied their performance for tungstated zirconia catalyst. Solvothermal reaction of zirconium(IV) *n*-butoxide in different solvent media such as 1,3-pentanediol, 1,4-butanediol, 1,5-pentanediol and 1,6-hexanediol resulted in the formation of zirconium dioxide (ZrO_2) nanostructure. The experimental results showed that the ZrO_2 particles prepared in 1,4-butanediol have a spherical shape, while in other glycols the samples were irregularly-shaped particles. Moreover, the zirconia prepared in 1,4-butanediol presented the highest activity in the esterification reaction of acetic acid and methanol attributed to its higher acidity.

2.7 Modification of support

The major advantages of heterogeneous system are producing the desired polymer morphology and avoiding reactor fouling with finely dispersed swelling polymers. On the other hand, this system still has several disadvantages. The heterogeneous metallocene catalysts generally have lower activity than homogeneous metallocene catalysts. This is widely attributed not only to limitation of monomer diffusion into active sites interior support pores, but may also be steric hindrance by the support resulting in fewer active sites for the heterogeneous catalyst. Catalyst active sites are probably deactivated during impregnation procedure. Starting from such viewpoints, some modifications of support or polymerization systems are usually required. Many studies have reported that the impregnation of metallocene catalyst or cocatalyst through modified surface support, such as thermal and chemical treatments, can improve the catalytic performance of heterogeneous system [16].

Most researchers reviewed that treating the support surface with hydrophobic functional groups such as aryl, alkyl, and silane can improve the catalytic behavior. Especially, the use of the silicon compound, which acted as spacer, was widely investigated for catalytic activity enhancement. Galland et al. [23] studied the results of grafting $(n\text{BuCp})_2\text{ZrCl}_2$ on silica modified with different spacer for ethylene/1-hexene copolymerization and compared their performance to the homogenous catalyst. Silica supports were modified with polymethylhydrosiloxane (PMHS), chlorotrimethylsilane (Me_3SiCl), chlorotrimethylsilane (Ph_3SiOH), tin(IV) chloride (SnCl_4), isodrin and aldrin. The $(n\text{BuCp})_2\text{ZrCl}_2$ grafted on PMHS-modified silica afforded the highest activity among spacer used. PMHS-modified silica exhibited catalyst activity which was the half of that of the homogeneous system, indicating a potential approach to increasing catalyst activity of supported metallocenes. Lee et al. [24] investigated the effect of silica modified with trisiloxane spacer (ZATS) and pentamethylene spacer (ZAPM) supported Cp[Ind]ZrCl$_2$ in combination with modified methylaluminoxane on ethylene polymerization. The silica supports modified with ZATS and ZAPM gave polyethylene with lower molecular weight but showed higher activity than unmodified silica. Therefore, it can conclude that the activity of silica

supported Cp[Ind]ZrCl$_2$ can enhance by introducing a spacer between silica surface and metallocene species. Jongsomjit et al. [26] employed SiCl$_4$-modified silica/MAO-supported Et[Ind]$_2$ZrCl$_2$ metallocene catalyst for ethylene/α-olefins copolymerization. The activities can be improved by using silane-modified silica/MAO system. However, the effect of silane on activity is diminished with higher α-olefin copolymerization (1-octene and 1-decene) due to effects of the longer chain insertion. The molecular weights and molecular weight distribution of copolymers decrease with the silane modification.

Moreover, some researchers accentuated that the increased surface acidity by a coordination of support surface with Lewis acid may play the significant role in the improvement of the polymerization activity in heterogeneous catalysts. The results of α-Diimine nickel(II) catalyst covalently linked to silica support on ethylene polymerization were revealed by Schrekker et al. [89]. Grace Davison SP9-496 silica supports were modified with the linkers including trimethylaluminum (TMA), tetrachlorosilane (SiCl$_4$), and trichloroborane (BCl$_3$) followed by covalent attachment of α-Diimine nickel(II) catalyst to the linkers of silica. Upon the modification of the linker on silica, TMA released methane while SiCl$_4$ and BCl$_3$ released HCl. The polymerizations were carried out in 100 mL of pentane at 150 psig of ethylene for 2 h. The results showed that TMA, SiCl$_4$, and BCl$_3$ were identified as efficient linkers, with TMA as the preferred one. These supported catalysts had no reactor fouling. Barbotin et al. [90] investigated the influence of the modified silica supported series of neodymium complexes on butadiene polymerization. The silica was modified with Lewis acids including BCl$_3$, AlCl$_3$, TiCl$_4$, ZrCl$_4$, SnCl$_4$, SbCl$_5$ and HfCl$_4$. The results revealed that all of modified silica supported catalysts presented active and highly stereospecific for butadiene polymerization, especially BCl$_3$ modification on silica, showed the most efficient. Jiamwijitkul et al. [91] studied the effects of boron modification on the MCM-41-supported dMMAO/zirconocene catalyst during copolymerization of ethylene with 1-octene. The enhanced catalytic activity achieved via the boron modification. This is probably because boron acted as a spacer between the support and dMMAO leading to lower interaction. However, the activity slightly decreased with large amounts of boron loading due to the migration of dMMAO into boron layer resulting in less surface concentration of [Al]$_{dMMAO}$. The boron

modification rendered narrower molecular weight distribution suggesting more uniform catalytic site.

There is another way except support modifications to improve activity of heterogeneous system. It has been reported that employing chemically modified MAO with aliphatic or aromatic diols as the cross-linking agent under methane evolving to form three-dimensional lattice of MAO had been greatly improved the Al content on support and the catalytic activity. Guan et al. [32] developed a novel spherical $MgCl_2$-supported MAO cocatalyst. The addition of cross-linking agents, namely glycol, glycerol and triethanolamine, during the impregnation of MAO on the support led to an increase in Al contents on the support surface from 3.8 to 9–12 wt%. The catalytic activity in ethylene polymerization increased with increasing amounts of Al. The highest activity in ethylene polymerization was achieved in the case of using glycerol as a cross-linking agent.

CHAPTER III

EXPERIMENTAL

In this chapter, equipment used in these experiments, chemicals used with each method, synthesis of support, synthesis of catalyst, catalyst precursor preparations, polymerization procedures as well as characterizations are specified as follows.

3.1 Equipment

The major equipment used in this research are compiled the following.

3.1.1 Schlenk line

Schlenk line was used to protect oxygen and moisture in all operations. It consists of nitrogen gas line and vacuum line with several stopcocks. Nitrogen gas line was vented through an oil bubbler, while solvent vapors or gas from evacuation was trapped by liquid nitrogen cold trap to prevent contaminating the vacuum pump. The Schlenk line is shown in **Figure 3.1**.
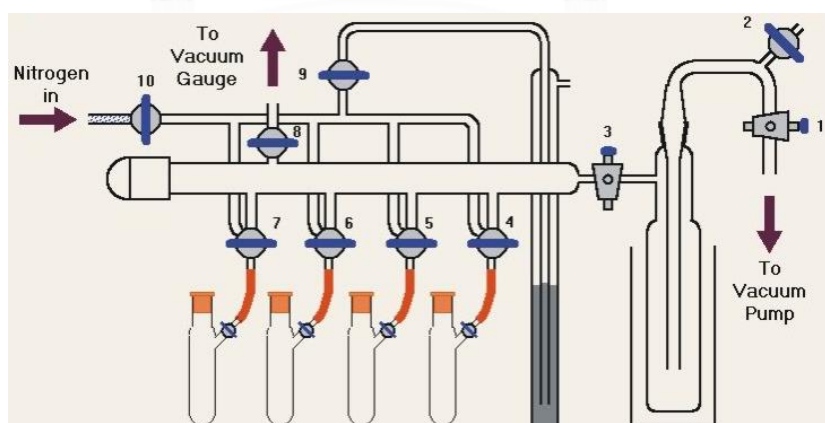
Figure 3.1 Schlenk line

3.1.2 Gas supply

All chemicals and polymerizations were manipulated under nitrogen atmosphere. Nitrogen gas was flowed through Schlenk line without purification.

3.1.3 Distillation systems

Distillation system has two methods as described below.

1) Solvent was distilled over sodium under nitrogen atmosphere for 6 h prior to use.

2) Comonomer was purified by stirring over calcium hydride (CaH_2) under nitrogen atmosphere overnight at room temperature, and then distilled prior to use.

3.1.4 Polymerization reactor

A 100 mL glass flask consisting of two necks which one neck was connected to three-ways glass valve while the other was closed with glass cock equipped with a magnetic stirrer was used as the polymerization reactor under atmospheric pressure gas.

3.1.5 Vacuum pump

One line of schlenk line was connected to vacuum pump for evacuating solvent or gas from operations. A pressure of 0.5 kPa was sufficient for vacuum system.

3.1.6 Centrifuge

Centrifuge was used to separate solid phase and liquid phase of mixture for synthesis of spherical zirconia, synthesis of catalyst and catalyst precursor preparations. Moreover, centrifuge tubes for the catalyst preparation and the catalyst precursor preparations were performed under nitrogen atmosphere.

3.2 Synthesis of *tert*-[butyl(dimethylfluorenylsilyl) amido]dimethyl titanium

3.2.1 Chemicals

The chemicals manipulated for synthesis of *tert*-[butyl(dimethylfluorenylsilyl) amido]dimethyl titanium ($Me_2Si(\eta^3\text{-}C_{13}H_8)(\eta^1\text{-}N^tBu)TiMe_2$) are shown in **Table 3.1**.

Table 3.1 The chemicals used for synthesis of the $Me_2Si(\eta^3\text{-}C_{13}H_8)(\eta^1\text{-}N^tBu)TiMe_2$

Chemical	Supplier	Purification
Fluorene	Tokyo Chemical Industry Co., Ltd.	Used as received
Dichrolodimethylsilane ($SiMe_2Cl_2$)	Tokyo Chemical Industry Co., Ltd.	Used as received
n-Buthyl lithium (*n*-BuLi)	Kanto Chemical Co., Inc.	Used as received
Methyl lithium (MeLi)	Kanto Chemical Co., Inc.	Used as received
tert-Butylamine (*t*-BuNH$_2$)	Aldrich Chemical company, Inc.	Used as received
Methyl magnesiumbromide (MeMgBr)	Aldrich Chemical company, Inc.	Used as received
Titanium (IV) chloride (TiCl$_4$)	Wako	Used as received
Diethylether (Et$_2$O)	Kanto Chemical Co., Inc.	Distilled
Tetrahydrofuoran (THF)	Kanto Chemical Co., Inc.	Distilled
Hexane	Kanto Chemical Co., Inc.	Dried over molecular sieve
Nitrogen gas	Iwatani Industrial Gases	Used as received

3.2.2 Synthesis procedure
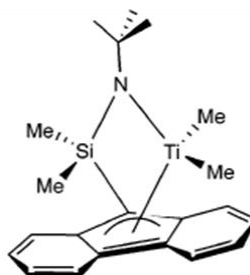
Figure 3.2 Structure of Me$_2$Si(η^3-C$_{13}$H$_8$)(η^1-N^{t}Bu)TiMe$_2$

The constrained geometry catalyst employed in this research was *tert*-[butyl(dimethylfluorenylsilyl) amido]dimethyl titanium. The structure is shown in **Figure 3.2**. The Me$_2$Si(η^3-C$_{13}$H$_8$)(η^1-N^{t}Bu)TiMe$_2$ catalyst was synthesized according to previous procedure reported by Nishii K. [52] which the synthetic procedure is shown in **Figure 3.3**.
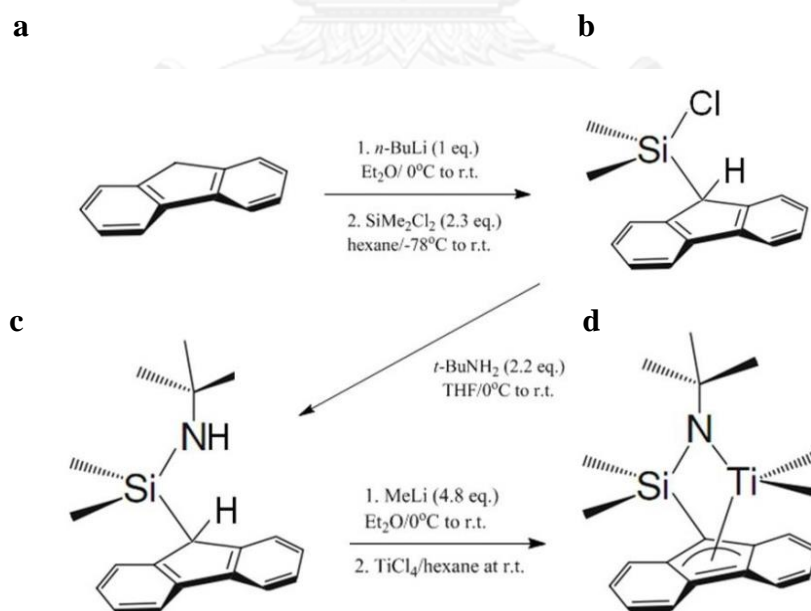
Figure 3.3 The pathway for Me$_2$Si(η^3-C$_{13}$H$_8$)(η^1-N^{t}Bu)TiMe$_2$ synthesis

3.2.2.1 Synthesis of ligand

First, 5 g of fluorene (30 mmol) was suspended in 60 ml of Et_2O and then this reactor was kept at $0°C$ using ice bath. Next, 30 mmol of *n*-BuLi was slowly added. After the mixture was stirred for 3 h at room temperature, solvent was removed under vacuum to give Li[Flu]. The suspension of Li[Flu] in Et_2O was gradually transferred to the solution of excess $SiMe_2Cl_2$ in hexane (40 ml) at $-78°C$. After stirring overnight at room temperature, the solvent and unreacted $SiMe_2Cl_2$ was removed under vacuum followed by the addition of 150 ml of hexane into precipitate lithium chloride salt (LiCl). After that, clear solution was decanted to another reactor, and then the solvent was evacuated to give 9-(chlorodimethylsilyl)fluorene as white solid. Next, the solution of white solid in THF was reacted with *t*-BuNH$_2$ (55 mmol) at $0°C$ followed by stirring for 5 h at room temperature to occur lithium chloride precipitation. Then, yellow-clear solution was transferred to another reactor and the solvent was removed under vacuum to obtain $Me_2Si(\eta^3\text{-}C_{13}H_8)(\eta^1\text{-}N^tBu)$ ligand (**Figure 3.3a – 3.3c**).

3.2.2.2 Synthesis of catalyst

The solution of 5 mmol of ligand in Et_2O was reacted with excess MeLi at $0°C$. After stirring the reaction at room temperature for 5 h, this resultant was transferred to the solution of TiCl$_4$ (5 mmol) in 50 ml of hexane. Then, the mixture was stirred for 1 h to give dark brown suspension. After evaporation of the solvent, 100 ml of hexane was injected into the residual solid. The decanted solution was reacted with MeMgBr (10 mmol), and then the mixture was stirred for 1 h. Next, the solvent was removed under vacuum followed by adding of hexane into the resulting solid. Then, the red brown solution was separated to another reactor followed by concentrated. The result was kept overnight at $-30°C$. Red-orange crystal was then obtained (**Figure 3.3d**).

3.3 Synthesis of spherical zirconia supports via solvothermal method

3.3.1 Chemicals

The chemicals applied to synthesize the spherical zirconia are shown in **Table 3.2**.

Table 3.2 The chemicals applied to synthesis of the spherical zirconia

Chemical	Supplier	Purification
Zircronium (IV) n-butoxide (ZNB) 80 wt% solution in 1-butanol	Aldrich Chemical company, Inc.	Used as received
1,4-Butainediol	Aldrich Chemical company, Inc.	Used as received
Methanol	Aldrich Chemical company, Inc.	Used as received

3.3.2 Synthesis procedure

Spherical zirconia was synthesized according to synthetic method reported by Wongmaneenil et al.[88]. Zircronium (IV) n-butoxide (35 g) was suspended in 100 mL of 1,4 butainediol in the inner tube. This tube was put in the outer tube contained with 30 mL of 1,4-butainediol. After entered these tubes in autoclave, it was purged with N_2 and kept under vacuum. Then, it was heated to 300 °C at heating rate 2.5 °C/min followed by keeping the reaction at this temperature for 2 h. After that, the autoclave was cooled down to room temperature. Next, solid part was washed with methanol 5 times and dried at 100°C overnight to obtain white powder of spherical zirconia. The scheme of instrument for spherical zirconia synthesis is shown in **Figure 3.4**.
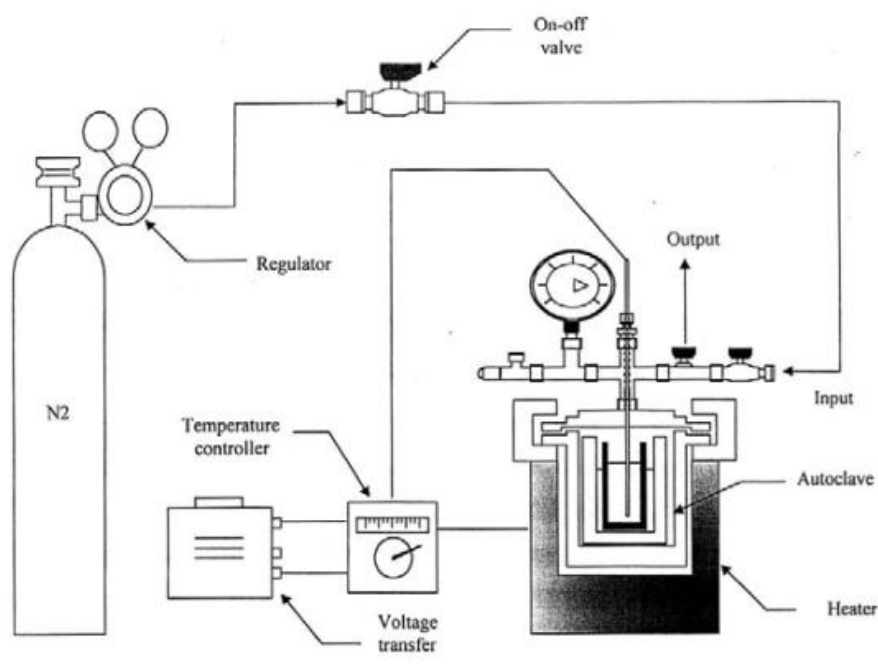
Figure 3.4 The instruments for spherical zirconia synthesis

3.4 Preparation of metal oxides supported cocatalysts

3.4.1 Chemicals

The chemicals were employed in this procedure as mentioned in **Table 3.3**.

Table 3.3 The chemicals used for preparation of metal oxide supported cocatalysts

Chemical	Supplier	Purification
n-Buthyl lithium (*n*-BuLi)	Kanto Chemical Co., Inc.	Used as received
Sodium hydroxide (NaOH) 0.1 M (standard solution)	Aldrich Chemical company, Inc.	Used as received
Hydrochloric acid (HCl) 0.1 M (standard solution)	Aldrich Chemical company, Inc.	Used as received
Phenolphthalein	Aldrich Chemical company, Inc.	Used as received

Silica (grade P-10)	Fuji Silysia Chemical Ltd.	Calcined
Methylaluminoxane (MAO) 6.9% in toluene	Tosoh Finechem Co., Ltd.	Used as received
Modified- methylaluminoxane (MMAO) 6.5% in toluene	Tosoh Finechem Co., Ltd.	Used as received
Silicon tetrachloride 99%	Aldrich Chemical company, Inc.	Used as received
Boron trichloride (BCl_3) 1 M in hexane		Used as received
Glycerol ($\geq$ 99% v/v) reagent grade	Aldrich Chemical company, Inc.	Used as received
Toluene	Kanto Chemical Co., Inc.	Distilled
Hexane	Kanto Chemical Co., Inc.	Dried over molecular sieve

3.4.2 Analysis hydroxyl group on metal oxides

Metal oxides consisting of spherical zirconia and silica were calcined under argon at 400 °C for 6 h. The suspension of calcined support (0.5 g) in 20 mL of toluene was reacted with excess *n*-butyl lithium. After stirring at 60 °C for 5 h, the reaction was cooled down to room temperature, and then dried under vacuum. The obtained solid was washed with 20 mL of hexane seven times. For the last washing, the solid was dried under vacuum. Then, 0.1 g of the resulting solid was added with phenolphthalein as indicator followed by excess standard hydrochloric acid solution. This mixture was titrated with the standard sodium hydroxide solution. The titration results were calculated to find amount of hydroxyl group of the support.

3.4.3   Preparation of dried MMAO

The desired amount of MMAO was evaporated the solvent, and then it was washed with heptane seven times for removing TMA and TIBA in MMAO to obtain dried MMAO as white solid.

3.4.4   Immobilization of cocatalysts on supports

3.4.4.1 Preparation of metal oxides-supported cocatalysts

One gram of metal oxide was suspended in 20 mL of toluene followed by the addition of appropriate amount of MAO. After stirring the mixture at room temperature for 30 min, solvent was evaporated under vacuum. The activated zirconia was washed seven times with hexane followed by dried under vacuum for 6 h at room temperature. The metal oxide supported MMAO and dried-MMAO was prepared with similar procedure of MAO. The Al content on catalyst precursor was measured by ICP.

3.4.4.2 Preparation of BCl_3-mofified metal oxide-supported MAO

The desired amount of BCl_3 was added to 2 g of metal oxide in 50 mL of hexane. Then, the mixture was stirred for 1 h at room temperature. After evaporating solvent under vacuum, it was washed three times with 50 mL of toluene and finally dried under vacuum. The BCl_3-modified metal oxide was impregnated by MAO according to prior method.

3.4.4.3 Preparation of $SiCl_4$-mofified metal oxides-supported MAO

The suspension of calcined metal oxide (2 g) in 40 mL of toluene was reacted with desired amount of $SiCl_4$. After stirring 1 h at room temperature, the solvent was removed under vacuum. Next, the modified metal oxide was washed three times with toluene followed by dried under vacuum. The $SiCl_4$-modified metal oxide was treated with MAO as above-mentioned procedure.

3.4.4.4 Preparation of metal oxide with cross linking agent-supported MAO

The desired amount of MAO was reacted with 1 g of calcined metal oxide in 20 mL of toluene followed by adding suitable amount of glycerol. After stirring this mixture for 4 h at room temperature, toluene was eliminated by evacuation. Then, the resulting solid was washed three times with toluene followed by drying under vacuum at room temperature.

3.5 Polymerization procedures

3.5.1 Chemicals

The chemicals used polymerizations are displayed in **Table 3.4**.

Table 3.4 The chemicals used for polymerization procedures

Chemical	Supplier	Purification
rac-Et(Ind)ZrCl$_2$	Aldrich Chemical company, Inc.	Used as received
Ethylene	Sumitomo Seika Chemicals Co., Ltd.	Used as received
Propylene	Sumitomo Seika Chemicals Co., Ltd.	Used as received
1-hexene	Tokyo Chemical Industry Co., Ltd.,	Distilled
Toluene	Kanto Chemical Co., Inc.	Distilled
Methanol (purity 99.5%)	Kanto Chemical Co., Inc.	Used as received
Hydrochloric acid (35.37% conc.)	Kanto Chemical Co., Inc.	Used as received

Polymerization procedure was divided into three methods depending on each part of this research as follows.

3.5.2 Ethylene/1-hexene copolymerization at atmospheric pressure (Part 1)

The ethylene/1-hexene copolymerization was carried out in a 100 mL glass reactor equipped with a magnetic stirrer. In the reactor, the appropriate amount of catalyst precursor ($[Al]_{MAO}/[Zr]_{cat} = 1135$) was added, and the total volume was adjust to 30 mL with toluene. Then, 1-hexene was injected into the reactor. After that the mixture was saturated with atmospheric pressure of ethylene at the copolymerization temperature (70 °C). The solution of *rac*-Et(Ind)$_2$ZrCl$_2$ catalyst in toluene (5×10^{-5} M) was injected to start copolymerization. During the reaction, the ethylene pressure and the copolymerization temperature were kept constantly. The ethylene was delivered for a prescribed amount of time. The polymerization was terminated by stopping the ethylene pressure and adding with acidic methanol. The precipitated copolymer was filtrated followed by washing with methanol and drying under vacuum at 60 °C for 6 h.

3.5.3 Propylene polymerization at atmospheric pressure (Part 2 and 3)

Polymerization of propylene was conducted in a 100-mL glass reactor equipped with a magnetic stirrer. A certain amount of the supported cocatalyst was suspended in toluene whose volume was adjusted to a total volume of 30 mL. The toluene slurry was saturated with an atmospheric pressure of propylene. Polymerization was started by the addition of Me$_2$Si(η^3-C$_{13}$H$_8$)(η^1-N^{t}Bu)TiMe$_2$ in toluene (20 μmol in 1 mL). The polymerization was operated for a prescribed time under atmospheric pressure of propylene, and the rate of propylene consumption was monitored by a mass flow meter. The polymerization was terminated with acidic methanol. The resulting polymer was filtrated and dried under vacuum at 60 °C for 6 h.

3.5.4 Ethylene/1-hexene copolymerization at atmospheric pressure (Part 3)

Ethylene/1-hexene copolymerization was conducted by the same method with the propylene polymerization except the introduction of 1-hexene after the toluene slurry was saturated with an atmospheric pressure of ethylene.

3.6 Characterizations

3.6.1 X-ray diffraction (XRD)

The bulk crystalline phase and crystallite size of support was determined using the Siemens D-5000 X-ray diffractometer connected with a computer with Diffract ZT version 3.3 programs for fully control of the XRD analyzer. The characterization was performed with CuK_α radiation with Ni filter in the 2θ range of $20°$ to $80°$ degrees resolution $0.04°$. The crystallite size was computed from the Scherrer's equation.

3.6.2 N$_2$ physisorption

Micromeritics ASAP 2000 automated system was used to analyze the BET surface area, average pore diameter and pore volume of zirconia. The sample was determined under nitrogen gas physisorption.

3.6.3 Fourier transform infrared spectroscopy (FT-IR)

The powder samples for IR analysis were casted as thin films on NaCl disks under the protection from moisture and oxygen. The prepared samples were analyzed by Nicolet 6700 FTIR spectrometer with ATR mode. The spectra were collected in the scanning range from 400-4000 cm^{-1} with 100 numbers of scans at a resolution of 4 cm^{-1}. The FTIR spectra were recorded on ATI Mattson Infinity Series spectrometer.

3.6.4 Proton nuclear magnetic resonance spectroscopy (^{1}H NMR)

The structure of $Me_2Si(\eta^3\text{-}C_{13}H_8)(\eta^1\text{-}N^tBu)TiMe_2$ synthesized was confirmed with a BRUKER AVANCE II 400 spectrometer operating at 100 MHz with an acquisition time of 1.5 s and a delay time of 4 s. The samples were transferred to a NMR tube under N_2 atmosphere and dissolved in benzene-d_6 (C_6D_6) as solvent and the resonance of non-deuterated benzene was used as an internal reference (7.15 ppm).

3.6.5 ^{13}Carbon nuclear magnetic resonance spectroscopy (^{13}C NMR)

The comonomer incorporation in the copolymers and the stereoregularity of polypropylenes were determined by ^{13}C NMR. The ^{13}C NMR spectra were recorded using a JEOL GX 500 spectrometer at 130 °C. About 10000 scans were assembled in a pulse repeating of 4.0 s. The sample solution was prepared by dissolution of acquired polymer in 1,1,2,2 tetrachloroethane-d_2 as solvent and the resonance of the center peak of the solvent was used as an internal reference (74.47 ppm).

3.6.6 Inductively-coupled plasma (ICP)

The amounts of aluminum on the supported MAOs were analyzed by ICP using an iCAP 6500 DUO spectrometer. Standard solutions of aluminum from 5 to 30 ppm were prepared by diluting the standard solution purchased from Aldrich for the calibration curve. Approximately, 0.01 g of supported MAO was dissolved in 5 mL of hydrofluoric acid and stirred at room temperature. After the sample solution became clear, it was diluted exactly to 100 mL with deionized water to provide sample solution.

3.6.7 X-ray photoelectron spectroscopy (XPS)

The metal compositions on surface layer and the binding energy (BE) of the supported MAO were evaluated using the AMICUS photoelectron spectrometer and a KRATOS VISION 2 software. The experiment was carried out at 0.1 eV/step of resolution, 75 eV pass energy and the operating pressure approximately 1×10^{-6} Pa. The

sample was prepared in glove box and transferred to the XPS under an argon atmosphere.

3.6.8 Scanning electron microscope (SEM) and energy dispersive X-ray spectroscopy (EDX)

SEM of JEOL model JSM-5800LV was used to measure the morphological feature of support. The samples were coated with gold by means of ion sputtering before characterization. Moreover, the elemental distribution on cross-sectional surface of the supported MAO was investigated with the EDX using Link Isis series 300 program. For the cross-sectional particle prepared, the sample was casted with resin and sliced in the cross-section direction by microtome technique.

3.6.9 Thermogravimetric analysis (TGA)

The interaction force between $[Al]_{MAO}$ and surface of support was determined by TGA instrument SDT Q 600 analyzer. Approximately, 10 mg of the supported MAO were used for thermogravimetric analysis in the temperature range of 30-800 °C at a heating rate of 10 °C/min using N_2 UHP as a carrier gas.

3.6.10 Gel Permeation Chromatography (GPC)

The molecular weight and molecular weight distribution of polymer were determined by gel permeation chromatography with a PL 210 equipped with Shodex columns of HT-806M (x 2) and HT-803 (x 1) at 140 °C using *o*-dichlorobenzene (ODCB) as a solvent. The calibration curve was made with monodisperse polystyrene standards from 3000 to 3900000. The parameters for universal calibration were as follows: polystyrene, $K = 1.38 \times 10^{-4}$, $\alpha = 0.7$; polypropylene, $K = 1.03 \times 10^{-4}$, $\alpha = 0.78$; ethylene copolymer, $K = 4.77 \times 10^{-4}$, $\alpha = 0.70$. The sample solution was prepared by dissolving approximately 4 mg of polymer in 4 mL of ODCB.

CHAPTER IV

RESULTS AND DISCUSSION

The results and discussion are divided into three sections composing of the effect of spherical zirconia with various modifiers on ethylene/1-hexene copolymerization (section 4.1), the influence of cocatalysts on propylene polymerization (section 4.2) and the modification effect of spherical zirconia modified with $SiCl_4$ for heterogeneous single-site catalyst (section 4.3).

4.1 The effect of spherical zirconia with various modifiers on ethylene/1-hexene copolymerization

This part has been focused on the effect of the modified spherical zirconia with $SiCl_4$, BCl_3, and glycerol supported *rac*-Et(Ind)$_2$ZrCl$_2$/MAO catalyst on ethylene/1-hexene copolymerization in term of catalyst precursor properties, catalytic activity and copolymer properties.

4.1.1 Characteristics of catalyst precursors

The zirconia (ZrO_2) supports modified surface with three kinds of modifiers including boron trichloride (BCl_3), silicon tetrachloride ($SiCl_4$) and glycerol were used as carrier for zirconocene/MAO catalyst in the order to compare the catalytic activity with the unmodified zirconia. The polymer morphology strongly depends on the shape and structure of the support particle. Thus, it is necessary to employ the support with desired morphology. First, the zirconia synthesized according to mentioned procedure was characterized prior to impregnation with MAO by means of SEM and N_2 physisorption. The BET surface area, pore volume and average pore diameter were 160 $m^2{\cdot}g^{-1}$, 0.18 $mL{\cdot}g^{-1}$ and 2.84 nm, respectively. In addition, the morphology of the synthesized zirconia after calcination is presented in **Figure 4.1a)**. It exhibited spherical shape having micron size particles as seen in the previous research [88].
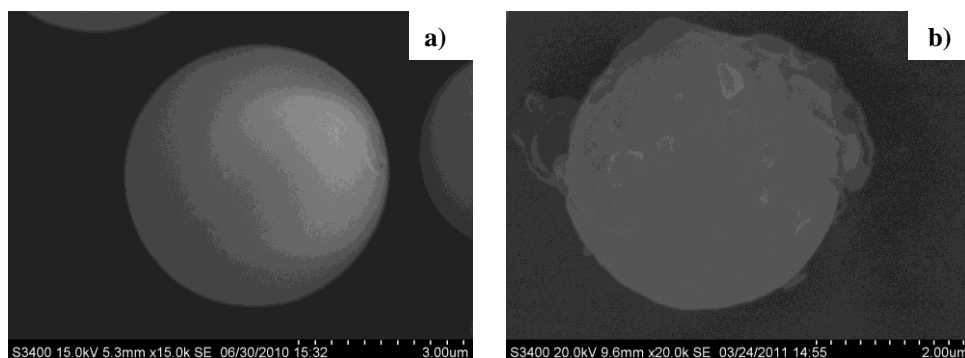
Figure 4.1 SEM micrographs of a) ZrO_2 and b) MAO/ZrO_2

The zirconia supports were modified surface followed by impregnation with MAO composing of MAO/ZrO_2, MAO/ZrO_2-BCl_3, MAO/ZrO_2-$SiCl_4$ and MAO/ZrO_2-glecerol. The morphology of the MAO/ZrO_2 is shown in **Figure 4.1b)**. The smooth surface of calcined zirconia became rough after the treatment with MAO as seen in **Figure 4.1b)**. The amount of Al supported on various supports was determined by ICP analysis as shown in **Table 4.1**. It can be seen that concentrations of Al in various supported systems are quite different probably owing to the different adsorption ability of each supported system. The Al contents on the modified zirconia supports were higher than that of the unmodified one, suggesting that the adsorption ability of zirconia can be improved by the modification with BCl_3, $SiCl_4$ and glycerol. Among the modified supported systems, the MAO/ZrO_2-glycerol exhibited the highest amount of Al. It can be mentioned that some MAOs were co-oligomerized through the hydroxyl groups of glycerol to form oligo-MAO as three dimensional lattices on zirconia resulting in enhancing amount of Al compared to the unmodified zirconia [32,59]. Furthermore, the elemental distributions within the modified and unmodified zirconia supported MAO were observed using EDX measurement after slicing of sample particles. The EDX mappings of the cross-sectioned particles of each supported system are illustrated in **Figure 4.2**. A large quantity of Al was dispersed over the outer surface of a zirconia support while a little amount of Al was diffused into pores inside particle in all supported systems. This was suggested that pore diameter and pore volume of the zirconia support were rather small. Therefore, MAO was difficultly diffused into pores. However, it can be seen that the MAO/ZrO_2-BCl_3 had more amounts of Al within

zirconia particle than other supported systems. In addition, the unmodified and modified zirconia supports after impregnated with MAO were still spherical morphology as the original one, which would benefit for good morphology of the polymer particle.

In order to investigate how the modification of zirconia affects on the MAO anchorage, the IR spectroscopy was conducted. The absorption bands at 700-800 cm^{-1} can be interpreted as -Al-O- structural units of MAO [32,92]. Moreover, the spectrum of the C-H stretching signal is located around 2900 cm^{-1} [93]. From Fig. 3, the spectra of all modified zirconia supported MAO systems did not much differ from the spectrum of the zirconia-supported MAO without modification. It is concluded that the modification did not change the structure of MAO adsorbed.

Table 4.1 Contents of Al in various supported systems determined by ICP

Supported system	Al content of supported MAO (mmol·g^{-1})
MAO/ZrO$_2$	2.55
MAO/ZrO$_2$-BCl$_3$	3.33
MAO/ZrO$_2$-SiCl$_4$	2.76
MAO/ZrO$_2$-glycerol	3.80
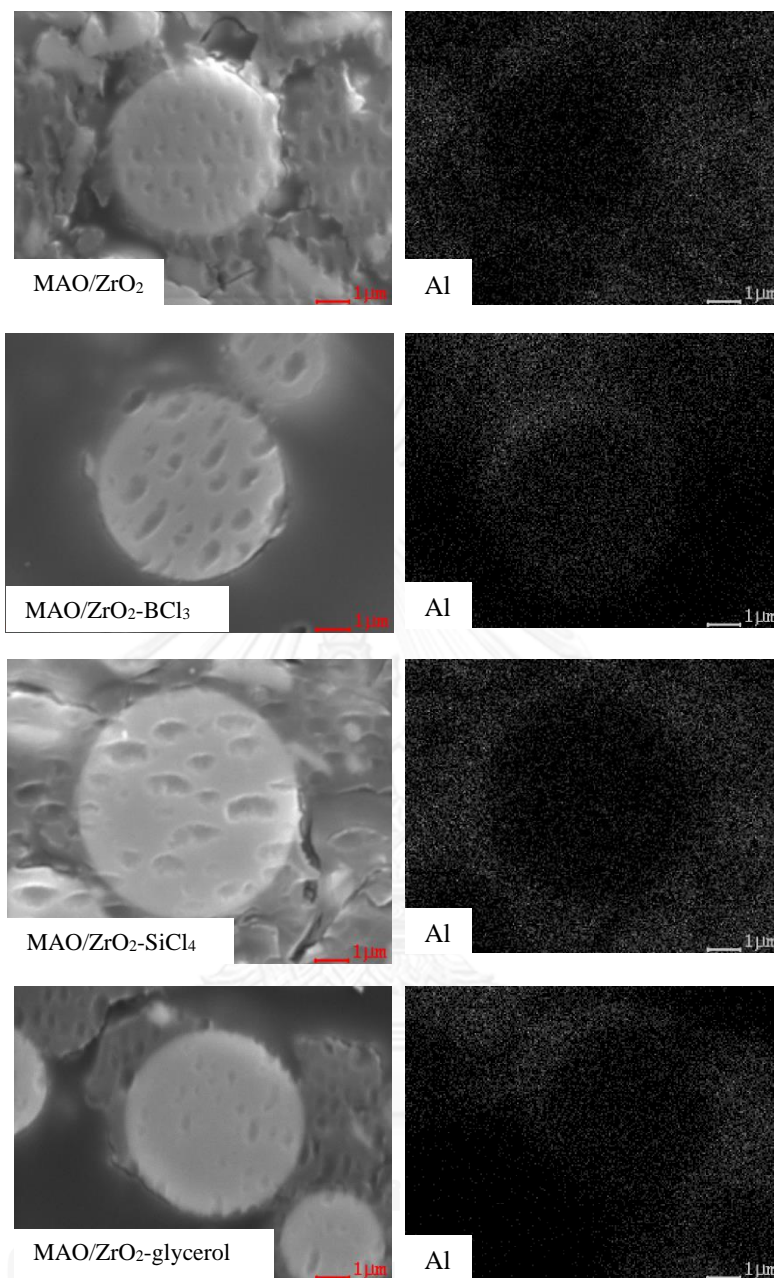
Figure 4.2 SEM/EDX mappings of Al distribution on cross-sectional particles
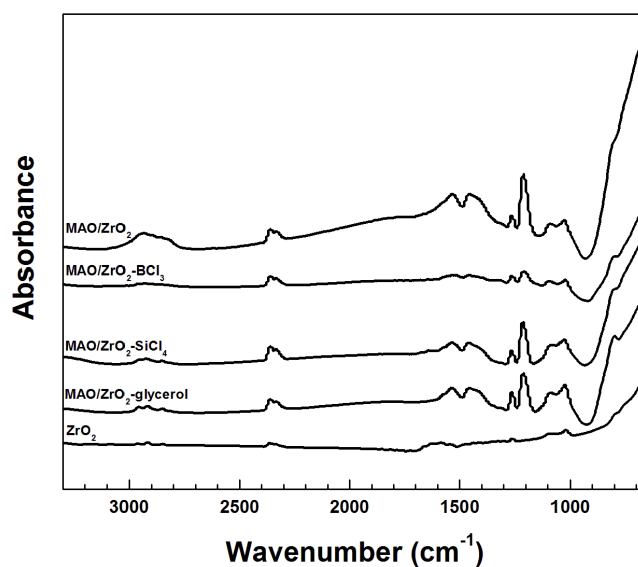
Figure 4.3 IR spectra of the unmodified and
the modified spherical ZrO_2-supported MAO

4.1.2 Catalytic activity

Then, the different modified and unmodified zirconia supports after impregnation with MAO were tested to evaluate the catalytic activity. To measure the catalytic activity, copolymerization of ethylene with 1-hexene using the modified and unmodified zirconia-supported MAO with *rac*-Et(Ind)$_2$ZrCl$_2$ catalyst was conducted under slurry process via semi-batch method.

The rate of ethylene consumption against polymerization time is plotted in **Figure 4.4**. It indicated that the highest ethylene consumption rate was achieved with the SiCl$_4$-modified zirconia supported MAO system within the prescribed polymerization time. It can be observed that the ethylene consumption from the beginning of polymerization apparently increased with time, whereas other supported systems showed about less than half of ethylene consumption in the MAO/ZrO$_2$-SiCl$_4$ system.
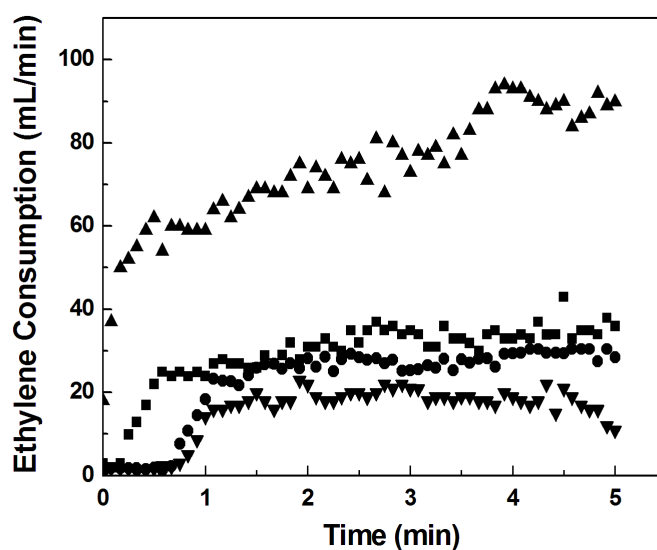
Figure 4.4 Rate-time profiles of ethylene/1-hexene copolymerization with *rac*-Et(Ind)$_2$ZrCl$_2$ catalyst in different supported systems; MAO/ZrO$_2$ (▼), MAO/ZrO$_2$-BCl$_3$ (■), MAO/ZrO$_2$-SiCl$_4$ (▲) and MAO/ZrO$_2$-glycerol (●)

The MAO/ZrO$_2$ and the MAO/ZrO$_2$-glycerol systems show the induction period because metallocene catalyst was probably difficult to contact with MAO anchored on the ZrO$_2$ or the ZrO$_2$-glycerol supports for formation of active site possibly attributed to steric effect on the support surface. On the other hand, for the MAO/ZrO$_2$-SiCl$_4$ system, it might be easier to form the active site in consequence of MAO anchored on the modified zirconia surface through the Si atom, which is presented as spacer, consequently resulting in less steric hindrance on the support surface. Considering the unmodified zirconia supported MAO, the lowest ethylene consumption rate occurred in this system and the rate gradually decreased after 3 min.

The copolymerization activities of immobilized MAO on each supported system are summarized in **Table 4.2**. The catalytic activity increased in the following order of; MAO/ZrO$_2$-SiCl$_4$ > MAO/ZrO$_2$-BCl$_3$ > MAO/ZrO$_2$-glycerol > MAO/ZrO$_2$. It can be seen that all the modified zirconia systems were capable of improving the catalytic activity compared to the unmodified one. The maximum activity could be obtained from zirconia modified with SiCl$_4$ system, which is about three times higher than the unmodified zirconia system.

Table 4.2 Copolymerization activities

Entry	Supported system	Yield (g)	Activity[a] [kg polymer·mol Zr^{-1}·min^{-1}]
1	MAO/ZrO$_2$	0.18	26
2	MAO/ZrO$_2$-BCl$_3$	0.41	54
3	MAO/ZrO$_2$-SiCl$_4$	0.63	84
4	MAO/ZrO$_2$-glycerol	0.32	40

[a] Polymerization conditions: [Zr] = 5×10^{-5} M, [A]$_{MAO}$/[Zr]$_{cat}$ = 1135, liquid volume (toluene) = 30 ml, ethylene = 1 atm, 1-hexene = 0.15 M, temperature = 70 °C, time = 5 min.

In order to investigate the modification effect of zirconia, XPS analysis was conducted on different supported systems. The binding energy (BE) for Al 2p core-level spectra and the full width at half maximum intensity (FWHM) of each supported system were measured, as seen in **Table 4.3**. The BE of Al 2p values were in the order of MAO/ZrO$_2$-BCl$_3$ (75.2 eV) > MAO/ZrO$_2$-SiCl$_4$ (74.8 eV) ≈ MAO/ZrO$_2$ (74.8 eV) > MAO/ZrO$_2$-glycerol (74.5 eV). The binding energy for Al 2p core-level of the cocatalyst was about 74.5-75.2 eV in unmodified and modified systems. These values are in agreement to those of the cocatalysts present in previous reports [7,94]. From this result, it is suggested that no significant change in the oxidation state of [Al]$_{MAO}$ occurred upon these supports. In contrast, the BE of the MAO/ZrO$_2$-BCl$_3$ was slightly higher than the unmodified one due to the enhancement in Lewis acidity of MAO by modification with BCl$_3$ since B is a Lewis acid metal atom [95]. This can result in a decrease in electron density of Al in the cocatalyst. It can be noted that the surface acidity property of the support plays an important role in the catalytic activity enhancement [30]. However, the MAO/ZrO$_2$-BCl$_3$ system did not render the highest activity. This is presumable because the MAO/ZrO$_2$-BCl$_3$ systems had much MAO locating within zirconia particles (**Figure 4.2**) resulting in more difficult to activate the catalyst than other systems. In addition, the EDX results are in accordance with the surface concentration of Al measured by XPS technique. Based on XPS measurement, the surface concentration of Al in the MAO/ZrO$_2$-SiCl$_4$ support was ca. 28.4 wt%,

whereas that on the MAO/ZrO$_2$-BCl$_3$ support was only ca. 25.9 wt%. This was corresponding to the EDX mapping result, where most of MAO in the MAO/ZrO$_2$-BCl$_3$ support was located in the bulk.

Table 4.3 XPS data of Al 2p core-level of each supported system

Entry	Supported system	BE (eV)	FWHM (eV)
1	MAO/ZrO$_2$	74.8	2.396
2	MAO/ZrO$_2$-BCl$_3$	75.2	2.086
3	MAO/ZrO$_2$-SiCl$_4$	74.8	1.973
4	MAO/ZrO$_2$-glycerol	74.5	2.344

It is worth noting that besides acidity, other factors should be considered. It is known that the amount of [Al]$_{MAO}$ and the interaction between [Al]$_{MAO}$ and the support have great influences on the change in the activity of the supported system. Considering the [Al]$_{MAO}$ contents on supports, it can be controlled by fixing the same [Al]$_{MAO}$/[Zr]$_{cat}$ ratio, which is 1135 when copolymerization was proceeded. As a consequent, the significant effect on the copolymerization activity should be only focused on the support interaction with [Al]$_{MAO}$. In fact, too strong interaction may cause difficulty for metallocene catalyst activation with cocatalyst anchored on the support. On the contrary, too weak interaction could result in leaching of MAO from the support. Thus, the optimum interaction should be required since both mentioned cases apparently resulted in low activity. Severn et al. [2] reported that the support and cocatalyst interact via O$_{support}$-Al$_{cocatalyst}$ linkage. The TGA measurement was used to determine the interaction of MAO cocatalyst bound to various supports in terms of the weight loss and removal temperature. From **Figure 4.5**, the weight loss during thermogravimetric analysis is plotted with removal temperature showing the weight loss in the order of MAO/ZrO$_2$-SiCl$_4$ (14.32%) < MAO/ZrO$_2$-BCl$_3$ (14.81%) < MAO/ZrO$_2$-glycerol (15.28%) < MAO/ZrO$_2$ (15.54%). In order to clarify TGA results, the curve of derivative weight loss is also presented. The first weight loss at ca. 100 °C can be attributed to moisture elimination. At the second stage, the MAO/ZrO$_2$-BCl$_3$ and the MAO/ZrO$_2$-SiCl$_4$ exhibited removal temperature at ca. 351 °C and 386°C, respectively.

Besides, the unmodified zirconia showed the removal temperature at ca. 338-404 °C. In the case of MAO/ZrO$_2$-glycerol system, the species were removed at ca. 205-380 °C. They were removed at lower temperature than other systems, probably due to the MAO/ZrO$_2$-glycerol system have high Al contents obtained from MAO anchored with the cross-linking reaction with glycerol to form three-dimensional lattices. This demonstrates that the MAO/ZrO$_2$-SiCl$_4$ system exhibited the strongest interaction among other supported systems. To support this result, Schrekker et al. [7] also revealed that α-diimine nickel (II) catalyst was reacted with silica treated with SiCl$_4$, AlMe$_3$ and BCl$_3$ to afford the covalently linked catalyst. Refer to the catalytic activity in **Table 4.2**, the highest copolymerization activity was observed in the MAO/ZrO$_2$-SiCl$_4$ system. Besides, the orders of interaction degree between MAO and each support indicated the similar trend with copolymerization activity. It should be mentioned that the absence of induction period coupled with the stronger interaction of cocatalyst bound to the support play important roles on an increased catalytic activity for the modified supported system. Moreover, the location of MAO on the zirconia particle was probably an important factor for increased activity as well.
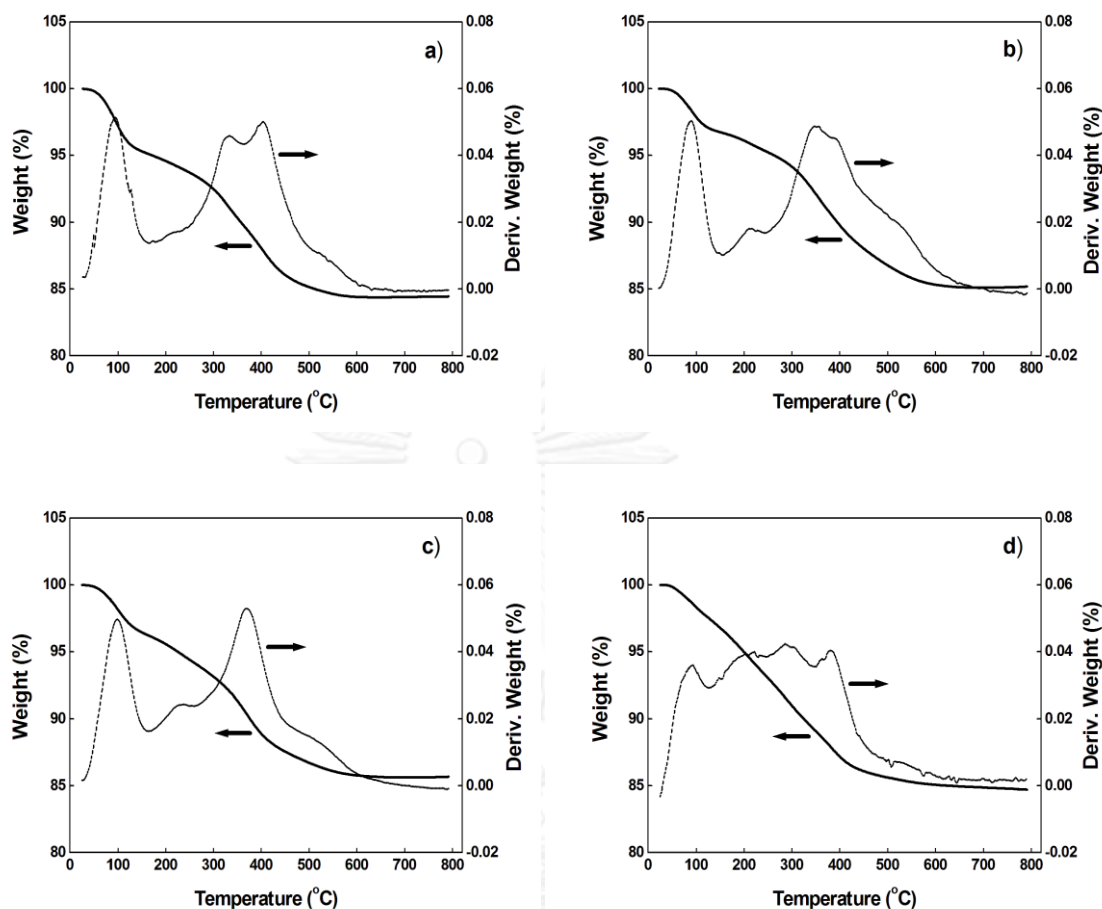
Figure 4.5 TGA and DTA profiles of various supported systems; a) MAO/ZrO$_2$, b) MAO/ZrO$_2$-BCl$_3$, c) MAO/ZrO$_2$-SiCl$_4$ and d) MAO/ZrO$_2$-glycerol

4.1.3 Copolymers properties

The molecular weight (M_w and M_n) and the molecular weight distribution (M_w/M_n) of copolymers produced were measured using the GPC. The microstructure of ethylene/1-hexene copolymers was determined by ^{13}C NMR. **Table 4.4** presents the GPC results from different supported systems. It can be observed that the M_n of the copolymers obtained with the modified zirconia supports except for the BCl$_3$ modification was slightly lower than copolymer obtained from the unmodified one. This is due to an increase in 1-hexene insertion that encourages in more chain transfer reactions when SiCl$_4$ and glycerol leading to a decrease in copolymer molecular weight

[94]. However, with the BCl_3 modification, the M_n was slightly higher than the unmodified system, suggesting that the active species of the present system is an ion pair of the active metal cation and the MAO anion. The increase in Lewis acidity of MAO by modification with BCl_3 results in the abstraction of methyl from catalyst by MAO more strongly. Therefore, the active species are promoted, and the propagation rate is accelerated [7]. In addition, only the unimodal molecular weight distribution was achieved in all copolymers obtained. The M_w/M_n of all the modified zirconia supports became slightly narrower, which may be due to the formation of more uniform active sites in such the supported systems. To give further information, the FWHM values of MAO cocatalyst from XPS data shown in **Table 4.3** became broader in the order of MAO/ZrO_2-$SiCl_4$ (1.973 eV), < MAO/ZrO_2-BCl_3 (2.086 eV) < MAO/ZrO_2-glycerol (2.344 eV) < MAO/ZrO_2 (2.396 eV). This can be confirmed by an increase of the M_w/M_n values. It can be mentioned that the different support surface properties should provide the heterogeneity of surface Al species obtained from MAO cocatalyst [7].

Table 4.4 Properties of ethylene/1-hexene copolymers produced

Entry	Supported system	M_n^a	M_w^a	M_w/M_n^a	H (%)[b]
1	MAO/ZrO_2	9755	25727	2.64	23.5
2	MAO/ZrO_2-BCl_3	10844	26444	2.44	16.7
3	MAO/ZrO_2-$SiCl_4$	9253	21907	2.37	26.9
4	MAO/ZrO_2-glycerol	8050	20779	2.58	24.4

[a] determined by GPC
[b] 1-hexene insertion calculated from ^{13}C NMR spectra

The quantitative analysis of triad distribution for all copolymers produced was performed by ^{13}C NMR spectroscopy. The results of the triad distribution of ethylene/1-hexene copolymers and reactivity ratios are summarized in **Table 4.5**. All copolymers obtained from each supported system showed the similar triad distribution. The absence

of 1-hexene triblock (HHH) was observed in these copolymers. Moreover, considering the 1-hexene insertion from **Table 4.4**, it indicated that the SiCl₄ modification evidently yielded the highest degree of 1-hexene insertion. This was presumable on account of less steric hindrance on the zirconia surface when SiCl₄ was used. The SiCl₄ might perform like a spacer group to anchor MAO to zirconia support resulting in facilitating 1-hexene incorporation. The reactivity ratio calculated from ^{13}C NMR data revealed that random copolymers were obtained from all supported systems.

Table 4.5 Triad distribution of copolymers from each supported system

Entry[a]	supported system	HHH	EHH	EHE	HEH	EEH	EEE	$r_E r_H$
1	MAO/ZrO₂	0.000	0.146	0.167	0.089	0.302	0.296	0.57
2	MAO/ZrO₂-BCl₃	0.000	0.075	0.142	0.057	0.244	0.482	0.70
3	MAO/ZrO₂-SiCl₄	0.000	0.187	0.168	0.106	0.312	0.227	0.52
4	MAO/ZrO₂-glecerol	0.000	0.159	0.166	0.089	0.313	0.273	0.57

[a] Determined by ^{13}C NMR that E and H stand for ethylene and 1-hexene, respectively

4.2 Supporting effect of different cocatalysts on living behavior, catalytic activity, polymer properties

In our previous research, the effect of different kinds of modifier in term of catalytic activity and polymer properties were investigated. All kind of modifiers can enhance the catalytic activity of this heterogeneous catalyst system compared to unmodified-ZrO₂ system. However, no detailed studies have so far been carried out to investigate the reasons of the activity enhancement in term of the kinetic parameters. Recently, the living polymerization has turned out to be one of the most powerful methods for studying the kinetic features because the number of active centers and the propagation rate can be easily evaluated from the number of polymer chains and the number average molecular weight, respectively. There are research reported that Me₂Si(η^3-C₁₃H₈)(η^1-N^{t}Bu)TiMe₂-based catalytic systems can conduct living polymerization of propylene in homogeneous system [69,70]. However, the living

behavior of olefin polymerization was dependent on the cocatalyst employed [7,57,69,70]. Although MAO is by far the prominent cocatalyst for activation of metallocene catalysts [1], the living polymerization probably was accomplished with other cocatalysts.

In order to investigate supporting effects of different methylaluminoxanes on living behavior, catalytic activity, polymer properties, spherical zirconia-supported different cocatalysts were prepared. The dMMAO/ZrO$_2$ which was almost free from trialkylaluminums, MAO/ZrO$_2$ and MMAO/ZrO$_2$ were used as a cocatalyst on propylene polymerization with Me$_2$Si(η^3-C$_{13}$H$_8$)(η^1-N^{t}Bu)TiMe$_2$ catalyst.

4.2.1 Synthesis of catalyst

The *tert*-butyl(dimethylfluorenylsilyl)amido]dimethyl titanium complex [Me$_2$Si(η^3-C$_{13}$H$_8$)(η^1-N^{t}Bu)TiMe$_2$] was synthesized according to synthetic method reported by Nishii K. et al. [52]. The dimethylfluorenylsilylamine [Me$_2$Si(η^3-C$_{13}$H$_8$)(η^1-N^{t}Bu)] ligand was produced as light yellow oil. The ^{1}H NMR spectrum of the Me$_2$Si(η^3-C$_{13}$H$_8$)(η^1-N^{t}Bu) ligand is shown in **Figure 4.6**, it correspond to the results of Nishii K. et al. Consequently, it can confirm that the ligand was accomplished by cited method giving about 76% yield.
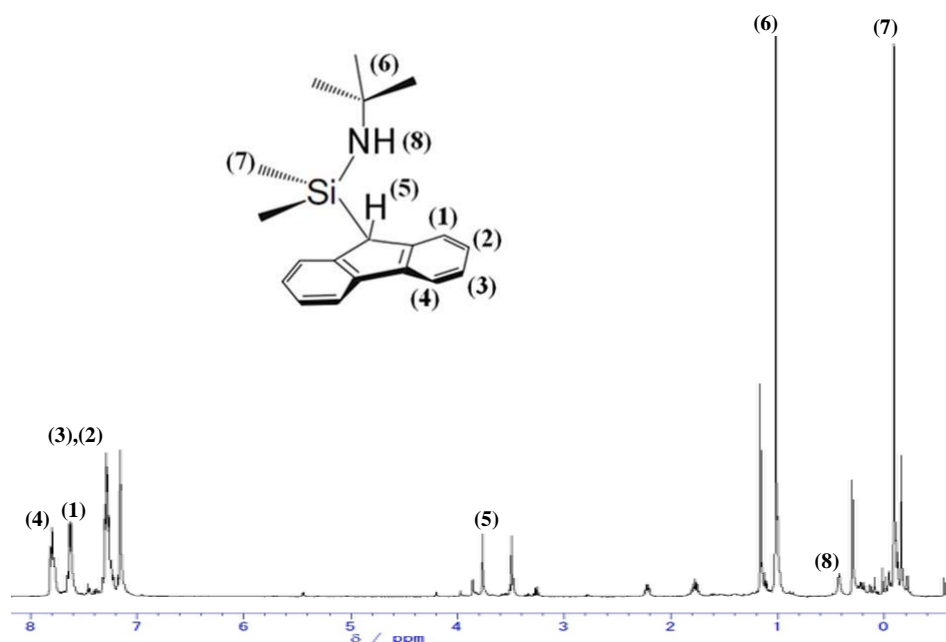
Figure 4.6 ^{1}H NMR spectrum of $Me_2Si(\eta^3\text{-}C_{13}H_8)(\eta^1\text{-}N^tBu)$ ligand

The ligand was used to synthesize the $Me_2Si(\eta^3\text{-}C_{13}H_8)(\eta^1\text{-}N^tBu)TiMe_2$ complex. The Ti complex can be crystallized as dark red crystals by the synthesis method mentioned. The ^{1}H NMR spectrum of the $Me_2Si(\eta^3\text{-}C_{13}H_8)(\eta^1\text{-}N^tBu)TiMe_2$ complex is shown in the **Figure 4.7**. It can be observed that the result accorded with the reference data of Nishii K.; therefore, this complex was successfully synthesized via the mentioned method, obtained the yield of 44%.
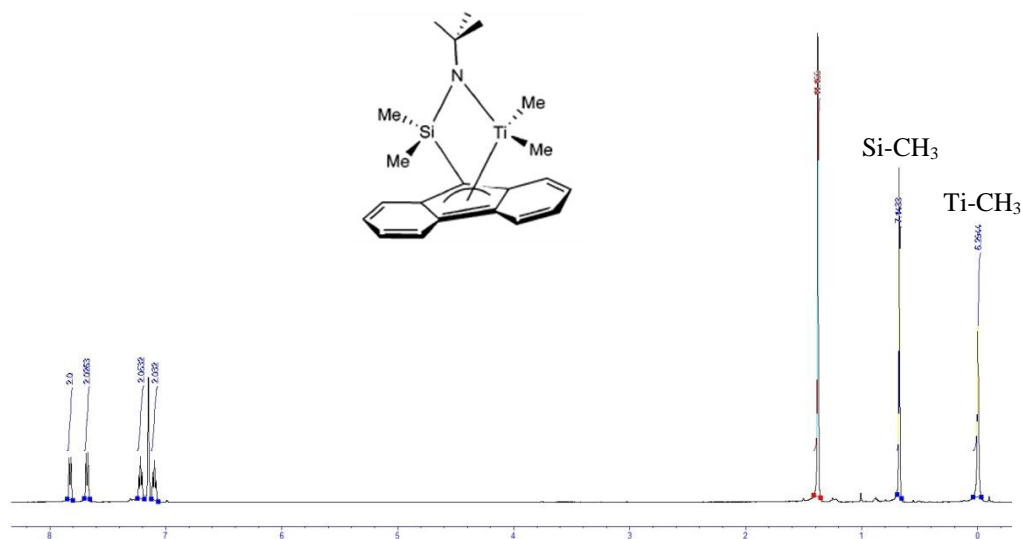
Figure 4.7 ^{1}H NMR spectrum of [*t*-BuNSiMe$_2$Flu]TiMe$_2$ complex

4.2.2 Effect of cocatlysts on the catalytic activity

Propylene polymerizations were carried out with Me$_2$Si(η^3-C$_{13}$H$_8$)(η^1-N^{t}Bu)TiMe$_2$ using different aluminoxane compounds supported on spherical zirconia as a cocatalyst. The propylene consumption rates plotted against polymerization time are shown in **Figure 4.8**.

The MAO/ZrO$_2$ system showed a steady propylene consumption rate, indicating that deactivation did not take place in this cocatalyst. In the MMAO/ZrO$_2$ system, the consumption rate was higher than MAO/ZrO$_2$ system at the initial stage, then decreased with polymerization time attributed to the deactivation in this system. For the dMMAO/ZrO$_2$ system, which free-alkylaluminums were removed, the highest consumption rate was achieved within the first 5 minutes, but the rate gradually decreased with increasing polymerization time. This is because a large amount of produced polymer increased the viscosity in the slurry resulting in prohibiting effective stirring. It led to the evident decrease in the propylene consumption rate. Therefore, the polymerization feature was clearly dependent upon the types of supported cocatalysts.
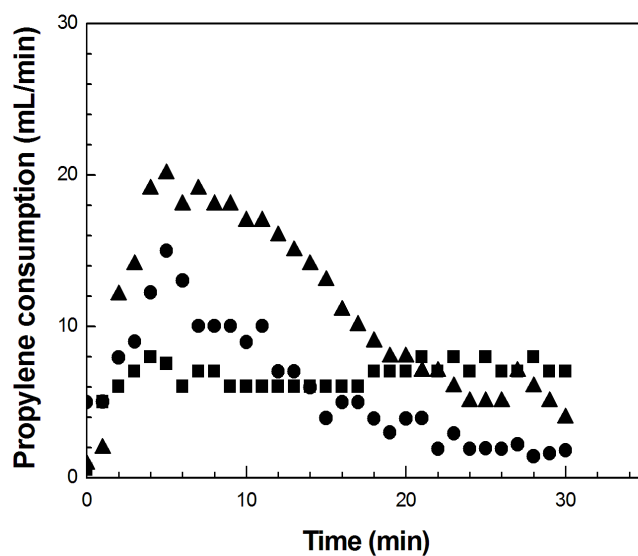
Figure 4.8 Rate-time profiles of propylene polymerization with different cocatalyst systems: MAO/ZrO$_2$ (■), MMAO/ZrO$_2$ (●), dMMAO/ZrO$_2$ (▲).
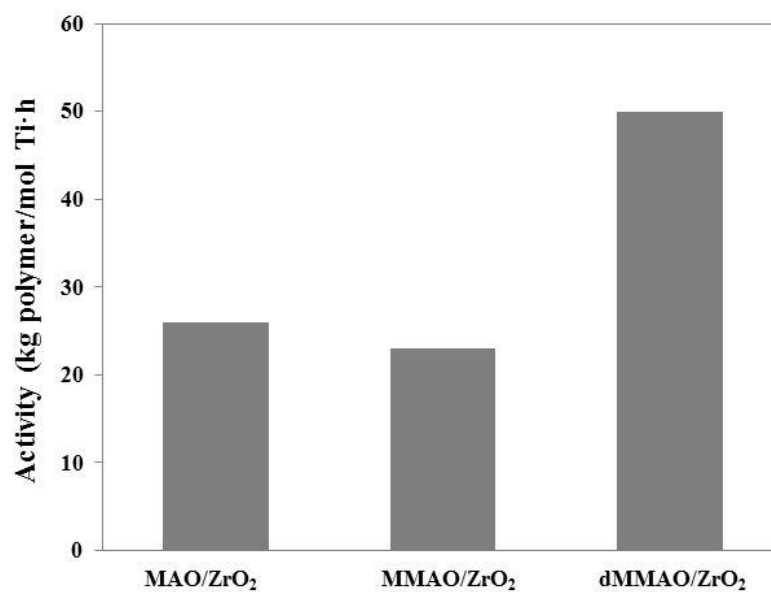
Figure 4.9 Catalytic activity in propylene polymerization; Ti = 20 μmol, propylene = 1 atm, temperature = 0 °C, Al$_{(MAO/ZrO2)}$ = 3.5 mmol, Al$_{(MMAO/ZrO2)}$ = 2.9 mmol, Al$_{(dMMAO/ZrO2)}$ = 2.6 mmol, polymerization time = 30 min

The activities obtained with different cocatalysts are presented in **Figure 4.9**, which clearly show that the polymerization activities strongly depend on the types of supported cocatalysts. The activities decreased as the following order: dMMAO/ZrO$_2$ > MAO/ZrO$_2$ > MMAO/ZrO$_2$. This was probably due to the supporting effect, which can impact the reactivity of cocatalysts towards Ti active species. For the activation process of metallocene catalyst, it is accepted that the formation of active sites undergoes by cocatalyst, which generally consists of alkylaluminoxane and residual trialkylaluminum, via alkylation of transition metal complexes subsequent to methyl anion abstract to yield cationic transition metal species [12]. Moreover, the influences of the supported cocatalysts also came from the nature and structure of alkylaluminoxane themselves. Since the MAO contains free-TMA while the MMAO have both free-TMA and free-TIBA, they possibly participated in the activation of active sites. For the supported systems, the higher activity of dMMAO/ZrO$_2$ comparing to MMAO/ZrO$_2$ could be attributed to higher actual amount of free-trialkylaluminum MMAO presented on the spherical zirconia supports. Furthermore, trialkylaluminum can promote chain transfer reaction [96]. From **Table 4.6**, although Al/Ti ratio in the MMAO/ZrO$_2$ system was less than in the MAO/ZrO$_2$ system, the number of polymer chains with the MMAO/ZrO$_2$ was larger than the number with the MAO/ZrO$_2$. It is probably because trialkylaluminums in the MMAO/ZrO$_2$, which have both TIBA and TMA, were more efficient chain transfer reagent than only TMA in the MAO/ZrO$_2$. The lowest molecular weight and a decay of propylene consumption rate in the MMAO/ZrO$_2$ system also suggested that trialkylaluminums in the MMAO/ZrO$_2$ acted as chain transfer reagent. On the contrary, the steady propylene consumption rate and the narrow M_w/M_n value on the MAO/ZrO$_2$ system suggest the living nature of propylene polymerization with this catalytic system.

Table 4.6 Effects of cocatalyst systems on propylene polymerization with
$Me_2Si(\eta^3\text{-}C_{13}H_8)(\eta^1\text{-}N^tBu)TiMe_2$ catalyst

Entry[a]	Cocatalyst	Yield (g)	M_n[b] ($\times 10^3$)	M_w/M_n[b]	N/Ti[c]
1[d]	MAO/ZrO$_2$	0.26	36	1.53	0.35
2[e]	MMAO/ZrO$_2$	0.21	27	1.97	0.41
3[f]	dMMAO/ZrO$_2$	0.50	287	2.00	0.09

[a] Polymerization conditions: toluene = 30 mL, Ti = 20 µmol, propylene = 1 atm, temp. = 0 °C.

[b] Number average molecular weight (M_n) and molecular weight distribution (M_w/M_n) was determined by GPC using polystyrene standard with universal calibration.

[c] Number of polymer chains calculated from yield and M_n.

[d] Al = 3.5 mmol.

[e] Al = 2.9 mmol.

[f] Al = 2.6 mmol.

4.2.3 Effect of cocatlysts on the polymer properties

The investigation has also been extended for the evaluation of different supported cocatalysts effect on the polymer properties towards $Me_2Si(\eta^3\text{-}C_{13}H_8)(\eta^1\text{-}N^tBu)TiMe_2$ catalyst. The triad analysis of polypropylene in all entries are summarized in **Table 4.7**. These results indicate that the supported cocatalysts did not affect the stereospecificity of catalyst. All polymers produced were syndiotactic polypropylene. The results were in agreement with $Me_2Si(\eta^3\text{-}C_{13}H_8)(\eta^1\text{-}N^tBu)TiMe_2$ catalyst in toluene solvent that gave syndiotactic-rich of polypropylene, regardless of the cocatalysts employed as reported by Ioku et al. [61].

Table 4.7 Effects of cocatalyst systems on polypropylene obtained by $Me_2Si(\eta^3\text{-}C_{13}H_8)(\eta^1\text{-}N^tBu)TiMe_2$catalyst with different cocatalysts

Entry	Cocatalyst	rr^a (%)	Td_5^b (°C)	Polymer^c (wt%)
1	MAO/ZrO$_2$	68	337	33.8
2	MMAO/ZrO$_2$	68	325	14.7
3	dMMAO/ZrO$_2$	70	352	44.8

^{a} Determined by ^{13}C NMR.

^{b} Td reported as the 5% and 10% weight loss temperature under nitrogen determined by TGA.

^{c} Determined by TGA.

Thermal gravimetric analysis was carried out in order to obtain better idea of the thermal stability of polymer and the polymer particle composition in terms of polymeric versus zirconia material. TGA profiles of the present polymers in nitrogen are shown in **Figure 4.10**. For a specific polymerization time, the maximum weight losses for all cocatalysts were in the order of dMMAO/ZrO$_2$ (43.8%) > MAO/ZrO$_2$ (33.3%) > MMAO/ZrO$_2$ (13.7%). The maximum weight loss may be attributed to decomposition of all polymer material and the remained weight in TGA profiles may be attributed to zirconia support. For the dMMAO/ZrO$_2$, the particle is made up the highest percent of polymer (43.8%) and contained the lowest percent of zirconia (56.2%). These results conform to polymer yields received by weight measurement as shown in **Table 4.6**. The temperatures at 5% decomposition are listed in **Table 4.7**. The dMMAO/ZrO$_2$ also showed the highest thermal resistance with Td$_5$ = 352 °C. The thermal stability of the products increases with rising amount of polymeric materials on the zirconia support attributed to very compact polymer particle [80].
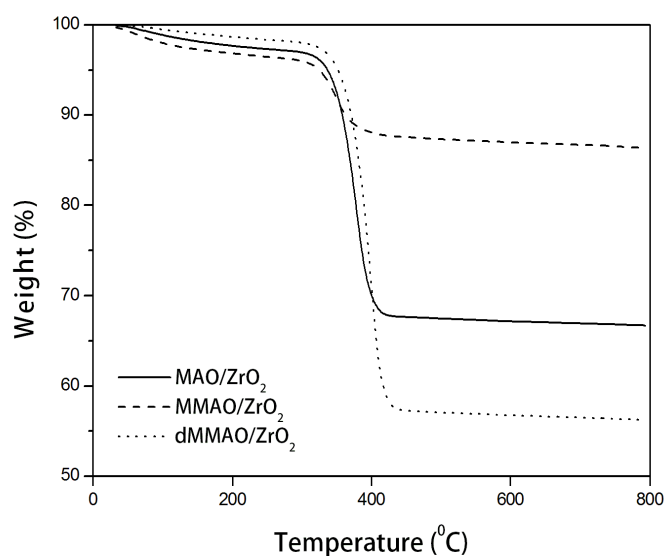
Figure 4.10 TGA profiles for polymers produced from different cocatalysts

From SEM micrographs in **Figure 4.11**, it demonstrates that the particles morphology of all polymers produced with different supported cocatalysts were quite different. The polymers were formed on the outer zirconia surfaces and the particles agglomerated. The fragmentations of zirconia particles were not observed. However, in MMAO/ZrO_2 cocatalyst, few polymers were produced on the outer zirconia surfaces and the agglomeration of particles did not occurred.
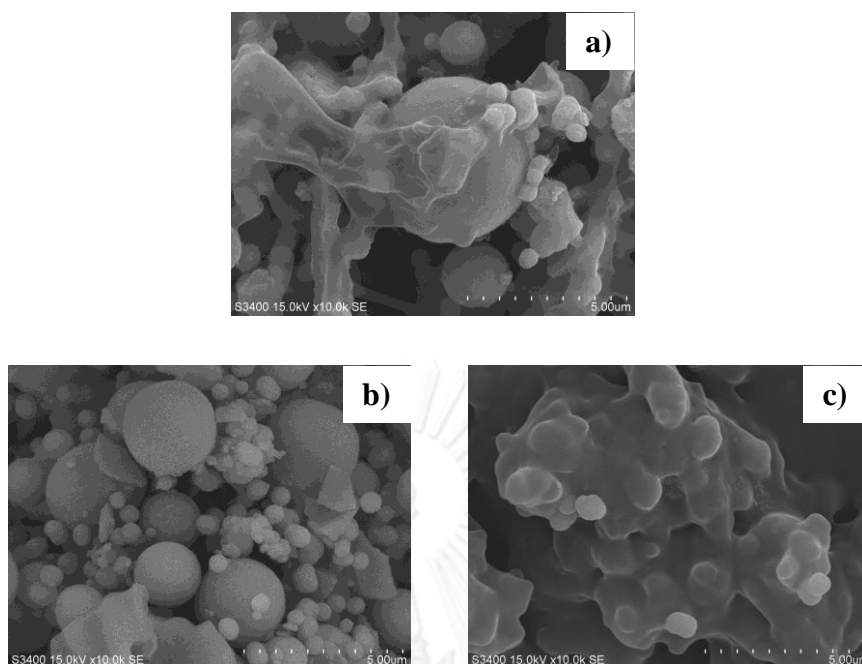
Figure 4.11 SEM micrographs of polypropylene obtained with different   cocatalysts; a) MAO/ZrO$_2$, b) MMAO/ZrO$_2$ and c) dMMAO/ZrO$_2$

4.3   The modification effect of spherical zirconia modified with SiCl$_4$ for heterogeneous single-site catalyst

Regarding the results from section 4.1, it was found that the SiCl$_4$ modification on zirconia before supporting MAO showed the highest catalytic activity of ethylene/1-hexene copolymerization with *rac*-Et(Ind)$_2$ZrCl$_2$. However, the reason of the activity improvement by the SiCl$_4$ modification has not been clear. In the event of living polymerization accomplished with the modified cocatalyst system, it becomes obvious whether the modification affects the number of active centers (C^*) or the propagation rate constant (k_p). In this part, propylene polymerization was conducted with Me$_2$Si(η^3-C$_{13}$H$_8$)(η^1-N^{t}Bu)TiMe$_2$ catalyst activated by MAO supported on the unmodified and the SiCl$_4$-modified spherical zirconia so as to study the feasibility of living polymerization for clarifying the modification effect of SiCl$_4$ on cocatalyst abilities.

4.3.1   Properties of supports

The physical properties of the synthesized zirconia and the conventional silica are shown in **Table 4.8**.

Table 4.8 Comparison physical properties of zirconia and silica

Support	Particle size (µm)	Surface area (m²/g)	Pore volume (mL/g)	Pore size (nm)
Zirconia	4.2	160[a]	0.18[a]	2.84 [a]
Silica[b]	40.8	273	1.30	-

[a] Characterization by N_2 physisorption.

[b] Commercial silica (P-10).

The support was calcined at 400 °C for 6 h, and then the 0.5 g of calcined support was reacted with *n*-BuLi as well as washed 7 times with hexane. After drying under vacuum, it was analyzed hydroxyl group by back titration method. The results are summarizes in the **Table 4.9**. It indicated that silica has more amount of hydroxyl group than zirconia at same calcination condition. This is probably due to high surface area and pore volume of silica.

Table 4.9 Amount of hydroxyl group on zirconia and silica after calcination

Support	Average hydroxyl group (mmol·g⁻¹)
Zirconia	3.75
Silica	4.38

4.3.2 Propylene polymerization

Propylene polymerization with 1 was carried out in a 100-mL glass reactor at 0 °C under atmospheric pressure of propylene. MAO/Zr_{O2} and MAO/ZrO_2–$SiCl_4$ were employed as a cocatalyst to investigate the feasibility of living polymerization with the heterogeneous catalytic systems. For comparison, silica was also used as a support in place of zirconia and prepared MAO/SiO_2 and MAO/SiO_2–$SiCl_4$. The rates of propylene consumption are plotted as a function of polymerization time in Figure 4.12. The similar trend of propylene consumption was observed in all the metal oxide-supported MAO systems: the propylene consumption gradually increased with polymerization time, then kept steady rate until terminating the polymerization. These results demonstrate that no deactivation occurred during the polymerization regardless of the cocatalyst used. In addition, the MAO/ZrO_2–$SiCl_4$ system rendered the highest consumption rate among the cocatalyst used.
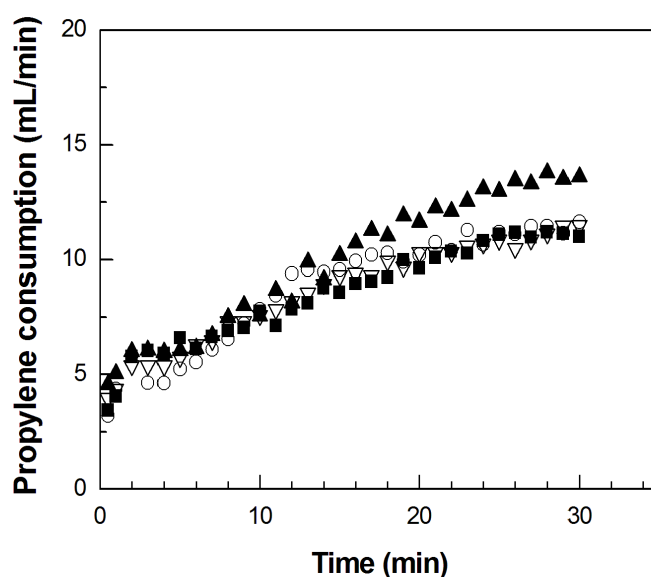
Figure 4.12 Rate-time profiles of propylene polymerization with various cocatalyst systems: MAO/ZrO_2 (■), MAO/ZrO_2-$SiCl_4$ (▲), MAO/SiO_2 (▽), MAO/SiO_2-$SiCl_4$ (○)

In order to confirm the living behavior of these heterogeneous systems, the time dependence of the number average molecular weight (M_n) and the molecular weight

distribution (M_w/M_n) was investigated by sampling the produced polymers from the reactor at certain interval during polymerization. The sampled polymers were analyzed by GPC. The results are plotted in **Figure 4.13**. The M_n values linearly increased with increasing polymerization time together with narrowing molecular weight distribution irrespective of the cocatalyst used. Moreover, the straight line of M_n against the polymerization time went through the origin. These results indicate that the propylene polymerizations by the present heterogenous catalytic systems proceeded in a living manner Therefore, the propagation rate constant (k_p) of these catalytic systems can be directly evaluated from the slope of M_n vs. polymerization time plot or the M_n value at a certain polymerization time [7,97]. Then, the number of active centers (C^*) can be evaluated by the number of polymer-chains (N) per Ti [7,97,98].
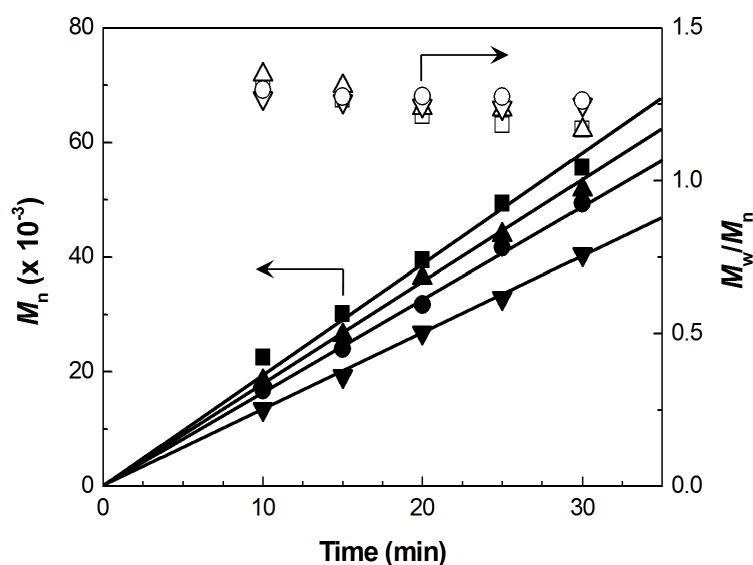

Figure 4.13 Plots of M_n and M_w/M_n against polymerization time in propylene polymerization with various cocatalyst systems: MAO/ZrO$_2$, M_n (■), M_w/M_n (□); MAO/ZrO$_2$-SiCl$_4$, M_n (▲), M_w/M_n (△); MAO/SiO$_2$, M_n (▼), M_w/M_n (▽); MAO/SiO$_2$-SiCl$_4$, M_n (●), M_w/M_n (○).

The results of propylene polymerization are summarized in **Table 4.10**, which clearly shows that the polymerization features strongly depend on the modification of support. The MAO/ZrO$_2$-SiCl$_4$ system rendered higher activity than the MAO/ZrO$_2$ system. However, the M_n value of polymer obtained with the MAO/ZrO$_2$-SiCl$_4$ system was lower than that with the MAO/ZrO$_2$ system implying that the average k_p value in the MAO/ZrO$_2$-SiCl$_4$ system was less than that in the MAO/ZrO$_2$ system. On the hand, the N/Ti value was increased by the SiCl$_4$ modification on zirconia, which is attributed to an increase of the C^* value probably due to less steric hindrance on support surface modified with SiCl$_4$ [99]. In case of the conventional silica, the yields were almost the same between the MAO/SiO$_2$ and the MAO/SiO$_2$-SiCl$_4$ systems. However, the M_n value increased and closed to that of the MAO/ZrO$_2$-SiCl$_4$ system, indicating the similar k_p values of these active species due to the modification with SiCl$_4$. The reason why the modification of SiO$_2$ with SiCl$_4$ decreased the C^* value is not clear at present.

Table 4.10 Results of propylene polymerization with Me$_2$Si(η^3-C$_{13}$H$_8$)(η^1-N^{t}Bu)TiMe$_2$ activated by supported MAOs

Entry[a]	Cocatalyst	Yield (g)	Activity[b]	M_n[c] ($\times 10^{-3}$)	M_w/M_n[c]	N[d]/Ti (mol/mol)
P-1	MAO/ZrO$_2$	0.48	48	48	1.32	0.48
P-2	MAO/ZrO$_2$-SiCl$_4$	0.50	50	33	1.29	0.78
P-3	MAO/SiO$_2$	0.25	25	29	1.27	0.44
P-4	MAO/SiO$_2$-SiCl$_4$	0.25	25	38	1.27	0.33

[a] Polymerization conditions: Ti = 20 µmol, Al/Ti = 200, solvent = toluene, total volume = 30 mL, propylene = 1 atm, temperature = 0 °C, polymerization time = 30 min.

[b] Activity = (kg polymer)·(mol cat)$^{-1}$·h^{-1}.

[c] Number average molecular weight (M_n) and molecular weight distribution (M_w/M_n) determined by GPC using universal calibration.

[d] Number of polymer chains calculated from yield and M_n.

4.3.3 Microstructure of polypropylenes

To study the modification effect on the microstructure of the produced polypropylene, the ^{13}C NMR analysis of the polypropylenes was performed. The results are summarized in **Table 4.11**, which indicate that the modification of SiCl$_4$ did not affect the regio- and stereoregularity of the living polypropylenes. Syndiotactic polypropylenes were produced with all the cocatalyst systems. This result corresponded to the finding of Hagimoto et al. [7] who studied propylene polymerization with a chelating (diamido)dimethyltitanium complex using several kinds of the metal oxide-supported MMAO as a cocatalyst. They found that all polymers produced were statistically atactic regardless of the cocatalyst used.

Table 4.11 Microstructure of polypropylenes obtained by ^{13}C NMR

Entry	Cocatalyst	mm	mr	rr
P-1	MAO/ZrO$_2$	0.02	0.23	0.75
P-2	MAO/ZrO$_2$-SiCl$_4$	0.03	0.22	0.75
P-3	MAO/SiO$_2$	0.03	0.21	0.76
P-4	MAO/SiO$_2$-SiCl$_4$	0.03	0.21	0.76

4.3.4 Ethylene/1-hexene copolymerization

Copolymerization of ethylene with 1-hexene was also performed in order to compare the modification effect with propylene polymerization. The ethylene consumption rate during ethylene/1-hexene copolymerization at 0 °C are illustrated in **Figure 4.14**. The steady rate of ethylene consumption was observed for all the cocatalyst systems, indicating that deactivation did not take place in these systems. The MAO/ZrO$_2$-SiCl$_4$ system gave the highest consumption rate among the cocatalysts used as observed in the propylene polymerization described above.
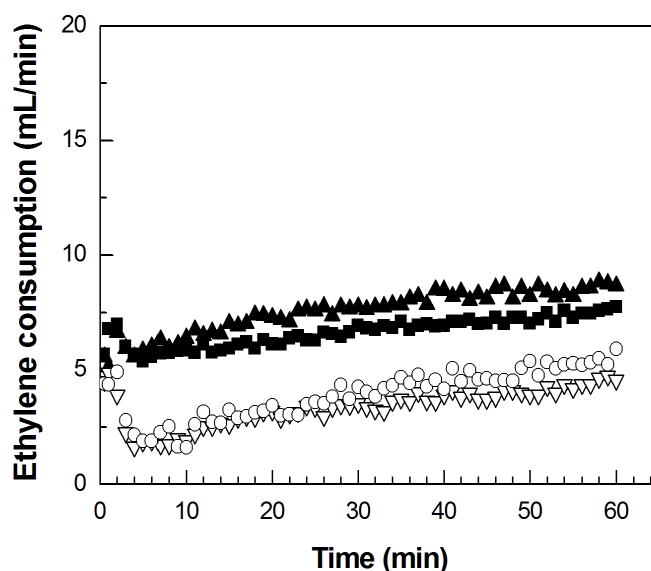
Figure 4.14 Rate-time profiles of ethylene/1-hexene copolymerization with various cocatalyst systems: MAO/ZrO$_2$ (■), MAO/ZrO$_2$-SiCl$_4$ (▲), MAO/SiO$_2$ (▽), MAO/SiO$_2$-SiCl$_4$ (○).

The results of ethylene/1-hexene copolymerization are displayed in **Table 4.12**, including the catalytic activities based on copolymer yield and the GPC results of the polymer produced. Although we could not confirm the livingness of the ethylene/1-hexene copolymerization by means of the sampling method due to low consumption rate, the steady consumption rates and the narrow M_w/M_n values (< 1.5) of the produced polymers suggest the living nature of the copolymerization with these catalytic systems. Therefore, the modification effects are discussed on the assumption that the copolymerization is living.

The modification of zirconia with SiCl$_4$ increased the copolymerization activity in about 30% accompanied with the reduction of the M_n value. Similar modification effects were also observed in the propylene polymerization. The results clearly indicated that the copolymerization features also depend on the modification of support. The N/Ti value obtained with the MAO/ZrO$_2$-SiCl$_4$ system was higher than that obtained with the MAO/ZrO$_2$ system. This should be attributed to an increase of the C^* value when zirconia was modified with SiCl$_4$ as observed in the propylene

polymerization. In case of the conventional silica, the activity was also increased by the SiCl$_4$ modification accompanied by the increase of the M_n and the N/Ti values.

Table 4.12 Ethylene/1-hexene copolymerization results

Entry[a]	Cocatalyst	Yield (g)	Activity[b]	M_n^c (× 10^{-3})	M_w/M_n^c	N^d/Ti (mol/mol)
EH-1	MAO/ZrO$_2$	0.55	28	52	1.49	0.52
EH-2	MAO/ZrO$_2$-SiCl$_4$	0.73	37	43	1.48	0.85
EH-3	MAO/SiO$_2$	0.14	7	31	1.42	0.23
EH-4	MAO/SiO$_2$-SiCl$_4$	0.25	13	35	1.40	0.25

[a] Polymerization conditions: Ti = 20 µmol, Al/Ti = 200, solvent = toluene, total volume = 30 mL, ethylene = 1 atm, 1-hexene = 0.45 M, temperature = 0 °C, polymerization time = 30 min.

[b] Activity = (kg polymer)·(mol cat)$^{-1}$·h^{-1}.

[c] Number average molecular weight (M_n) and molecular weight distribution (M_w/M_n) determined by GPC using universal calibration.

[d] Number of polymer chains calculated from yield and M_n.

4.3.5 Microstructure of copolymers

The structure of the ethylene/1-hexene copolymers was analyzed by ^{13}C NMR [99]. The triad distribution, 1-hexene incorporation and the product of reactivity ratios (r_Er_H) are shown in **Table 4.13**. The results indicate that the copolymer structure slightly depended on the kind of the cocatalysts. The silica support presented higher insertion ability for 1-hexene than the zirconia support. The modification with SiCl$_4$ slightly increased the 1-hexene insertion in both systems probably due to less steric hindrance on the modified metal oxide surface [25]. The product of monomer reactivity ratios is one of the factors for considering the nature of copolymerization. The products were approximately 0.85 for zirconia-supported cocatalysts and approximately 0.60 for

silica-supported cocatalysts, respectively indicating that the supporting material of MAO affects the copolymerization ability of the catalyst.

Table 4.13 Triad distribution of ethylene/1-hexene copolymers obtained by ^{13}C NMR

Cocatalyst	HHH	EHH	EHE	HEH	EEH	EEE	%H	r_E	r_H	$r_E r_H$
MAO/ZrO$_2$	0.012	0.207	0.139	0.119	0.248	0.275	35.9	4.76	0.16	0.76
MAO/ZrO$_2$-SiCl$_4$	0.048	0.191	0.144	0.099	0.281	0.237	38.3	3.89	0.24	0.93
MAO/SiO$_2$	0.041	0.218	0.168	0.151	0.271	0.151	42.8	3.10	0.19	0.59
MAO/SiO$_2$-SiCl$_4$	0.051	0.217	0.168	0.128	0.297	0.139	43.6	3.02	0.20	0.60

CHAPTER V

CONCLUSIONS AND RECOMMENDATIONS

5.1 Conclusions

5.1.1 Effect of spherical zirconia modified with different modifiers including $SiCl_4$, BCl_3, and glycerol on the ethylene/1-hexene copolymerization behavior

The modification effects of each modifier on ethylene/1-hexene copolymerization were investigated using metallocene catalyst combined with MAO. The catalytic activity strongly depended on the supported system employed. The modification of zirconia with BCl_3, $SiCl_4$ and glycerol can improve the activity of ethylene/1-hexene copolymerization, especially for the $SiCl_4$ modification that renders the highest activity. The results clearly revealed that the catalytic activity enhancement arisen from both in the absence of induction period and the stronger interaction between MAO cocatalyst and the support. Moreover, $SiCl_4$ acting as a spacer decreased steric effect resulting in an increase in activity and 1-hexene insertion. The narrow molecular weight distribution was observed with all modifiers compared to the unmodified zirconia. The $SiCl_4$ and the glycerol modification caused a decrease in molecular weight while the improvement in the Lewis acidity property of the support with the BCl_3 modification led to higher molecular weight. Finally, the support modifications had effect on the catalytic activity, but had no significant influence on the copolymer microstructure.

5.1.2 Supporting effects of different cocatalysts on living behavior, catalytic activity, polymer properties

The supporting effects of different methylaluminoxanes were investigated in propylene polymerization with $Me_2Si(\eta^3\text{-}C_{13}H_8)(\eta^1\text{-}N^tBu)TiMe_2$ catalyst. The supported

cocatalysts showed different Al contents depending on the adsorption ability between zirconia surface and cocatalysts. The MAO/ZrO_2 showed a steady propylene consumption rate with narrow molecular weight distribution suggesting the living behavior of this catalytic system. The dMMAO/ZrO_2 presented the highest activity. On the contrary, the MMAO/ZrO_2 rendered the lowest activity together with a decrease in consumption rate of propylene probably due to lower actual amount of free-trialkylaluminum MMAO and deactivation of this system. Moreover, trialkylaluminums in the MMAO/ZrO_2 cocatalyst, which were TIBA and TMA, were effective chain transfer reagent. The zirconia supported different methylaluminoxanes affects the polymerization behaviors and catalytic activities, whereas no significant changes in the polymer microstructure and polymer morphology.

5.1.3 Possibility of living polymerization for clarifying the modification effect of $SiCl_4$ on cocatalyst abilities

Living polymerization of propylene proceeded with $Me_2Si(\eta^3\text{-}C_{13}H_8)(\eta^1\text{-}N^tBu)TiMe_2$ catalyst combined with the unmodified and the $SiCl_4$-modified metal oxide-supported MAO as a cocatalyst at 0 °C. The steady polymerization rates and the narrow M_w/M_n values of the produced polymers were observed in all the cocatalyst systems, indicating the living nature of the propylene polymerization. The k_p value and the C^* value depended on the cocatalyst used. The $SiCl_4$ modification on zirconia decreased the k_p value accompanied by an increase in the C^* value. The enhancement of the catalytic activities by the $SiCl_4$ modification was therefore ascribed to the increase of the C^* value. The modification did not affect the structure of living polypropylene. Copolymerization of ethylene/1-hexene with the same catalytic systems also proceeded in a controlled manner. For the $SiCl_4$ modification on zirconia, the similar effects on the propylene polymerization were also observed in on the k_p value and the C^* value. The 1-hexene incorporation was slightly improved by the $SiCl_4$ modification. The $SiCl_4$ might act as a spacer on the zirconia support leading to a higher number of active centers and higher comonomer incorporation.

5.2 Recommendations

- The optimization of modifiers content i.e. $SiCl_4$, BCl_3 and glycerol in the spherical zirconia supports should be investigated.

- The chemical bond analysis between modifiers, i.e. BCl_3 and $SiCl_4$, and zirconia surface should be investigated through Raman spectroscopy and Diffuse Reflectance Infrared Fourier Transform spectroscopy for obtaining a better understanding of their chemical bond.

- Characterization of spherical zirconia-supported MAOs such as surface area, pore size and the degree of interactions between support and cocatlysts should be studied.

- Cross-section SEM imaging and EDX of polymer should be characterized in order to clearly distinguish between zirconia particle and the polymer building upon the surface.

- To verify living behavior of zirconia supported MMAO and dMMAO, the time dependence of the number average molecular weight (M_n) and the molecular weight distribution (M_w/M_n) should be investigated.

- Postpolymerizations of propylene with unmodified and modified spherical zirconia supported MAO should be conducted in order to confirm living nature of these systems.

- The modification effect of spherical zirconia with BCl_3 and glycerol for heterogeneous single-site catalyst should be investigated in order to clarify their effects on cocatalyst abilities.

REFERENCES

[1] Kaminsky, W., Laban, A. Metallocene catalysis. Applied Catalysis A 222 (2001): 47-61.

[2] Severn, J.R., Chadwick, J.C., Duchateau, R., Friederichs, N. ''Bound but not gagged''-Immobilizing single-site α-olefin polymerization catalysts. Chemical Reviews 105 (2005): 4073-4147.

[3] Wu, L., Zhou, J.M., Lynch, D.T., Wanke, S.E. Polymer supported metallocene catalysts for gas-phase ethylene/1-hexene polymerization. Applied Catalysis A 293 (2005): 180-191.

[4] Ribour, D., Monteil, V., Splitz, R. Strong a of $MgCl_2$-supported Ziegler-Natta catalysts by treatments with BCl_3: evidence and application of the ''cluster'' model of active sites. Journal of Polymer Science Part A: Polymer Chemistry 47 (2009): 5784-5791.

[5] Chum, P.S., Swogger, K.W. Olefin polymer technologies-history and recent progress at the Dow Chemical Company. Progress in Polymer Science 33 (2008): 797-819.

[6] Hasan, T., Shiono, T., Ikeda, T. Highly efficient Ti-based catalyst system for vinyl addition polymerization of norbornene. Macromolecules 37 (2004): 7432-7443.

[7] Hagimoto, H., Shiono, T., Ikeda, T. Supporting effects of methylaluminoxane on the living polymerization of propylene with a chelating(diamide) dimethyl titanium complex. Macromolecular Chemistry and Physics 205 (2004): 19-26.

[8] Pullukat, T.J., Hoff, R.E. Silica-based Ziegler–Natta catalysts: a patent review. Catalysis Reviews - Science and Engineering 41 (1999): 389-428.

[9] Kaminsky, W., Arndt, M. Metallocenes for polymer catalysis. Advances in Polymer Science 127 (1997): 143.

[10] Li, K.T., Dai, C.L., Li, C.Y. Synthesis of linear low density polyethylene with a nano-sized silica supported Cp_2ZrCl_2/MAO catalyst. Polymer Bulletin 64 (2010): 749-759.

[11] Galland, G.B., Seferin, M., Mauler, R.S., Santos, J.H.Z.D. Linear low-density polyethylene synthesis promoted by homogeneous and supported catalysts. Polymer International 48 (1999): 660-664.

[12] Ciardellia, F., Altomarea, A., Michelotti, M. From homogeneous to supported metallocene catalysts. Catalysis Today 41 (1998): 149-157.

[13] Mcknight, A. L., Waymouth, R. M. Group 4 ansa-cyclopentadienyl-amido catalysts for olefin polymerization. Chemical Reviews 98 (1998): 2587-2598.

[14] Braunschweig, H., Breitling, F.M. Constrained geometry complexes Synthesis and applications. Coordination Chemistry Reviews 250 (2006): 2691–2720.

[15] Hlatky, G.G. Heterogeneous single-site catalyst for olefin polymerization. Chemical Reviews 100 (2000): 1347-1376.

[16] Chien, J.C.W. Supported metallocene polymerization catalysis. Topics in Catalysis 7 (1999): 23-36.

[17] Santos, J.H.Z.D., Greco, P.P., Stedile, F.C., Dupont, J. Organosilicon-modified silicas as support for zirconocene catalyst. Journal of Molecular Catalysis A: Chemical 154 (2000): 103-113.

[18] Chaichana, E., Khaubunsongserm, S., Praserthdam, P., Jongsomjit, B. Effect of Ga modification on different pore size silicas in synthesis of LLDPE by copolymerization of ethylene and 1-hexene with [t-BuNSiMe$_2$Flu]TiMe$_2$/MMAO catalyst. Polymer Bulletin 66 (2011): 1301–1312.

[19] Wongwaiwattanakul, P., Jongsomjit, B. Copolymerization of ethylene/1-octene via different pore sized silica-based-supported zirconocene/dMMAO catalyst. Catalysis Communications 10 (200): 118-122.

[20] Babushkin, D.E., Panchenko, V.N., Timofeeva, M.N., Zakharov, V.A., Brintzinger, H.H. Novel zirconocene hydride complexes in homogeneous and in SiO$_2$-supported olefin-polymerization catalysts modified with diisobutylaluminum hydride or triisobutylaluminum. Macromolecular Chemistry and Physics 12 (2008): 1210-1219.

[21] Pothirat, T., Jongsomjit, B., Praserthdam, P. A comparative study of SiO$_2$- and ZrO$_2$-supported zirconocene/MAO catalysts on ethylene/1-olefin copolymerization. Catalysis Communications 9 (2008): 1426-1431.

[22] Hammawa, H., Wanke, S.E. Influence of support friability and concentration of α-olefins on gas-phase ethylene polymerization over polymer-supported metallocene/methylaluminoxane catalysts. Journal of Applied Polymer Science 104 (2006): 514-527.

[23] Galland, G.B., Santos, J.H.Z.D., Stedile, F.C., Greco, P.P., Campani, A. Ethylene homo- and copolymerization using (nBuCp)$_2$ZrCl$_2$ grafted on silica modified with different spacers. Journal of Molecular Catalysis A: Chemical 210 (2004): 149-156.

[24] Lee, D.H., Yoon, K.B., Noh, S.K. Polymerization of ethylene by using zirconocene catalyst anchored on silica with trisiloxane and pentamethylene spacers. Macromolecular Rapid Communications 18 (1997): 427-431.

[25] Chao, C., Pratchayawutthirat, W., Praserthdam, P., Shiono, T., Rempel, G.L. Copolymerization of ethylene and propylene using silicon tetrachloride-modified silica/MAO with Et[Ind]$_2$ZrCl$_2$ metallocene catalyst. Macromolecular Rapid Communications 23 (2002): 672-675.

[26] Jongsomjit, B., Kaewkrajang, P., Praserthdam, P. Effect of silane-modified silica/MAO-supported Et[Ind]$_2$ZrCl$_2$ metallocene catalyst on copolymerization of ethylene. European Polymer Journal 40 (2004): 2813-2817.

[27] Lee, K.S., Oh, C.G., Yim, J.H., Ihm, S.K. Characteristics of zirconocene catalysts supported on Al-MCM-41 for ethylene polymerization. Journal of Molecular Catalysis A: Chemical 159 (2000): 301-308.

[28] Camposa, J.M., Lourençob, J.P., Fernandesc, A., Regod, A.M., Ribeiro, M.R. Mesoporous Ga-MCM-41 as support for metallocene catalysts: Acidity-activity relationship. Journal of Molecular Catalysis A: Chemical 310 (2009): 1-8.

[29] Pédeutour, J.N., Radhakrishnan, K., Cramail, H., Deffieux, A. Reactivity of metallocene catalysts for olefin polymerization: influence of activator nature and structure. Macromolecular Rapid Communications 22 (2001): 1095-1123.

[30] Kaivalchatchawal, P., Samingprai, S., Shiono, T., Praserthdam, P., Jongsomjit, B. Effect of Ga- and BCl$_3$-modified silica-supported [t-BuNSiMe$_2$(2,7-t-Bu$_2$Flu)]TiMe$_2$/MAO catalyst on ethylene/1-hexene copolymerization. European Polymer Journal 48 (2012): 1304-1312.

[31] Severn, J.R., Chadwick, J.C. Tailor-Made Polymers. Morlenbach: WILEY-VCH Verlag GmbH & Co. KGaA. 2008.

[32] Guan, Z., Zheng, Y., Jiao, S. Spherical $MgCl_2$-supported MAO pre-catalysts: preparation, characterization and activity in ethylene polymerization. Journal of Molecular Catalysis A: Chemical 188 (2002): 123-131.

[33] Rappaport, H. Ethylene and Polyethylene Global Overview [slides]. SPI Film & Bag, Houston, 2011.

[34] Heurtefeu, B., Bouilhaca, C., Clouteta, E., Tatona, D., Deffieuxa, A., Cramaila, H. Polymer support of "single-site" catalysts for heterogeneous olefin polymerization. Progress in Polymer Science 36 (2011): 89-126.

[35] Odian, G. Principles of polymerization. 4th ed. New Jersey: John Wiley & Sons, 2004.

[36] Malpass, D.B. Introduction to industrial polyethylene. Massachusetts: Scrivener, 2010.

[37] Peacock, A.J. Handbook of Polyethylene. New York: Marcel Dekker, 2000.

[38] Frank, P.T.J. Crystallization of isotactic polypropylene: The influence of stereo-defects. Eindhoven. 2002.

[39] Jongsomjit B. Metallocene Catalysis. Bangkok: Department of Chemical Engineering, Chulalongkorn University.

[40] Albizzati, E., Galimberti, M. Catalysts for olefins polymerization. Catalysis Today 41 (1998) 159-168.

[41] Jalali Dil E., Pourmahdian S., Vatankhah M., Afshar Taromi F. Effect of dealcoholation of support in $MgCl_2$-supported Ziegler–Natta catalysts on catalyst activity and polypropylene powder morphology. Polymer Bulletin 64 (2010): 445-457.

[42] Huang, J., Rempel, G.L. Ziegler-Natta catalysts for olefin polymerization: Mechanistic insights from metallocene system. Progress in Polymer Science 20 (1995): 459-526.

[43] McKnight, A.L., Waymouth, R.M. Group 4 ansa-cyclopentadienyl-amido catalysts for olefin polymerization. Chemical Reviews 98 (1998): 2587-2598.

[44] Zhang, J., Wang, X., Jin, G.X. Polymerized metallocene catalysts and late transition metal catalysts for ethylene polymerization. <u>Coordination Chemistry Reviews</u> 250 (2006): 95–109.

[45] Helmu, G., Koppl, A. Effect of the nature of metallocene complexes of groupIV metals on their performance in catalytic ethylene and propylene polymerization. <u>Chemical Reviews</u> 100 (2000): 1205-1222.

[46] Carnahan, E.M., Jacobsen, G.B. Supported metallocene catalysts. <u>Cattech</u> 4 (2000): 1-15.

[47] Hamielec, A.E., Soares, J.B.P. Polymerization reaction engineering-Metallocene catalysts. <u>Progress in Polymer Science</u> 21 (1996): 651-706.

[48] Cano, J., Kunz, K. How to synthesize a constrained geometry catalyst (CGC) - A survey. <u>Journal of Organometallic Chemistry</u> 692 (2007): 4411-4423.

[49] Nomura, K., Liu, J. Half-titanocenes for precise olefin polymerisation: effects of ligand substituents and some mechanistic aspects. Dalton Transactions 40 (2011): 7666-7682.

[50] Chen, Y.X., Marks, T.J. "Constrained geometry" dialkyl catalysts. Efficient, syntheses, C-H bond activation chemistry, monomer-dimer equilibration, and α-olefin polymerization catalysis. <u>Organometallics</u> 16 (1997): 3649-3657.

[51] Okuda, J., Musikabhumma, K., Sinnema, P. The kinetic stability of cationic benzyl titanium complexes that contain a linked amido-cyclopentadienyl ligand: the influence of the amido-substituent on the ethylene polymerization activity of "constrained geometry catalysts". <u>Israel Journal of Chemistry</u> 42 (2002): 383-392.

[52] Nishii, K., Hagihara, H., Ikeda, T., Akita, M., Shiono, T. Stereospecific polymerization of propylene with group 4 ansa-fluorenylamidodimethyl complexes. <u>Journal of Organometallic Chemistry</u> 691 (2006): 193-201.

[53] Zurek, E., Ziegler, T. Theoretical studies of the structure and function of MAO (methylaluminoxane). <u>Progress in Polymer Science</u> 29 (2004): 107-148.

[54] Kaminsky, W. Discovery of methylaluminoxane as cocatalyst for olefin polymerization. <u>Macromolecules</u> 45 (2012): 3289-3297.

[55] Harlan, C.J., Mason, M.R., Barron, A.R. *Tert*-butylaluminum hydroxides and oxides: structural relationship between alkylalumoxanes and alumina gels. Organometallics 13 (1994): 2957-2969.

[56] Chen, E.Y.X., Marks, T.J. Cocatalysts for metal-catalyzed olefin polymerization: activators, activation processes, and structure-activity relationships. Chemical Reviews 100 (2000): 1391-1434.

[57] Hagimoto, H., Shiono, T., Ikeda, T. Living polymerization of propene with a chelating(diamide) dimethyltitanium complex using silica-supported methylaluminoxane. Macromolecules 35 (2002): 5744-5745.

[58] Janiak, C., Rieger, B., Voelkel, R., Braun, H.G. Polymeric aluminoxanes: A possible cocatalytic sypport material for Ziegler-Natta-type metallocene catalysts. Journal of Polymer Science Part A: Polymer Chemistry 31 (1993): 2959-2968.

[59] Jin, J., Uozumi, T., Soga, K. Polymerization of olefins with zirconocene catalysts using methylaluminoxane modified with hydroquinone as cocatalyst. Macromolecular Chemistry and Physics 197 (1996): 849-854.

[60] Busico, V., Cipullo, R., Cutillo, F., Friederichs, N., Ronca, S., Wang, B. Improving the performance of methylalumoxane: A facile and efficient method to trap "free" trimethylaluminum. Journal of the American Chemical Society 125 (2003): 12402-12403.

[61] Ioku, A., Hasan, T., Shiono, T., Ikeda, T. Effects of cocatalysts on propene polymerization with [*t*-BuNSiMe$_2$(CSMe$_4$)]TiM$_{e2}$. Macromolecular Chemistry and Physics 203 (2002): 748-755.

[62] Intaragamjon N. "Comparative study of solvent effect and activators with titanocene catalysts on ethylene/α-olefins polymerization,". (Doctoral dissertation, Chemical Engineering, Engineering, Chulalongkorn University, 2005), pp. 39-55.

[63] Tsutsui, T., Mizuno, A., Kashiwa, N. Effect of hydrogen on propene polymerization with ethylenebis(1-indenyl)zirconium dichloride and methylalumoxane catalyst system. Macromolecular Rapid Communications 11 (1990): 565-570.

[64] Resconi, L., Camurati, I., Sudmeijer, O. Chain transfer reactions in propylene polymerization with zirconocene catalysts. <u>Topics in Catalysis</u> 7 (1999): 1457163.

[65] Kolodka, E.B. "Synthesis, characterization, thermomechanical and rheological properties of long chain branched metallocene polyolefins," (Doctoral dissertation the School of Graduate, McMaster University, 2002), pp. 13-16.

[66] Gottfried A.C., Brookhart M. Living and block copolymerization of ethylene and α-olefins using palladium(II)-α-diimine catalysts. <u>Macromolecules.</u> 36 (2003): 3085-3100.

[67] Coates, G.W., Hustad, P.D., Reinartz, S. Catalysts for the living insertion polymerization of alkenes: access to new polyolefin architectures using Ziegler-Natta chemistry. <u>Angewandte Chemie International Edition</u> 41 (2002): 2236-2257.

[68] Azoulay, J.D., Schneider, Y., Galland, G.B., Bazan, G.C. Living polymerization of ethylene and α-olefins using a nickel α-keto-β-diimine initiator. <u>Chemical Communications</u> 41 (2009): 6177-6179.

[69] Hagihara, H., Shiono, T., Ikeda, T. Living polymerization of propene and 1-hexene with the [t-BuNSiMe$_2$Flu]TiMe$_2$/B(C$_6$F$_5$)$_3$ Catalyst. <u>Macromolecules</u> 31 (1998): 3184-3188.

[70] Hasan, T., Ioku, A., Nishii, K., Shiono, T., Ikeda, T. Syndiospecific living polymerization of propene with [t-BuNSiMe$_2$Flu]TiMe$_2$ using MAO as cocatalyst. <u>Macromolecules</u> 34 (2001): 3142-3145.

[71] Camacho, D.H., Guan, Z. Living polymerization of α-olefins at elevated temperatures catalyzed by a highly active and robust cyclophane-based nickel catalyst. <u>Macromolecules</u> 38 (2005): 2544-2546.

[72] Coates, G.W., Hustad, P.D., Reinartz, S. Catalysts for the living insertion polymerization of alkenes: access to new polyolefin architectures using Ziegler-Natta chemistry. <u>Angewandte Chemie International Edition</u> 41(2002): 2236-2257.

[73] Chen, E.Y.X., Marks, T.J., Cocatalysts for metal-catalyzed olefin polymerisation: Activators, activation processes, and structure-activity relationships. <u>Chemical Reviews</u> 100 (2000): 1391 – 1434.

[74] Keii, T. <u>Heterogeneous kinetics</u>. Japan: Kodansha and Springer-Verlag Berlin Heidelberg, 2004.

[75] Hlatky G.G. Heterogeneous single-Site catalysts for olefin polymerization. <u>Chem. Rev</u>. 100 (2000): 1347-1376.

[76] Choi Y., Soares J.B.P., Supported single-site catalysts for slurry and gas-phase olefin polymerization. <u>Can. J. Chem. Eng</u>. 9999 (2011): 1-26.

[77] Ribeiro, M.R., Deffieux, A. and Portela, M.F., Supported metallocene complexes for ethylene and propylene polymerization: preparation and activity, Ind. <u>Eng Chem Res</u>. 36 (1997): 1224-1237.

[78] Fink G., Steinmetz B., Zechlin J., Przybyla C., Tesche B. Propene polymerization with silica-supported metallocene/MAO catalysts. <u>Chem Rev</u>.100 (2000): 1377-1390.

[79] Soga, K., Kim, H.J., Shiono, T. Polymerization of propene with highly isospecific SiO_2-supported zirconicene catalysts activated with common alkylaluminums. <u>Macromolecular Chemistry and Physics</u> 195 (1994): 3347-3360.

[80] Galli, P., Vercellio, G. Technology: Driving force behind innovation and growth of polyolefins. Progress in Polymer Science 26 (2001): 1287-1336.

[81] Steinmetz, B., Tesche, B., Przybyla, C., Zechlin, J., Fink, G. Polypropylene growth on silica-supported metallocene catalysts: A microscopic study to explain kinetic behavior especially in early polymerization stages. <u>Acta Polymerica</u> 48 (1997): 392-399.

[82] Paredes, B., Soares, J.B.P., Grieken, R.V., Carrero, A., Suarez, I. Characterization of ethylene-1-hexene copolymers made with supported metallocene catalysts: Influence of support type. <u>Macromolecular Symposium</u> 257 (2007): 103-111.

[83] Tanabe, K. Surface and catalytic properties of ZrO_2. <u>Materials Chemistry and Physics</u> 13 (1985): 347.

[85] Jongsomjit, B., Panpranot, J., Okada, M., Shiono, T., Praserthdam, P. Characteristics of $LLDPE/ZrO_2$ nanocomposite synthesized by the in situ polymerization using a zirconocene/MAO catalyst. <u>Iran Polymer Journal</u> 15 (2006): 431–437.

[86] Jongsomjit, B., Panpranot, J., Praserthdam, P. Effect of nanoscale SiO_2 and ZrO_2 as the fillers on the microstructure of LLDPE nanocomposites synthesized via *in situ* polymerization with zirconocene. <u>Materials Letters</u> 61 (2007): 1376-1379.

[87] Dow W.P., Wang Y.P., Huang T.J. Yttria-stabilized zirconia supported copper oxide catalyst I. Effect of oxygen vacancy of support on copper oxide reduction. <u>Journal of Catalysis</u> 160 (1996): 155-170.

[88] Wongmaneenil, P., Jongsomjit, B., Praserthdam, P. Solvent effect on synthesis of zirconia support for tungstated zirconia catalysts. <u>Journal of Industrial and Engineering Chemistry</u> 16 (2010): 327-333.

[89 Schrekker, H., Kotov, V., Preishuber-Pflugl, P., White, P., Brookhart, M. Efficient slurry-phase homopolymerization of ethylene to branched polyethylenes using α-diimine nickel(II) catalysts covalently linked to silica supports. <u>Macromolecules</u> 39 (2006): 6341-6354.

[90] Barbotin, F., Spitz, R., Boisson, C. Heterogeneous Ziegler-Natta catalyst based on neodymium for the stereospecific polymerization of butadiene. <u>Macromolecular Rapid Communications</u> 22(2001): 1411-1414.

[91] Jiamwijitkul, S., Jongsomjit, B., Praserthdam, P. Effect of boron-modified MCM-41-supported dMMAO/zirconocene catalyst on copolymerization of ethylene/1-Octene for LLDPE synthesis. <u>Iran Polymer Journal</u> 16 (2007): 549-559.

[92] Giannetti, E., Nicoletti, GM., Mazzocchi, R. Homogeneous Ziegler–Natta catalysis. II. Ethylene polymerization by IVB transition metal complexes/methyl aluminoxane catalyst systems. <u>Journal of Polymer Science Part A: Polymer Chemistry</u> 23 (1985): 2117-2134.

[93] Pol, A.V.D., Heel, J.P.C., Meijers, R., Meier, R.J., Kranenburg, M. Characterization of a metallocene/co-catalyst system supported on silica by fourier-transform Raman spectroscopy. <u>Journal of Organometallic Chemistry</u> 651 (2002): 80-89.

[94] Jongsomjit, B., Ngamposri, S., Praserthdam, P. Observation of bimodal polyethylene derived from TiO_2-supported zirconocene/MAO catalyst during polymerization of ethylene and ethylene/1-hexene. <u>Catalysis Letters</u> 117 (2007):177-181.

[95] Severn, J.R., Chadwick, J.C. <u>Tailor-made polymers via immobilization of alpha-olefin polymerization catalysts</u>. Weinheim: Wiley, 2004, p. 177.

[96] Shiono, T., Yoshida, S., Hagihara, H., Ikeda, T. Additive effects of trialkylaluminum on propene polymerization with (t-BuNSiMe$_2$Flu)TiMe$_2$-based catalysts. Applied Catalysis A: General 200 (2000): 145-152.

[97] Nishii, K., Matsumae, T., Dare, E.O., Shiono, T., Ikeda, T. Effect of solvents on living polymerization of propylene with [t-BuNSiMe$_2$Flu]TiMe$_2$-MMAO catalyst system. <u>Macromolecular Chemistry and Physics</u> 205 (2004): 363-9.

[98] Cai, Z., Ikeda, T., Akita, M., Shiono, T. Substituent effects of $tert$-butyl groups on fluorenyl ligand in syndiospecific living polymerization of propylene with ansa-fluorenylamidodimethyltitanium complex. <u>Macromolecules</u> 38 (2005): 8135-9.

[99] Soga, K., Uozumi, T., Park, J.R. Effect of catalyst isospecificity on olefin copolymerization. <u>Markromolekulare Chemie</u> 191 (1990): 2853-64.

[100] Busico, V., Cipullo, R., Monaco, G., Vacatello, M., Segre, A.L. Full assignment of the ^{13}C NMR spectra of regioregular polypropylenes: methyl and methylene region. <u>Macromolecules</u> 30 (1997): 6251-6263.

APPENDICES

APPENDIX A

(CALCULATION OF HYDROXYL GROUP)

A.1 Calculation of hydroxyl group on the support

Amount of hydroxyl group on the support was calculated from back titration method. The equation is shown below.

$$\text{-OH group} = \frac{N_{HCl}V_{HCl} - N_{NaOH}V_{NaOH}}{Wt}$$

Where   -OH group   =   amount of hydroxyl group per gram of support (mmol/g)

           N_{HCl} =   concentration of HCl solution (mol/L)

           V_{HCl} =   volume of HCl solution (mL)

           N_{NaOH} =   concentration of NaOH solution (mol/L)

           V_{NaOH} =   volume of NaOH solution (mL)

           Wt   =   weight of support (g)

APPENDIX B

(CALCULATION OF POLYMER MICROSTRUCTURE)

B-1 Calculation of copolymer microstructure

Copolymer microstructure and triad distribution of monomer were calculated according to the ^{13}C NMR spectra assignment of Soga et al. [99] in the list of reference. The detail of calculation for ethylene/1-hexene copolymer is interpreted as follow.

The integral area of ^{13}C NMR spectrum in the specify range are listed.

T_A	=	39.5 - 42	ppm
T_B	=	38.1	ppm
T_C	=	33-36	ppm
T_D	=	28.5-31	ppm
T_E	=	26.5-27.5	ppm
T_F	=	24-25	ppm
T_G	=	23.4	ppm
T_H	=	14.1	ppm

Triad distribution was calculated as the followed formula.

k[HHH]	=	$2T_A+T_b-T_g$
k[EHH]	=	$2(T_g-T_b-T_a)$
k[EHE]	=	T_B
k[EEE]	=	$0.5(T_a+T_d+T_f-2T_g)$
k[HEH]	=	T_F
k[HEE]	=	$2(T_g-T_a-T_f)$

All copolymer was calculated for the relative comonomer reactivity (r_E for ethylene and r_H for the 1-hexene) and monomer insertion by using the general formula as below.

$$r_E = 2[EE]/([EH]X) \qquad , \qquad r_H = 2[HH]X/[EH]$$

where

r_E	=	ethylene reactivity ratio
r_H	=	1-hexene reactivity ratio
[EE]	=	[EEE] + 0.5[HEE]
[EH]	=	[HEH] + 0.5[HEE] + [EHE] + 0.5[EHH]
[HH]	=	[HHH] + 0.5[EHH]
X	=	[E]/[H] in the feed
	=	concentration of ethylene (mol/l) / concentration of comonomer (mol/l) in the feed.
%E	=	[EEE] + [EEH] + [HEH]
%H	=	[HHH] + [HHE] + [EHE]

B-2 Calculation of propylene microstructure

Assignments of the methyl resonances in ^{13}C NMR spectrum of polypropylene [100].

mmmm	=	22.0–21.7	ppm
mmmr	=	21.7–21.4	ppm
rmmr	=	21.4–21.2	ppm
mmrr	=	21.2–21.0	ppm
mmrm + rmrr	=	21.0–20.7	ppm
rmrm	=	20.7–20.5	ppm
rrrm + rrrr	=	20.5–20.0	ppm
mrrm	=	20.0–19.7	ppm

The triad values can calculate as following [52]:

mm	=	mmmm + mmmr + rmmr
mr	=	mmrr + (mmrm + rmrr) + rmrm
rr	=	(rrrm + rrrr) + mrrm

APPENDIX C

(NUCLEAR MAGNETIC RESONANCE)
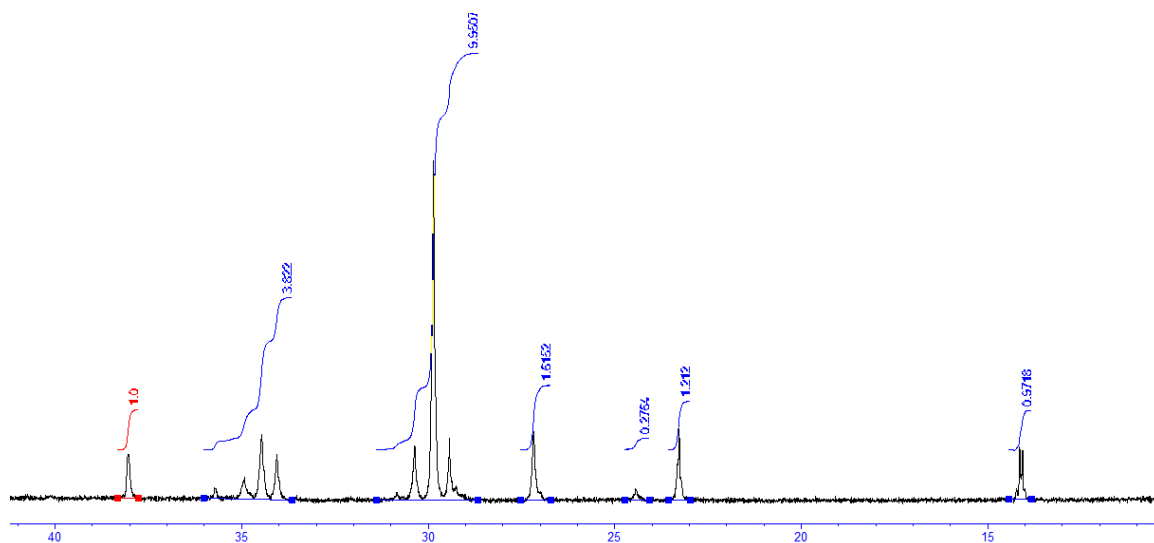
Figure C-1 ^{13}C NMR spectrum of ethylene/1-hexene copolymer
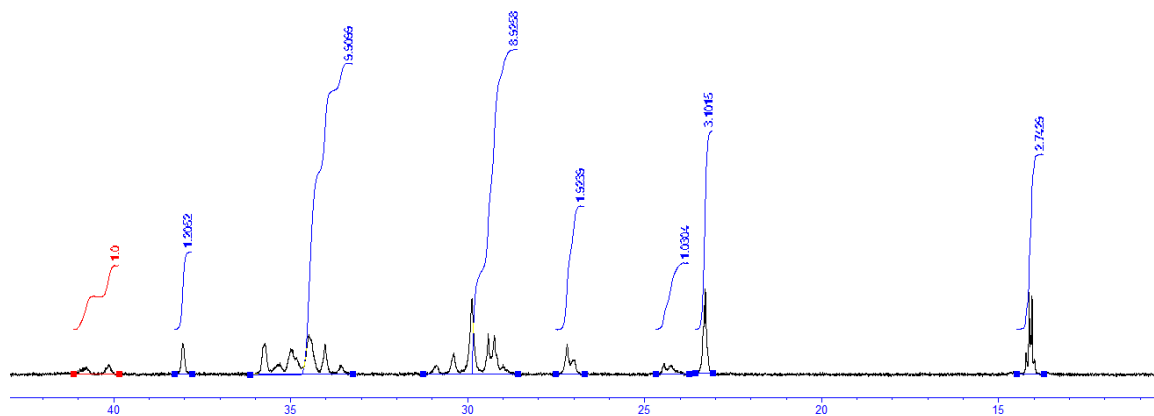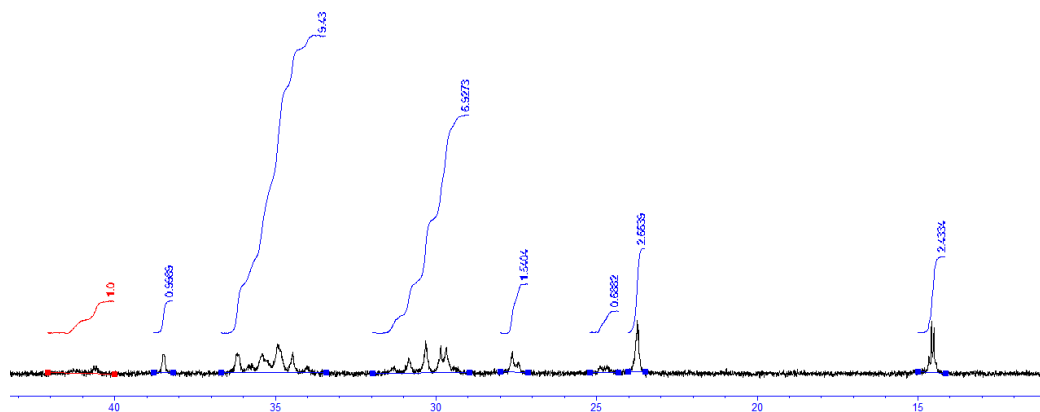obtained from MAO/ZrO$_2$-BCl$_3$ system (Part 1)
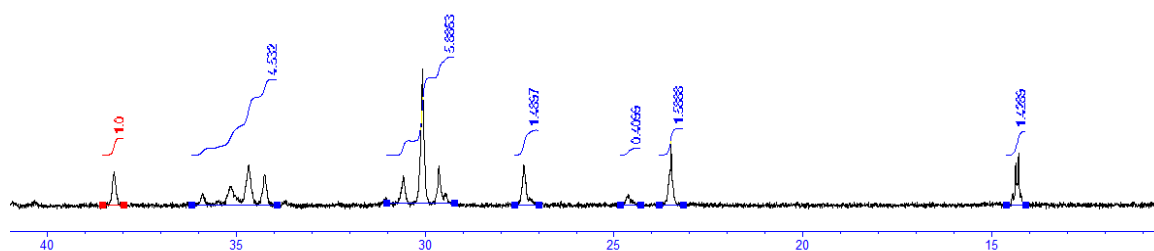
Figure C-2 ^{13}C NMR spectrum of ethylene/1-hexene copolymer
obtained from MAO/ZrO$_2$-glycerol system (Part 1)
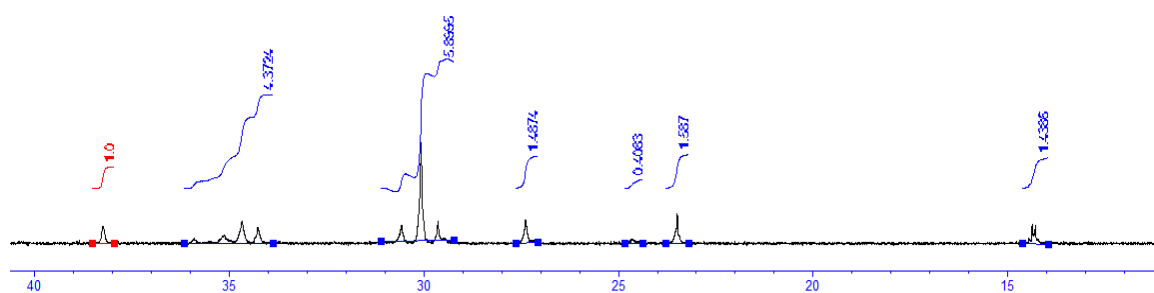
Figure C-3 ^{13}C NMR spectrum of ethylene/1-hexene copolymer
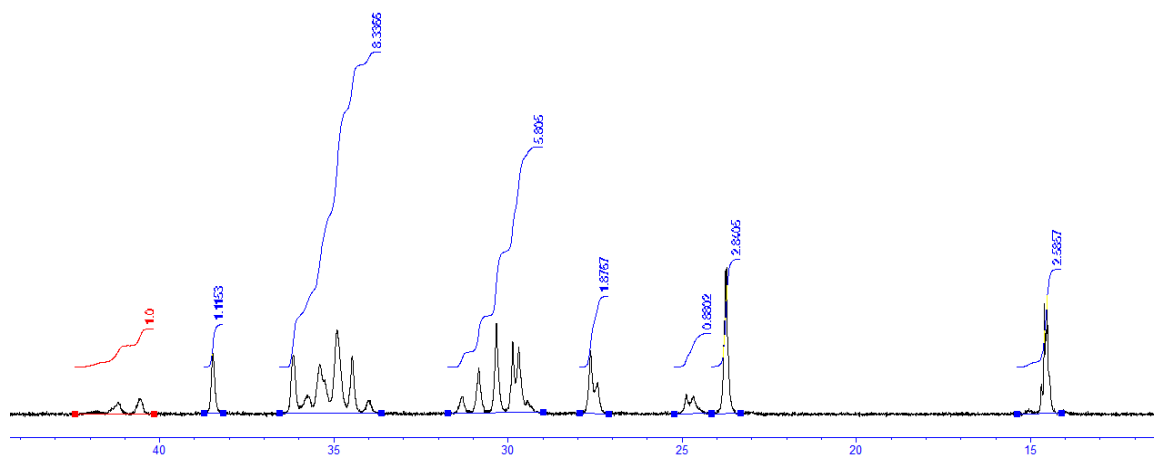obtained from MAO/ZrO$_2$-SiCl$_4$ system (Part 1)
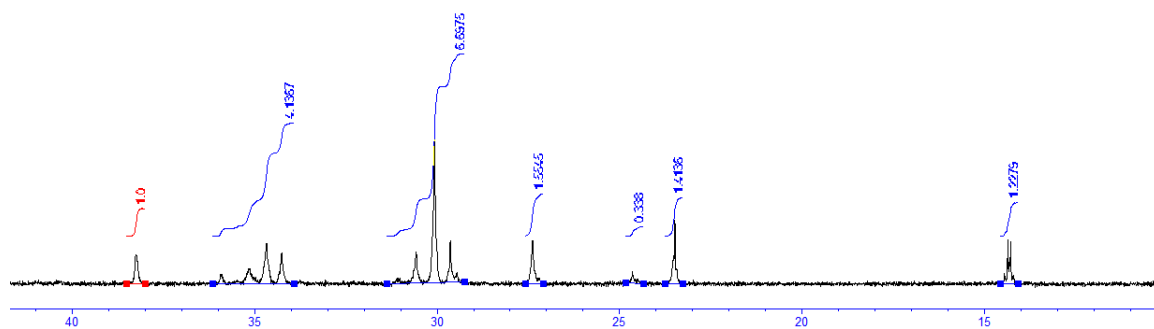
Figure C-4 ^{13}C NMR spectrum of ethylene/1-hexene copolymer
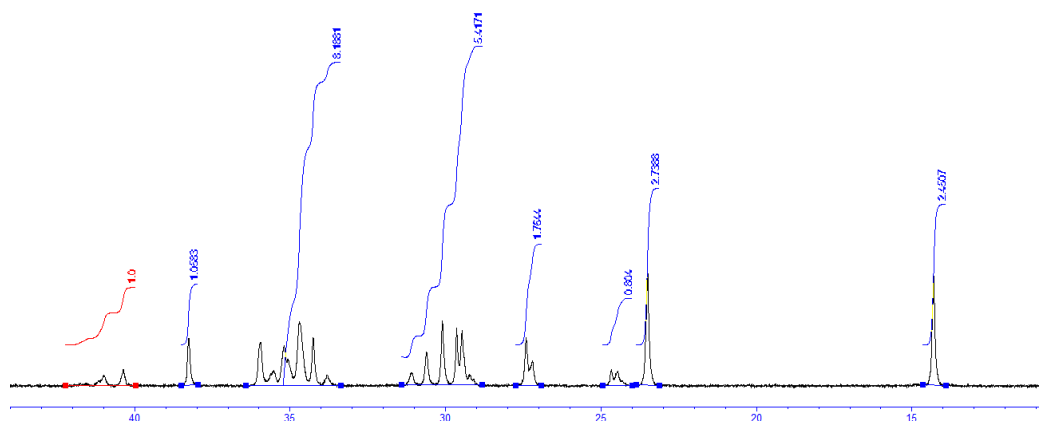obtained from MAO/ZrO$_2$ system (Part 1)
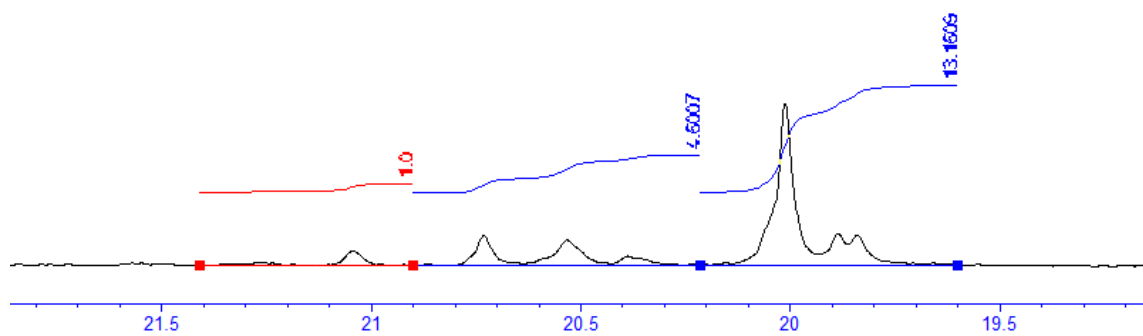
Figure C-5 ^{13}C NMR spectrum of polypropylene
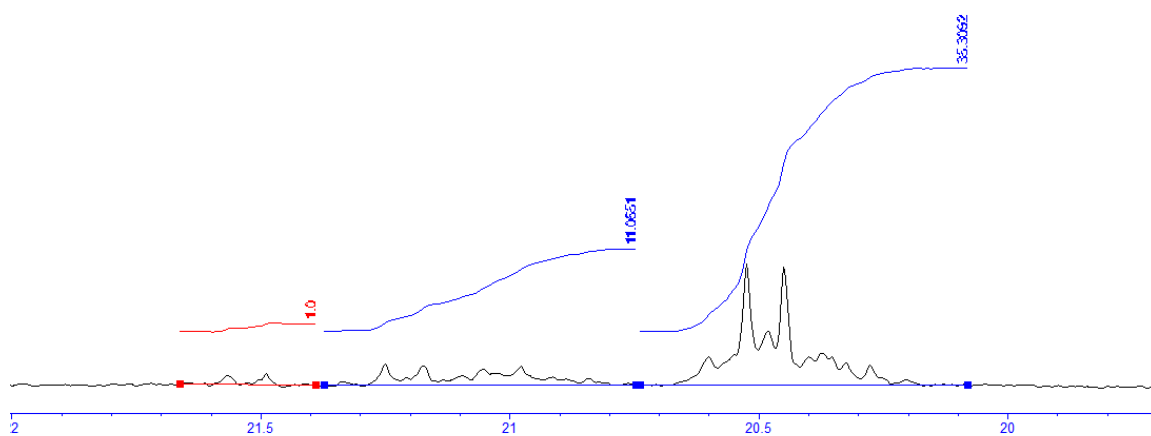obtained from dMMAO/ZrO$_2$ system (Part 2)
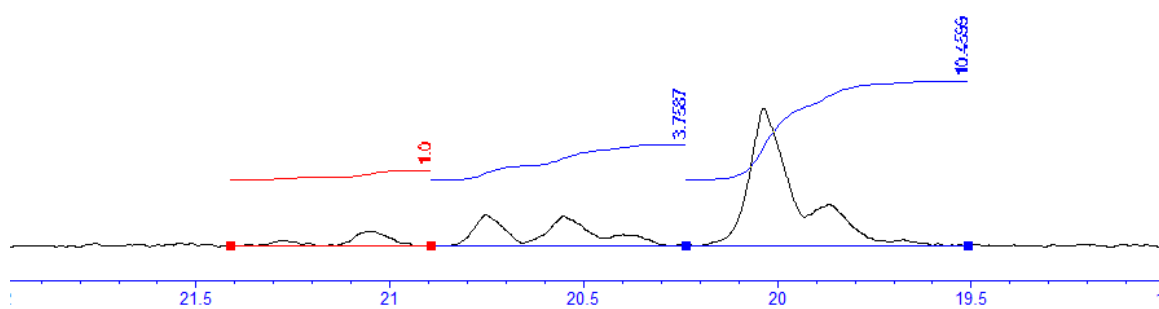
Figure C-6 ^{13}C NMR spectrum of polypropylene
obtained from MAO/ZrO$_2$ system (Part 2)
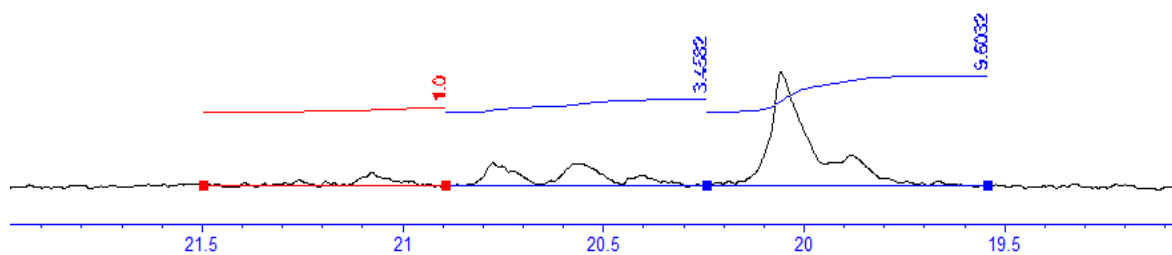
Figure C-7 ^{13}C NMR spectrum of polypropylene
obtained from MMAO/ZrO$_2$ system (Part 2)

Figure C-8 ^{13}C NMR spectrum of ethylene/1-hexene copolymer
obtained from MAO/ZrO$_2$ system (Part 3)

Figure C-9 ^{13}C NMR spectrum of ethylene/1-hexene copolymer
obtained from MAO/ZrO$_2$-SiCl$_4$ system (Part 3)

Figure C-10 ^{13}C NMR spectrum of ethylene/1-hexene copolymer
obtained from MAO/SiO$_2$ system (Part 3)

Figure C-11 ^{13}C NMR spectrum of ethylene/1-hexene copolymer
obtained from MAO/SiO$_2$-SiCl$_4$ system (Part 3)

Figure C-12 ^{13}C NMR spectrum of polypropylene
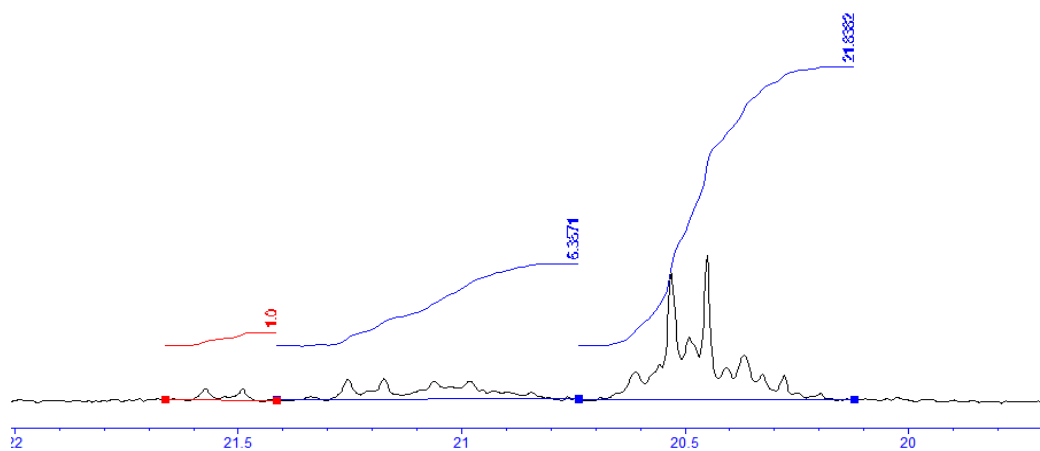obtained from MAO/ZrO$_2$ system (Part 3)

Figure C-13 ^{13}C NMR spectrum of polypropylene
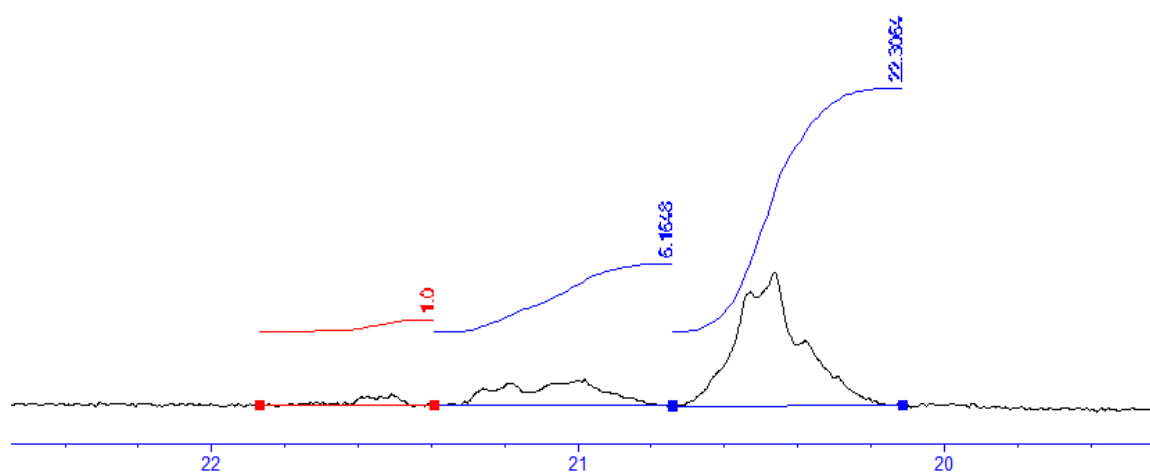obtained from MAO/ZrO$_2$-SiCl$_4$ system (Part 3)

Figure C-14 ^{13}C NMR spectrum of polypropylene
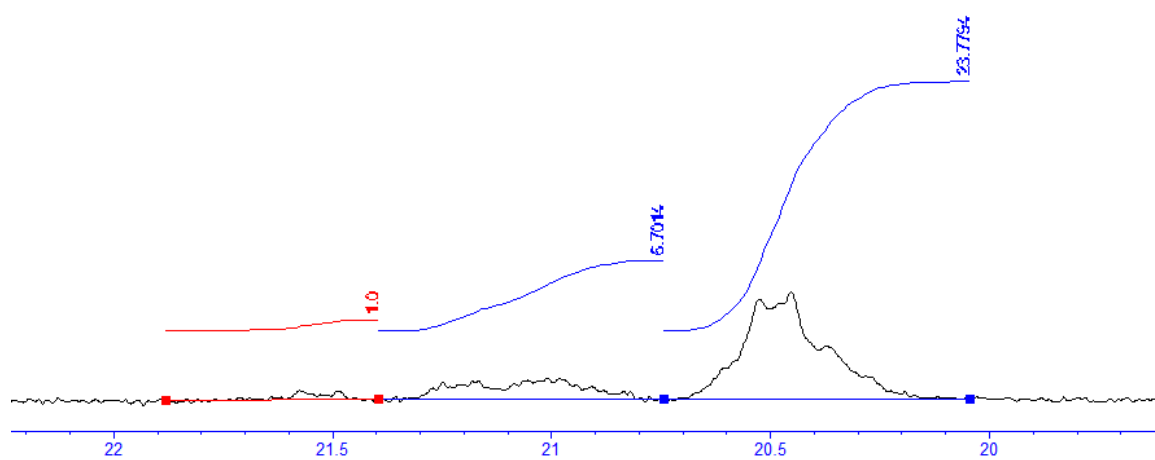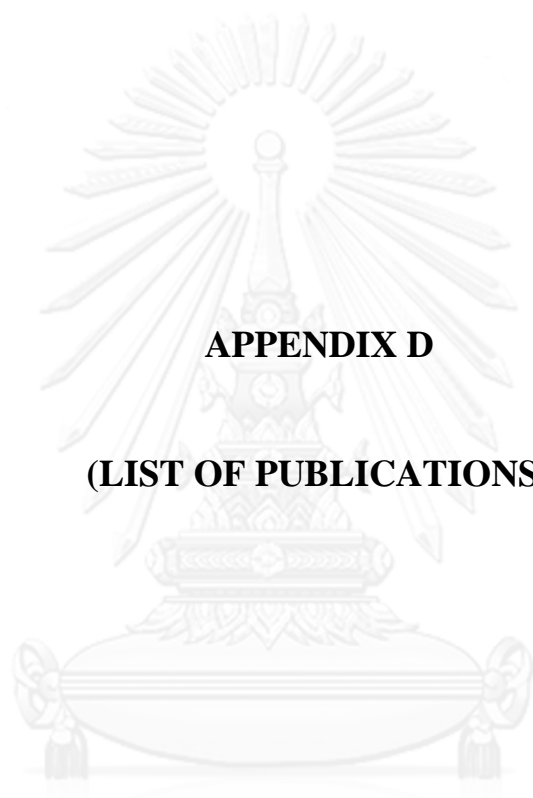obtained from MAO/SiO$_2$ system (Part 3)

Figure C-15 ^{13}C NMR spectrum of polypropylene
obtained from MAO/SiO$_2$-SiCl$_4$ system (Part 3)

APPENDIX D

(LIST OF PUBLICATIONS)

Articles

❖ Jantasee, S., Shiono, T., Jongsomjit, B. Copolymerization of ethylene/1-hexene with zirconocene/MAO catalyst supported on spherical zirconia modified with BCl_3, $SiCl_4$, and glycerol. <u>Polymer Bulletin</u> 70 (2013): 1753-1768.

❖ Jantasee, S., Jongsomjit, B., Shiono, T. Modification effect of spherical zirconia with $SiCl_4$ as a support of methylaluminoxane for heterogeneous single-site catalyst. <u>European Polymer Journal</u> 49(2013): 4195-4200.

❖ Lee, J.W., Jantasee, S., Jongsomsjit, B., Tanaka, R., Nakayama, Y., Shiono, T. Copolymerization of norbornene with ω-alkenylaluminum as a precursor comonomer for introduction of carbonyl moieties. <u>Journal of Polymer Science Part A: Polymer Chemistry</u> 51(2013): 5085-5090.

Conference contributions

❖ Jantasee, S., Shiono, T., Jongsomjit, B. Comparative effect of modified and unmodified spherical zirconia on living polymerization with [t-BuNSiMe₂Flu]TiMe₂ complex. <u>Proceedings of 8th International Colloquim on Heterogeneous Ziegler-Natta Catalysts</u>, Japan, 2012.

❖ Jantasee, S., Shiono, T., Jongsomjit, B. Effect of BCl_3- and $SiCl_4$-modified spherical zirconia supported metallocene/MAO catalyst on ethylene/1-hexene copolymerization. <u>Proceedings of the the 2nd International Conference on Engineering and Applied Science</u>, Japan, 2013.

❖ Jantasee, S., Shiono, T., Jongsomjit, B. Propylene polymerization over [*t*-BuNSiMe₂Flu]TiMe₂/MAO supported on zirconia support with $SiCl_4$ modification. <u>Proceedings of RGJ-Ph.D. Congress XIV</u>, Thailand, 2013.

❖ Jantasee, S., Shiono, T., Jongsomjit, B. Effect of $SiCl_4$-modified spherical zirconia-supported methylaluminoxane for heterogeneous single-site catalyst. Proceedings of 11th European Congress on Catalysis, France, 2013.

VITA

Miss Sasiradee Jantasee was born on May 20, 1987 in Bangkok, Thailand. She earned the Bachelor's Degree of Chemical Engineering from the Department of Chemical Engineering, Faculty of Engineer, King Mongkut's University of Technology Thonburi in April 2009 with a 1st class honor. Thereafter, she continued her Doctoral's study at the Department of Chemical Engineering, Chulalongkorn University under Royal Golden Jubilee program of Thailand Research Fund (TRF) in June 2009